

OPTIMIZATION OF LOCATION AND NUMBER OF LIGHTNING
ARRESTERS IN 420 kV SUBSTATIONS IN TURKISH HIGH VOLTAGE
ELECTRICITY SYSTEM

A THESIS SUBMITTED TO
THE GRADUATE SCHOOL OF NATURAL AND APPLIED SCIENCES
OF
MIDDLE EAST TECHNICAL UNIVERSITY

BY

MERT OZAN TULAZ

IN PARTIAL FULFILLMENT OF THE REQUIREMENTS
FOR
THE DEGREE OF MASTER OF SCIENCE
IN
ELECTRICAL AND ELECTRONICS ENGINEERING

FEBRUARY 2014

Approval of the Thesis

**OPTIMIZATION OF LOCATION AND NUMBER OF LIGHTNING
ARRESTERS IN 420 kV SUBSTATIONS IN TURKISH HIGH VOLTAGE
ELECTRICITY SYSTEM**

submitted by **MERT OZAN TULAZ** in partial fulfillment of the requirements
for the degree of **Master of Science in Electrical and Electronics Engineering
Department, Middle East Technical University** by,

Prof. Dr. Canan Özgen
Dean, Graduate School of **Natural and Applied Sciences** _____

Prof. Dr. Gönül Sayhan Turhan
Head of Department, **Electrical and Electronics Engineering** _____

Prof. Dr. Ali Nezih Güven
Supervisor, **Electrical and Electronics Engineering Dept., METU** _____

Examining Committee Members:

Prof. Dr. Nevzat Özay
Electrical and Electronics Engineering Dept., METU _____

Prof. Dr. Ali Nezih Güven
Electrical and Electronics Engineering Dept., METU _____

Prof. Dr. Arif Ertuş
Electrical and Electronics Engineering Dept., METU _____

Prof. Dr. Ahmet Rumeli
Electrical and Electronics Engineering Dept., METU _____

Dr. Erdal Bizkevelci
Consultant, ALSTOM POWER _____

Date: **06.02.2014**

I hereby declare that all information in this document has been obtained and presented in accordance with academic rules and ethical conduct. I also declare that, as required by these rules and conduct, I have fully cited and referenced all material and results that are not original to this work.

Name, Last name : Mert Ozan TULAZ

Signature :

ABSTRACT

OPTIMIZATION OF LOCATION AND NUMBER OF LIGHTNING ARRESTERS IN 420 kV SUBSTATIONS IN TURKISH HIGH VOLTAGE ELECTRICITY SYSTEM

Tulaz, Mert Ozan

M Sc, Department of Electrical and Electronics Engineering

Supervisor : Prof. Dr. Ali Nezh GÜVEN

February 2014, 96 pages

Insulation coordination is defined as the selection of the dielectric strength of equipment in relation to the voltages which can appear on the system for which the equipment is intended and taking into account the service environment and the characteristics of the available protective devices. In an insulation coordination study, the voltage levels of power system equipment are determined in order to ensure the protection of equipment against overvoltages. This proper design in terms of the insulation coordination provides the reliability of the system by decreasing insulation failures and reduces the cost of the system by preventing oversizing of the equipment. Hence, insulation coordination is an important study for power systems in order to prevent failures and overinvestment.

In this thesis, an insulation coordination study is performed for lightning overvoltages in 420 kV substations in Turkish High Voltage Electricity System.

The lightning impulse withstand voltage levels of the equipment are analyzed and evaluated as compared to current values in the system. In order to obtain optimum lightning arrester locations and numbers in the substation, different cases are defined and analyzed through computer simulations on Alternative Transient Program (ATP).

In this context, this thesis study proposes additional lightning arrester application at the line entrance to existing lightning arresters located at the front of power transformer in 420 kV substations of Turkish High Voltage Electricity System. With this additional application, it is concluded that lightning impulse withstand voltage levels of equipment can be reduced to voltages that are the standard values recommended in IEC for 420 kV systems, 1300 kV for power transformer and 1425 kV for other equipment.

Keywords: Insulation Coordination, Lightning Arresters, Lightning Impulse Withstand Voltage

ÖZ

TÜRKİYE YÜKSEK GERİLİM ELEKTRİK SİSTEMİNDE 420 kV TRAFO MERKEZİNDE PARAFUDRLARIN YERLERİNİN ve SAYILARININ OPTİMİZASYONU

Tulaz, Mert Ozan

Yüksek Lisans, Elektrik ve Elektronik Mühendisliği Bölümü

Tez Yöneticisi : Prof. Dr. Ali Nezh GÜVEN

Şubat 2014, 96 sayfa

İzolasyon koordinasyonu, ekipmanların dielektrik dayanımlarının, ekipmanların tasarlandığı ve işletme ortamı ile uygun koruma cihazlarının karakteristiklerinin dikkate alındığı sistemde oluşan gerilimler ile ilişkili seçilmesi olarak tanımlanır. İzolasyon koordinasyon çalışmasında, gerilim seviyesi, güç sistemi ekipmanlarının aşırı gerilime karşı korumasını garanti edecek şekilde belirlenir. İzolasyon koordinasyonu açısından uygun olan bu tasarım, izolasyon hatasını azaltarak sistemin güvenilirliğini sağlar ve olması gerekenden fazla ekipman boyutlandırmasını engelleyerek sistem maliyetini azaltır. Böylece, izolasyon koordinasyonu, güç sistemlerinde hataları ve fazla yatırımı engellemek için önemli bir çalışmadır.

Bu tez çalışmasında, Türkiye Yüksek Gerilim İletim Sistemi'nde 420 kV trafo merkezinde yıldırım aşırı gerilimleri için izolasyon koordinasyonu çalışması

gerçekleştirilmiştir. Ekipmanların yıldırım darbe dayanım gerilim seviyeleri, sistemdeki mevcut uygulamadaki değerler ile kıyaslanarak analiz edilmiş ve değerlendirilmiştir. Trafo merkezinde optimum parafudr lokasyonlarını ve sayılarını elde etmek için farklı durumlar tanımlanmakta ve Alternative Transient Program (ATP) üzerinden bilgisayar simülasyonları ile analiz edilmektedir.

Bu kapsamda, bu tez çalışması, Türkiye Yüksek Gerilim İletim Sistemi'nin 420 kV şalt merkezlerinde, mevcut güç trafoları önünde bulunan parafudrlara ilave olarak hat girişlerine parafudr yerleştirilmesini önermektedir. Bu ilave parafudr uygulaması ile ekipmanların yıldırım darbe dayanım gerilim seviyeleri IEC'de 420 kV sistemler için önerilen standart değerlere, güç trafosu için 1300 kV'a ve diğer ekipmanlar için 1425 kV'a, düşürülebileceği sonucuna ulaşılmıştır.

Anahtar Kelimeler: İzolasyon Koordinasyon, Parafudr, Yıldırım Darbe Dayanım Gerilimi

To My Niece and Nephew, Derin Mavi and Arin Deniz

ACKNOWLEDGEMENTS

First of all, I would like to thank my supervisor Prof. Dr. Ali Nezir Güzen for his guidance throughout the graduate study.

I wish to express my deepest gratitude to Prof. Dr. Nevzat Özyay for his insight, suggestions, advice, patience and encouragements throughout the research.

I would like to thank Burçak Kurt, Mustafa Daldal and Dr. Erdal Bizkevelci who patiently listened my problems, guided me and provided support for maturing my ideas and opinions.

Hamza Oğuz Ertuğrul and Çınar İnal, who are the members of Alstom Grid Enerji Endüstrisi AŞ, provided the technical support throughout the research. I express my special appreciation and I will remember them as the ones who enable me to conclude the study.

I would like to thank my manager Celal Öztop for his collaboration, tolerance, support and guidance.

I wish to express my special acknowledgements to my short-term housemates but long-term friends Baran Kurt and Yasemin Cansuz, who were with me at my hard times throughout the study.

My deepest thank is to my family for their charitably support, encouragements, patience and love.

TABLE OF CONTENTS

ABSTRACT	v
ÖZ.....	vii
ACKNOWLEDGEMENTS.....	x
TABLE OF CONTENTS.....	xi
LIST OF FIGURES	xiii
LIST OF TABLES	xvi
CHAPTERS	
1. INTRODUCTION.....	1
1.1. Motivation of the Thesis	1
1.2. Outline of the Thesis	6
2. INSULATION COORDINATION MODEL	7
2.1. Introduction	7
2.2. Lightning Strike Model	7
2.3. Overhead Line Model.....	17
2.4. Lightning (Surge) Arrester Model.....	24
2.5. Substation Equipment Models	26
2.6. Substation Model.....	27
2.7. Complete Simulation Models.....	34
3. SIMULATIONS AND RESULTS	37
3.1. Introduction	37
3.2. Effect of the Location of Lightning Arresters for Main Busbar Connection Type	38
3.3. Effect of the Location of Lightning Arresters for Transfer Busbar Connection Type	42

3.4. Effect of the Current Amplitude of Lightning Strike for Main Busbar Connection Type	45
3.5. Effect of the Current Amplitude of Lightning Strike for Transfer Busbar Connection Type	48
3.6. Effect of the Connection Length for Main Busbar Connection Type .	51
3.7. Effect of the Connection Length for Transfer Busbar Connection Type	54
3.8. Effect of the Lightning Strike Location for Main Busbar Connection Type	57
3.9. Effect of the Lightning Strike Location for Transfer Busbar Connection Type	60
4. DISCUSSION OF RESULTS.....	63
4.1. Introduction	63
4.2. Analyses of Effect of Location of Lightning Arresters	64
4.3. Analyses of Effect of Current Amplitude of Lightning Strike.....	68
4.4. Analyses of Effect of Connection Length	72
4.5. Analyses of Effect of Location of Lightning Strike	76
4.6. Analyses of Results	78
5. CONCLUSION AND FUTURE WORK.....	81
REFERENCES	83
APPENDIX A	87
APPENDIX B.....	96

LIST OF FIGURES

FIGURES

Figure 1 Geometric model of phase conductors and shield wires.....	8
Figure 2 Definition of I_m and expanded view.....	9
Figure 3 The annual frequency of thunderstorm days in the world	12
Figure 4 Turkey keraunic level map	13
Figure 5 Waist type in tower and equations	18
Figure 6 Standard 420 kV tower arrangement	19
Figure 7 Ionization model of the tower footing resistance.....	22
Figure 8 IEEE Working Group MO surge arrester model for fast front surges.....	25
Figure 9 Simplified Lightning Arrester Model	26
Figure 10 Typical capacitance to ground values for substation equipment [4]	27
Figure 11 Typical single line diagrams of 420 kV substation double busbar with transfer busbar for transformer feeder, line feeder and coupling and transfer feeder.....	29
Figure 12 Typical general layout of line feeder	31
Figure 13 Typical general layout of the bus coupler and transfer feeder.....	32
Figure 14 Typical general layout of the transformer feeder.....	33
Figure 15 Shielding failure model on ATP	35
Figure 16 Back flashover failure model on ATP	36
Figure 17 Resultant voltage waveforms for Case 1	40
Figure 18 Resultant voltage waveforms for Case 2	40
Figure 19 Resultant voltage waveforms for Case 3	41
Figure 20 Resultant voltage waveforms for Case 4	41
Figure 21 Resultant voltage waveforms for Case 5	43

Figure 22 Resultant voltage waveforms for Case 6	43
Figure 23 Resultant voltage waveforms for Case 7	44
Figure 24 Resultant voltage waveforms for Case 8	44
Figure 25 Resultant voltage waveforms for Case 9	46
Figure 26 Resultant voltage waveforms for Case 10	46
Figure 27 Resultant voltage waveforms for Case 11	47
Figure 28 Resultant voltage waveforms for Case 12	47
Figure 29 Resultant voltage waveforms for Case 13	49
Figure 30 Resultant voltage waveforms for Case 14	49
Figure 31 Resultant voltage waveforms for Case 15	50
Figure 32 Resultant voltage waveforms for Case 16	50
Figure 33 Resultant voltage waveforms for Case 17	52
Figure 34 Resultant voltage waveforms for Case 18	52
Figure 35 Resultant voltage waveforms for Case 19	53
Figure 36 Resultant voltage waveforms for Case 20	53
Figure 37 Resultant voltage waveforms for Case 21	55
Figure 38 Resultant voltage waveforms for Case 22	55
Figure 39 Resultant voltage waveforms for Case 23	56
Figure 40 Resultant voltage waveforms for Case 24	56
Figure 41 Resultant voltage waveforms for Case 25	58
Figure 42 Resultant voltage waveforms for Case 26	58
Figure 43 Resultant voltage waveforms for Case 27	59
Figure 44 Resultant voltage waveforms for Case 28	59
Figure 45 Resultant voltage waveforms for Case 29	61
Figure 46 Resultant voltage waveforms for Case 30	61
Figure 47 Resultant voltage waveforms for Case 31	62
Figure 48 Resultant voltage waveforms for Case 32	62
Figure 49 Effect of location of lightning arresters for main busbar connection type in Case 1, 2, 3 and 4	66

Figure 50 Effect of location of lightning arresters for transfer busbar connection type in Case 5, 6, 7 and 8	66
Figure 51 Effect of location of lightning arresters and connection type for back flashover failure in Case 1, 2, 5 and 6.....	67
Figure 52 Effect of location of lightning arresters and connection type for shielding failure in Case 3, 4, 7 and 8.....	67
Figure 53 Effect of current amplitude of lightning strike for main busbar connection type in Case 9, 10, 11 and 12.....	70
Figure 54 Effect of current amplitude of lightning strike for transfer busbar connection type in Case 13, 14, 15 and 16.....	70
Figure 55 Effect of current amplitude and connection type for back flashover failure in Case 9, 10, 13 and 14.....	71
Figure 56 Effect of current amplitude and connection type for shielding failure in Case 11, 12, 15 and 16	71
Figure 57 Effect of connection length for main busbar connection type in Case 17, 18, 19 and 20	74
Figure 58 Effect of connection length for transfer busbar connection type in Case 21, 22, 23 and 24	74
Figure 59 Effect of connection length and connection type for back flashover failure in Case 17, 18, 21 and 22.....	75
Figure 60 Effect of connection length and connection type for shielding failure in Case 19, 20, 23 and 24	75
Figure 61 Effect of location of lightning strike for main busbar connection type in Case 25, 26, 27 and 28	77
Figure 62 Effect of location of lightning strike for transfer busbar connection type in Case 29, 30, 31 and 32	77

LIST OF TABLES

TABLES

Table 1 Standard lightning impulse withstand voltage levels for 420 kV and 525 kV in [1]	3
Table 2 Group 1 Cases	38
Table 3 Group 2 Cases	42
Table 4 Group 3 Cases	45
Table 5 Group 4 Cases	48
Table 6 Group 5 Cases	51
Table 7 Group 6 Cases	54
Table 8 Group 7 Cases	57
Table 9 Group 8 Cases	60
Table 10 Results for Case 1.....	87
Table 11 Results for Case 2.....	87
Table 12 Results for Case 3.....	87
Table 13 Results for Case 4.....	88
Table 14 Results for Case 5.....	88
Table 15 Results for Case 6.....	88
Table 16 Results for Case 7.....	88
Table 17 Results for Case 8.....	89
Table 18 Results for Case 9.....	89
Table 19 Results for Case 10.....	89
Table 20 Results for Case 11.....	89
Table 21 Results for Case 12.....	90
Table 22 Results for Case 13.....	90

Table 23 Results for Case 14.....	90
Table 24 Results for Case 15.....	90
Table 25 Results for Case 16.....	91
Table 26 Results for Case 17.....	91
Table 27 Results for Case 18.....	91
Table 28 Results for Case 19.....	91
Table 29 Results for Case 20.....	92
Table 30 Results for Case 21.....	92
Table 31 Results for Case 22.....	92
Table 32 Results for Case 23.....	92
Table 33 Results for Case 24.....	93
Table 34 Results for Case 25.....	93
Table 35 Results for Case 26.....	93
Table 36 Results for Case 27.....	93
Table 37 Results for Case 28.....	94
Table 38 Results for Case 29.....	94
Table 39 Results for Case 30.....	94
Table 40 Results for Case 31.....	94
Table 41 Results for Case 32.....	95

CHAPTER 1

INTRODUCTION

1.1. Motivation of the Thesis

International Electrotechnical Commission (IEC) 60071-1 [1] classifies voltages and overvoltages into the following four classes; continuous (power frequency) voltage, temporary overvoltage, transient overvoltage and combined overvoltage based on their shape and duration. Power frequency voltage is continuously applied voltage to any part of an insulation configuration. Temporary overvoltage is defined as power frequency overvoltage for relatively long duration and is caused by load rejection, line short circuit fault and etc. Transient overvoltage is a short-duration overvoltage of few milliseconds or less and it consists of three type overvoltages; slow-front, fast-front and very fast-front. Combined overvoltage is the combination of two types of overvoltages.

Fast front overvoltages are the results of the lightning that is the reason why it is called as lightning overvoltages. It is known that lightning strikes inject steep front current impulses to the overhead transmission lines. This current impulses cause traveling waves which propagate along the overhead line and overvoltages. Also in substations, they cause lightning impulse overvoltages and pose a risk to any items of equipment. Thus, the dielectric withstand of the different equipment of substation must be higher than the resulting overvoltage.

There are two kinds of lightning impulse overvoltages which are taken into account due to the different position of the strike point. The first is the back flashover. In this type lightning impulse overvoltage, the lightning strikes on the tower or shielding wire, and then it increases the tower top voltage over the insulator strength. This leads to backward flashovers from the tower to an overhead line conductor. The second one is the shielding failure. In this type, the lightning strikes directly on the phase conductor of the overhead line due to the protection failure of shielding wire.

Lightning overvoltage is a dominant factor for determining the insulation level of equipment of a substation. It causes the highest overvoltages on the equipment and affects the insulation level. The insulation level at voltage levels higher than 245 kV refers to the standard lightning impulse withstand voltages according to [1].

In Turkish High Voltage Electricity System (THVES), 420 kV is one of standard voltage levels. Lightning impulse withstand voltage (LIWV) level of the primary equipment in THVES at 420 kV is determined as 1550 kV except power transformers. For power transformers, 1425 kV is specified as LIWV. However, in IEC 60071-1 [1], 1550 kV and 1425 kV standard lightning impulse withstand voltages are recommended for power systems where highest voltage for equipment is 525 kV. LIWV values recommended in IEC [1] for highest system voltages of 420 kV and 525 kV are given in Table 1. There are three groups in standard lightning impulse withstand voltage levels for both 420 kV and 525 kV, as seen from Table 1. Three groups are utilized according to the amplitude of standard LIWV. Each group consists of two values. The lower one is defined for equipment close to the lightning arrester and the higher one is for other equipment which is far from the lightning arrester. In [1], the highest standard LIWV values at 420kV for power transformer and other equipment are 1300 kV and 1425 kV, respectively. The values applied in THVES for 420 kV as LIWV, 1425 kV and

1550 kV, are at the highest group of 525 kV. Since, these LIWV values, used in THVES, is not standard, equipment of the power system in 420 kV THVES has to be custom production.

Table 1 Standard lightning impulse withstand voltage levels for 420 kV and 525 kV in [1]

Highest voltage for equipment U_m kV (r.m.s value)	Standard lightning impulse withstand voltage kV (peak value)
420	1050
	1175
	1175
	1300
525	1300
	1425
	1300
	1425
525	1425
	1550

When the standard lightning impulse voltages in 420 kV THVES are evaluated by considering the lightning arrester application, different situations could be observed. In standard Turkish Electricity Transmission Corporation (TEİAŞ) applications, lightning arresters are located only at front of the power transformers. At the outgoing and incoming feeders, there is no lightning arrester at the line entrance. However, besides TEİAŞ substations, the substations which are constructed by the power plant owners in order to connect the power plant to the interconnected high voltage system, lightning arresters are applied at the outgoing feeders at the line side. At these substations, the lightning arresters are also located at the transformer side similar to standard application of TEİAŞ. In other

countries, it is possible to observe different lightning arrester applications. In European countries, lightning arrester application is the same with the substations of power plants in Turkey. In other words, lightning arresters are located both at front of power transformers and at line entrances in European countries. However, LIWV levels for 420 kV substations are defined as 1300 kV and 1425 kV in accordance with recommended IEC [1] values [28]. Russia and most of former Soviet Bloc countries use lightning arresters also at the busbars connected via a disconnecter switch in addition to ones at the front of transformer and outgoing line feeders. In these countries, shielding line is not used in the substation or on the high voltage transmission line. Instead of this, lightning rods are applied at the top of the towers with a height of 3 to 6 meters.

The study which determines the insulation levels of the electrical equipment is called as insulation coordination. In [1], insulation coordination is defined as the selection of the dielectric strength of equipment in relation to the voltages which can appear on the system for which the equipment is intended and taking into account the service environment and the characteristics of the available protective devices. Two important past studies related with insulation coordination, especially for THVES, are by Ümit Hızıroğlu [9] and Sedef Şerifeken [10]. Although these studies were performed nearly 20 years ago, they are valuable sources for the general concept of insulation coordination and lightning overvoltages.

“Overvoltages in Electric Substations and Protection with Metal Oxide Surge Arresters”, Master’s thesis by Hızıroğlu, analyzes 154 kV Air Insulated System (AIS) by studying lightning overvoltages and single line to ground faults. Substation model is based on both constant parameter and frequency dependent line modeling approaches in system simulations. The differences of these modeling types are also evaluated with three phase and single phase system

representations. At this evaluation, surge arresters are located at front of transformer, at substation entrance and both at front of transformer and substation entrance for different cases. In these cases, maximum overvoltages for power transformer and voltage transformer are calculated. In this study, overvoltage values are decreased to the acceptable limits by utilization of metal oxide surge arresters.

The second important study is “Insulation Coordination Study for Hilal/İzmir Gas Insulated Substation” by Şerifeken. This study is performed for 154 kV Gas Insulated System (GIS) substation according to the lightning overvoltages. The variables are chosen as circuit configuration and lightning stroke parameters. Based on these variables, different cases are analyzed by changing the number of lines, peak current of lightning stroke, the front and tail time of waveform. After the analysis of these cases, the overvoltages at the surge arrester, power transformer and circuit breakers are observed. The result of these analyses is related with the insulation level of the 154 kV GIS. It concluded that the insulation level of 154 kV GIS should be decreased to 650 kV without sacrificing from the degree of the protection.

As described in [25], The location of lightning arresters, relative to the equipment being protected, must be given careful consideration if adequate protection is to be provided at reasonable cost and this is particularly true if equipment having reduced insulation levels is used for economy reasons.

The objective of this thesis study is to optimize the location and number of the lightning arresters in 420kV substations in Turkish High Voltage Electricity System and to determine the lightning impulse withstand voltage levels of the primary equipment in the substation. In line with this purpose, lightning overvoltages under different configuration cases are simulated and analyzed.

1.2. Outline of the Thesis

This thesis study starts with the introduction chapter. The overvoltage types are briefly classified according to [1] in this chapter. Lightning overvoltages are explained and failure types causing lightning overvoltages are given. Lightning impulse withstand voltage levels used in 420 kV Turkish High Voltage Electricity System are introduced in comparison with the standard lightning impulse withstand voltage levels defined in IEC [1]. In addition, lightning arresters application in Turkey and also in other countries is explained. In this way, the motivation of this thesis study is presented.

In chapter 2, the parts of insulation coordination model are presented. The calculations made to obtain the parameters defined in the model are explained. The complete insulation coordination models used in this thesis study are introduced for the shielding failure and the back flashover failure.

Chapter 3 presents the simulation cases performed on ATP in order to analyze the possible different configurations. The objective and the results of each simulation are also given in this chapter.

In chapter 4, the obtained results from the simulations are discussed. Effects of failure types, connection types, location of lightning arrester, current amplitude of lightning strike, connection length and location of lightning strike are explained through the results of simulations. Finally, in Chapter 5 the main conclusions reached throughout the study are stated and the work for future investigations is summarized.

CHAPTER 2

INSULATION COORDINATION MODEL

2.1. Introduction

In order to achieve the objective of this thesis study which is to optimize the lightning arresters in 420 kV substations in Turkish High Voltage Electricity System and determine the lightning impulse withstand voltage levels of the primary equipment in the substation, insulation coordination model designed and analyses are performed on the Alternative Transient Program (ATP) which is one of the most widely-used Power System Transient simulation program. IEC 60071-2 [2], IEC 60071-4 [3], “IEEE Modeling Guidelines for Fast Front Transients” [4] and “Guide to procedures for estimating the lightning performance of transmission lines” of CIGRE Study Committee of “Overvoltages and Insulation Coordination” [15] are the main references for the modeling the system in the ATP simulation program. The following sections present the modeling of lightning strike, overhead line (OHL), lightning arrester, equipment of substation and substation in detail.

2.2. Lightning Strike Model

Lightning overvoltages are caused in an electric network through two possible situations. The first situation is direct strokes to one of the phase conductors. In this type of lightning overvoltages, although shielding wire exists in order to

protect the phase conductors against the lightning strokes, lightning strikes directly to the phase conductor because of the shielding failure. The second possibility is called as back flashover. In this type of failure, lightning with higher amplitude than at the shielding failure, strikes to the tower or shielding wire, and then voltage wave is transferred to the phase conductor due to the breakdown of the insulator or air. As explained, since the shielding failure and back flashover failures occur under different conditions, they must be modeled according to their case specific situations. Hence, lightning strike is modelled separately for the shielding failure and the back flashover failure cases with related terms.

2.2.1. Shielding Failure

Shielding wires protect the phase conductors by attracting the lightning strokes to themselves. Until a limit value of current, however, the shielding wire may not protect the phase conductor. This limit current determines the maximum amplitude of the lightning stroke that directly strike to the phase conductor by bypassing the shielding wire. It is calculated according to the electro-geometric model which is defined in [5]. The geometric model, definitions of angles and distances are shown in Figure 1.

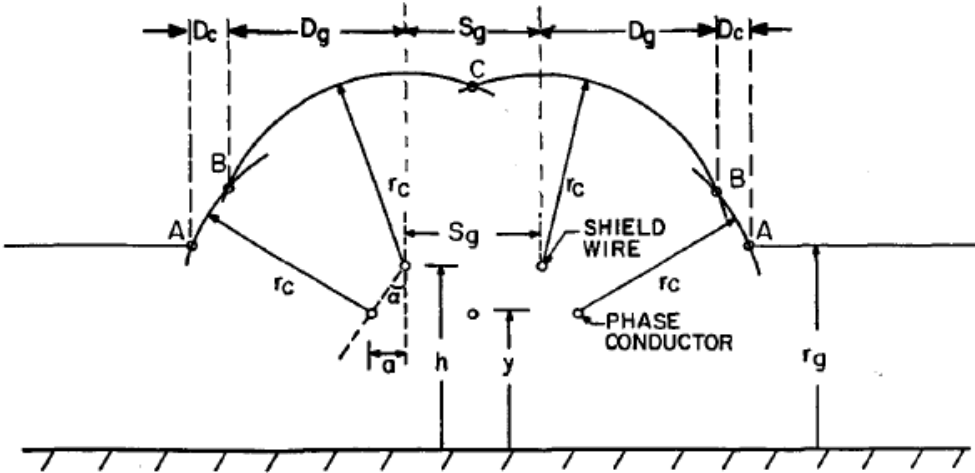


Figure 1 Geometric model of phase conductors and shield wires

Figure 1 illustrates the electro-geometric model, with a specific value of stroke current,

where r_c is the striking distance of phase conductors and shielding wires,

r_g is the striking distance to earth,

D_c and D_g are the exposure distance for phase conductors and shield wires.

Downward leaders that reach the arc between A and B will terminate on the phase conductor, while those reach the arc between B and C will terminate on the shield wires and those that terminate beyond A will terminate to the ground. As understood from Figure 1, across the arc between A and B, shielding wire cannot protect the phase conductor and lightning strokes terminate on the phase conductor bypassing the shielding wire. The horizontal distance between points A and B, D_c , has a correlation with current amplitude of lightning.

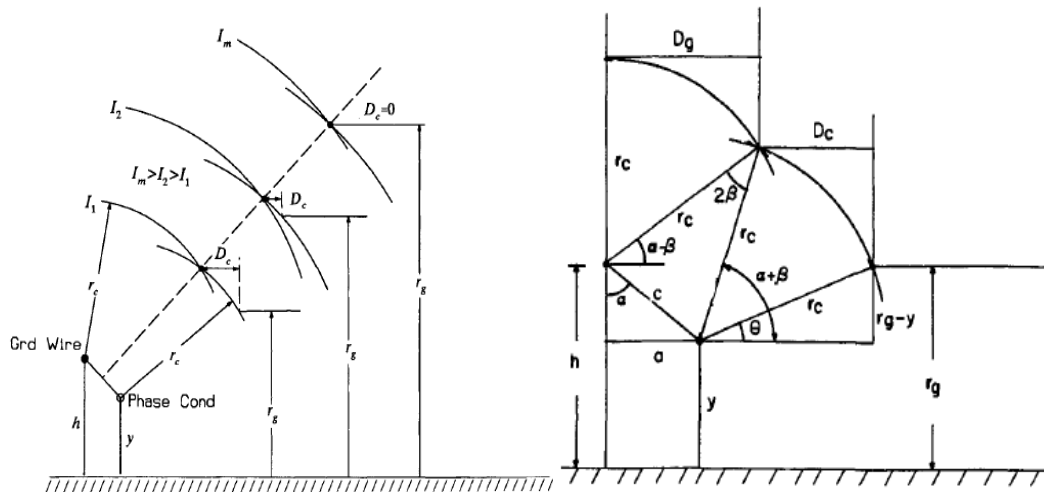


Figure 2 Definition of I_m and expanded view

Figure 2 presents that as the current amplitude of lightning increase, r_c and r_g increase and the distance D_c decrease, thus there exists a maximum value of current (I_{max}) where D_c can reach zero. Therefore, the lightning having higher current amplitude than I_{max} will always strike on the shielding wire or ground, and shielding failure is no more possible.

According to the procedure defined in [5], to calculate I_m which is the input parameter for simulation of shielding failure cases on ATP, first of all r_{gm} , the limited shielding distance between shielding wire and ground, is calculated.

$$r_{gm} = \frac{h+y}{2k_0} \left[1 + \sqrt{1 - k_0 \left[1 + \left(\frac{a}{h+y} \right)^2 \right]} \right] \quad (1)$$

where,

$$k_0 = 1 - \gamma^2 \sin^2 \alpha$$

$$\gamma = \frac{r_c}{r_g} = \left(\frac{y}{h} \right)^{0.6}$$

The maximum shielding failure current is calculated according to;

$$I_m = \left[\frac{r_{gm}}{0.67 \times h^{0.6}} \right]^{\frac{1}{0.74}} \quad (2)$$

In the situation modeled at this thesis study, the height of the shielding wire from ground (h) is 44.5 m, whereas phase conductor (y) is 36.40 m as shown in Figure 6. The third input parameter α which is the angel between the shielding wire and phase conductor can be seen as 20° also in Figure 6. The calculated values for these inputs are;

$$a = 2.9 \text{ m}$$

$$\gamma = 0.886$$

$$k_0 = 0.91$$

$$r_{gm} = 57.6 \text{ m}$$

$$I_m = 18.9 \text{ kA}$$

The calculated current value of I_m means that probability of lightning strike to the phase conductor with amplitude greater than 18.9 kA is zero. Therefore, in order to be at the pessimistic side and analyze the worst case scenarios, the lightning stroke is modeled with the current value of 19 kA.

2.2.2. Back Flashover Failure

Back flashovers occur when a lightning stroke with higher amplitude strikes to the tower or shielding wire. If the lightning strike current is high enough, lightning stroke is transferred from tower or shielding wire to the phase conductor. This transferred waveform creates a steeper waveform than direct strokes. This situation is called as a back flashover. Since the current amplitude is different from direct strokes and has different characteristics, back flashover lightning stroke is modeled separately from lightning stroke at the shielding failure. In addition, the parameters of related model for back flashovers are calculated.

In back flashover phenomena, ground flash density, limit distance, exposed width, probability of lightning current amplitude and acceptable failure rate terms appear and all of these factors should be calculated or defined. These factors are investigated in detail in following sections.

i. Ground Flash Density

The first parameter is ground flash density (N_g) which is related to the location of the substation. The most of the lightning flashes do not reach the ground; they are between clouds [15]. The flashes reaching the ground are recorded by CIGRE counters which are located in most of European countries. This system is used to obtain the ground flash density. Therefore, it is possible to establish a correlation between ground flash density and number of thunderstorm days. Reference [5] proposed an equation for this correlation which is given below;

$$N_g = k \times T_d^a \quad (3)$$

where k and a are constants and T_d is the number of the thunderstorm days per year which is called as the keraunic level. For k and a , different values are

proposed for countries by the researchers. One of these values recommended is from Eriksson [12]. In this recommendation, k and a are 0.04 and 1.25, respectively. This equation, shown below, is accepted also by CIGRE and IEEE.

$$N_g = 0.04 \times T_d^{1.25} \tag{4}$$

The annual registration of thunderstorm day (T_d) comes from the map of annual frequency of thunderstorm days in the world which is given from World Meteorological Organization [6] in Figure 3. The keraunic level map of Turkey is also given in Figure 4 [14].

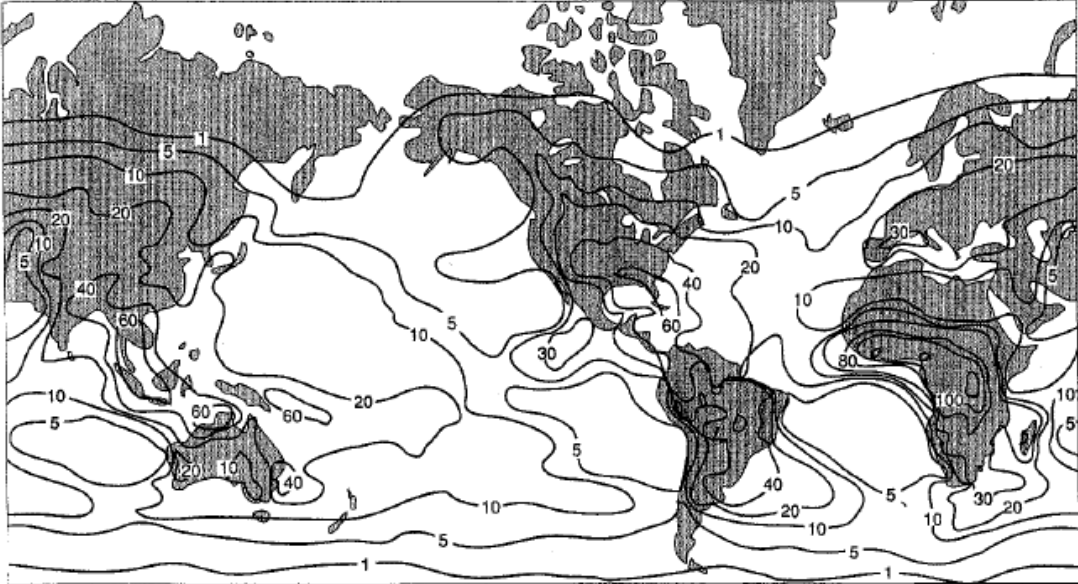


Figure 3 The annual frequency of thunderstorm days in the world

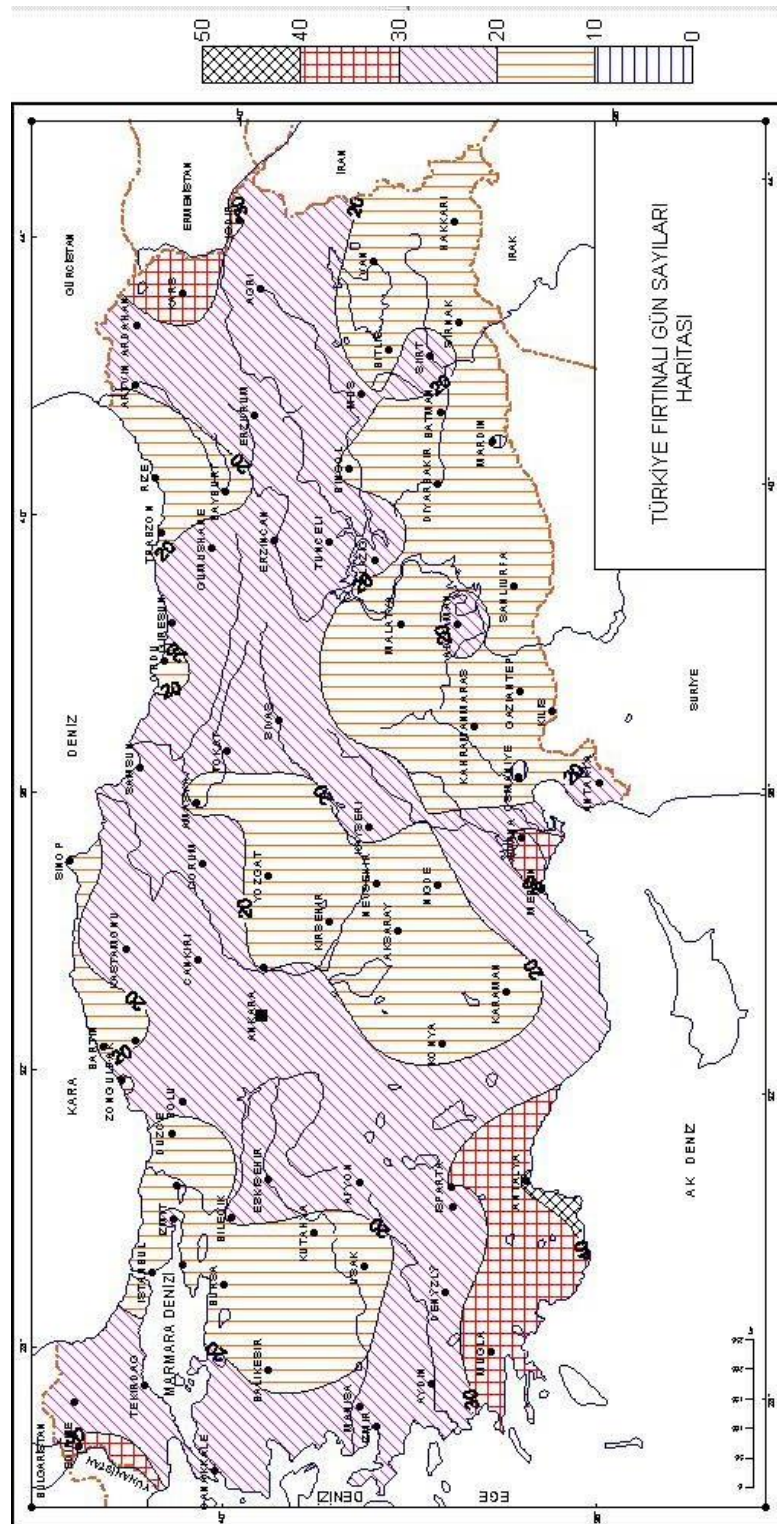


Figure 4 Turkey keraunic level map

As followed from Figure 4, at most parts of Turkey, the number of thunderstorm days (T_d) is between 10 and 30. However, it is possible to see that for certain locations, keraunic level is higher than 30. In order to be at safe side and analyze worst cases, the keraunic level, the number of thunderstorm days is determined as 40. According to this keraunic level of 40, ground flash density (N_g) is calculated as 4.024 flashes per km^2 per year.

ii. Limit Distance

The second factor is the limit distance (X_p) which is the critical distance between lightning stroke along the transmission line and entrance of the substation. The limit distance is the distance from the substation along the line which has been taken into account, to calculate the number of the lightning struck. Beyond this point, the stroke will not cause higher voltages. The limit distance is the length of the line in front of the substation in which all lightning events have to be considered. The lightning strokes only hitting this portion of line can produce dangerous overvoltages into the substation. The overvoltages generated outside of this limit distance have a reduced steepness. Therefore, the overvoltages are not dangerous for the equipment, irrespective of the surge amplitude.

According to [2], limit distance has to have a minimum value in order to correctly analyze. At the close tower to the substation, back flashover does not occur because of the low footing impedance due to connection to substation earthing. In addition, this prevents the interference between the reflection from the substation and the lightning. In [2], the limit distance for back flashover is defined as 2 towers. According to this information, for the modeled and analyzed case in this thesis study, the total distance between possible lightning strike point and substation which describes the limit distance (X_p) is 500 m.

iii. Exposed Width

The third factor in back flashover phenomena is exposed with (W) which should take into account the lateral strike distance (r_c). Lateral strike distance (r_c) is a point from there outward, the lightning would strike to ground rather than the shield wire, and from that distance inward (toward center of line) the lightning will strike shield wire rather than ground. Lateral strike distance (r_c) can be calculated according to the formula from CIGRE [15];

$$r_c = 0.67 \times H_T^{0.6} \times I^{0.74} \quad (5)$$

where H_T is the average height of shield wire close to substation and I is the critical stroke current. The average tower height (H_T) is specified as 30 m and the critical stroke current is accepted as 185 kA in order to satisfy the acceptable failure rates which are defined in [2] as in the range of 0.001/year up to 0.004/year, that means a value between 250 years to 1000 years are taken into account. r_c is calculated as 291.75 m. The exposed width (W) can be calculated related with the r_c according to the formula;

$$W = B + 2r_c \quad (6)$$

B is the distance between two shield wires and it is 9.49 m at model used as shown in Figure 6. Therefore the calculated exposed width (W) is 593m.

iv. Probability of Lightning Current Amplitude

The fourth term is the lightning current amplitude probability $P(I_f)$. Probability that random variable current amplitude will take on a value higher than I_f is;

$$P(I_f) = 1 - \int_0^{I_f} f(x) dx \text{ with } f(x) = \frac{1}{\sqrt{2\pi}\beta x} \exp\left(-\frac{1}{2} \times \left[\frac{\ln(x/M)}{\beta}\right]^2\right) \quad (7)$$

where M is the median parameter and β is the slope parameter as defined in CIGRE [15]. According to CIGRE [15], for back flashover case with current amplitude higher 20 kA, it is proposed that M and β have constant values as 33.33 and 0.605, respectively. According to Equation 7, the probability ($f(x)$) of the stroke, lower than or equal to I_f which is determined as 185 kA is 99.769%. Therefore, probability that a random variable current amplitude will take on a value higher than and equal to I_f is 0.00231.

v. Acceptable Failure Rate

The last term is the acceptable failure rate (R_a) which as explained above, is defined between 250 and 1000 years in [2]. According to this acceptable failure rate (R_a), the amplitude of the lightning strike current is determined.

A summarized equation representing the relationship between acceptable rate (R_a) and probability that the peak current in any stroke will exceed I_f ($P(I_f)$) is given below;

$$R_a = F \times P(I_f) \times n \quad (8)$$

where n is the number of the connected feeder.

In order to get the acceptable failure rate, the number of flashes to exposed area to lightning stroke per year per feeder (F) should be calculated which is;

$$F = N_g \times X_p \times W \times 10^{-6} \quad (9)$$

According to calculated N_g , X_p and W values 4.024, 500 m and 593 m, respectively, above the number of flashes to exposed area to lightning stroke per year per feeder (F) is derived as 1.193 flashes per year per feeder.

As seen from Equation 8, acceptable failure rate (R_a) is a function of the number of line connected to the substation (n). As a worst case situation, the number of line connected can be assumed as only one. This increases the failure rate probability. With the one line connection assumption, acceptable failure rate (R_a) is get as 0.00275 per year which means a failure probability in 363 years. This calculated R_a value is line with the [2] that require a probability between 250 and 1000 years. Therefore, the defined critical stroke current 185 kA is proper for the back flashover strike model.

When the statistics are observed, it is discovered that only a small portion of lightning strikes, only about 1%, has current amplitude higher than 200 kA according to CIGRE [15]. This shows that the calculated current amplitude 185 kA at the modeled back flashover case is in accordance with the statistics and literature.

2.3. Overhead Line Model

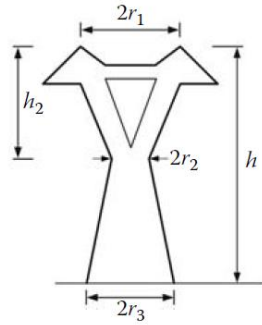
Overhead line (OHL) model consists of tower model, footing resistance model, phase conductor and shielding wire model and insulator model.

Tower models based on constant-parameter circuit representation are classified into three groups; single vertical lossless line, multi-conductor vertical line or multistory model, according to [7]. The single vertical lossless line models were developed by using electromagnetic field theory, and they are based on simple geometric forms like cylindrical and conical shapes of the tower and a vertical stroke to the tower top assumptions. In multi-conductor vertical line model, a multi-conductor vertical line shows each segment of the tower between crossarms separately, and then it is concluded as a single conductor. In the multistory model,

tower is represented with four sections, which consists of a lossless line in series with a parallel R–L circuit.

The tower arrangement used in this thesis study is shown in Figure 6. This is a typical tower arrangement for 954 MCM Cardinal Conductor in 420 kV THVES. This tower arrangement specified in this thesis corresponds to the waist type in the single vertical lossless line models which are described in [7]. According to [19] and [23], tower simulation model does not affect significantly the computed overvoltages, especially with increasing tower grounding resistance and thus, single vertical lossless line models are considered as satisfactory for simulating transmission line towers, due to their simplicity, in insulation coordination studies of substations. The type and related expressions are as the following;

Waist



$$Z = \sqrt{\frac{\pi}{4}} 60 \cdot \left(\ln \left(\cot \frac{\tan^{-1}(r/h)}{2} \right) - \ln \sqrt{2} \right)$$

$$r = \frac{r_1 h_2 + r_2 h + r_3 h_1}{h} \quad (h = h_1 + h_2)$$

$$t = \frac{h}{0.85 \cdot c}$$

Figure 5 Waist type in tower and equations

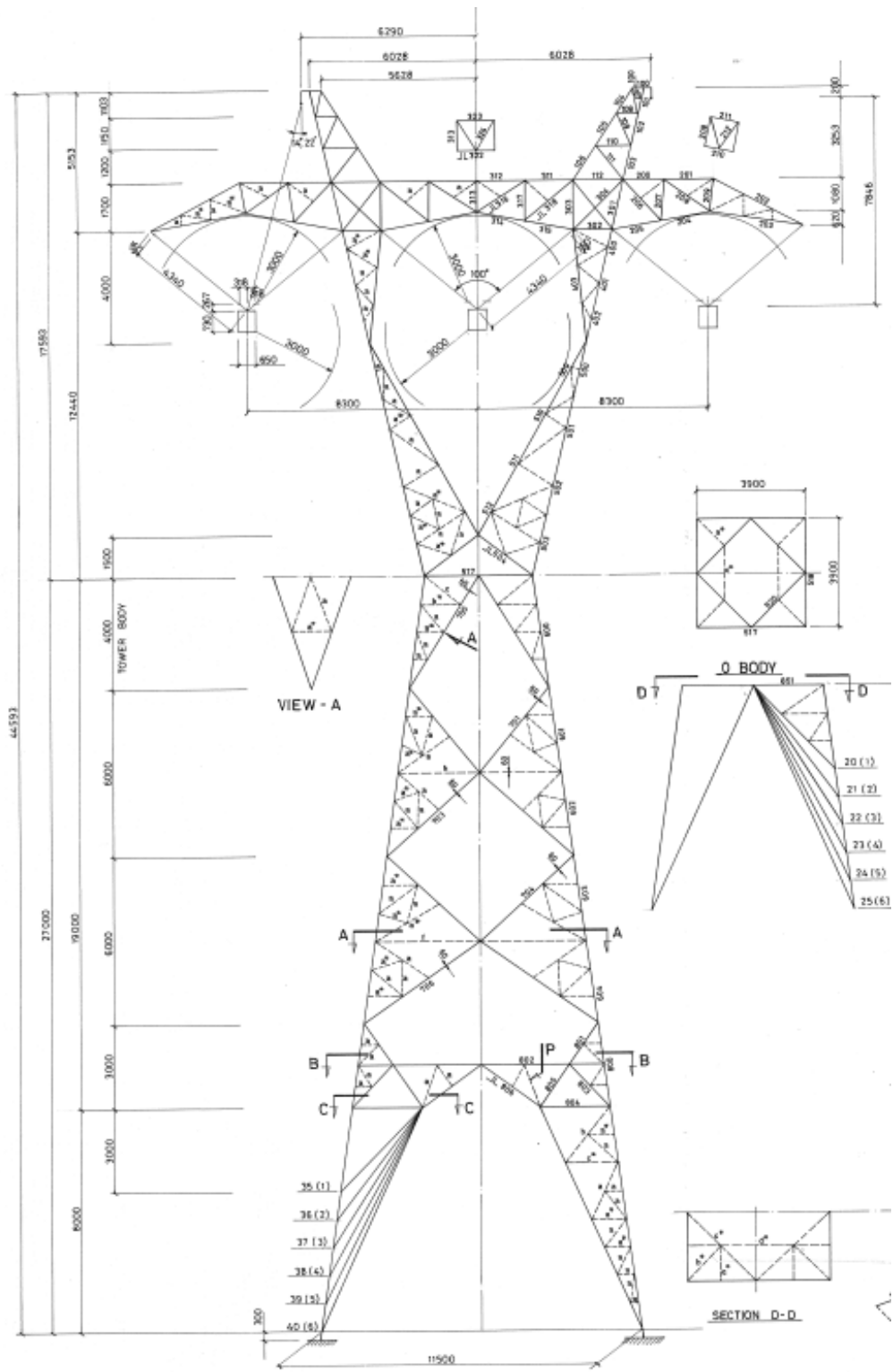


Figure 6 Standard 420 kV tower arrangement

According to Figure 6, the input parameters for calculating the surge impedance of the tower are;

Tower top radius	r_1	4.75 m
Tower waist radius	r_2	1.95 m
Tower base radius	r_3	5.6 m
Height from base to waist	h_1	27.00 m
Height from waist to top	h_2	17.50 m
Tower height	$h_1 + h_2$	44.50 m

The surge impedance of the tower (Z_t) is calculated as 115.52 ohms with the average radius (r) of 7.21 m. The value utilized in this thesis study, 115.52 ohms, is in accordance with the typical values range from 100 to 300 ohms [4].

The second model in the OHL is the tower footing resistance which is one of the primary parameters that affect the back flashover rate [8]. It is also an important parameter for the limitation of fast-front overvoltage occurrences as described in [2]. According to [5], there are three types of models for tower footing resistance; simplified, ionization and HF-model. Simplified model propose a resistance and inductance, parallel with capacitance or only a resistance. Ionization model considers the ionization during the lightning current which result in a non-linear resistor at the earth connection. In HF-model, each earthing network segment is represented as a propagation element.

As described in CIGRE [15], ground resistivity decreases with the current flowing because of the ionization of the earth by current. By taking into account this explanation, two types are used for the tower footing resistance model in this thesis. The tower footing resistances except for the tower that lightning struck are modeled according to the simplified model by a single resistance with 10 ohms which is typical value in THVES and satisfy the pessimistic view in order to

analyze worst case [21], [26]. However, for the tower that lightning struck to have ionization footing resistance model in order to take into account the ionization effect of the lightning current [17]. In this model, tower footing resistance decreases with the increase of the current flow through it. CIGRE [15] gives the following equations in order to calculate the tower footing resistance at the different current amplitudes;

$$\begin{aligned}
 R &= R_0, & \text{if } I < I_g \\
 R(I) &= \frac{R_0}{\sqrt{1 + \frac{I}{I_g}}}, & \text{if } I > I_g \\
 & \text{with } I_g = \frac{E_0 \rho}{2\pi R_0^2}
 \end{aligned} \tag{10}$$

where R_0 is the low-current and low-frequency resistance (Ω), I is the lightning current through the footing impedance (A), I_g is the limit current (A), ρ is the soil resistivity ($\Omega \times m$), E_0 is the soil ionization gradient which is recommended in [3] as $400 \text{ kV} \times m^{-1}$.

In this thesis study, recommended soil ionization gradient (E_0) is used. The values accepted in the model for low-frequency resistance and the soil resistivity (ρ) are 10Ω and $100 \Omega \times m$, respectively. According to these values, the limit current (I_g) is calculated as 63.66 kA . According to these input and calculated parameters, ionization model of tower footing resistance obtained is given in Figure 7.

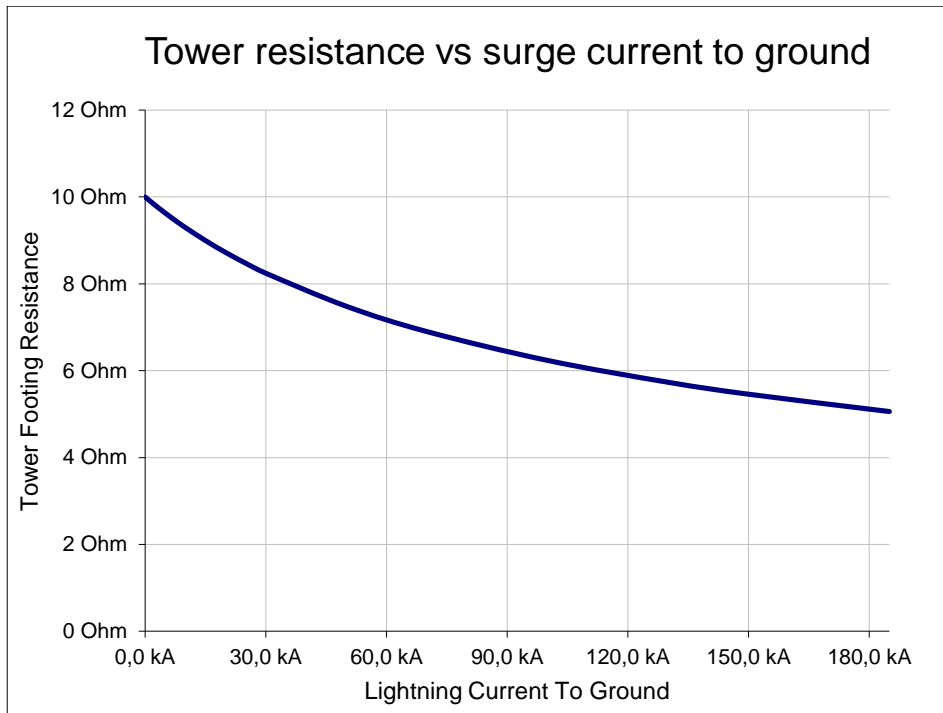


Figure 7 Ionization model of the tower footing resistance

The third parameter related with the OHL model is the surge impedances of the phase conductor and shielding wire. The calculation of related surge impedance and wave velocity is as below [5]:

$$Z_{Surge} = \sqrt{\frac{L}{C}} \quad v = \frac{1}{\sqrt{LC}} \quad (11)$$

where L is the line geometrical inductance (H/km) and C is the line geometrical capacitance (F/km).

The phase conductors at overhead line are modeled as 954 MCM Cardinal, three conductors per phase with 30 cm triangle bundle arrangement. The input parameters for this type conductor are;

- conductor number = 3
- conductor diameter = 0.0170 m
- bundle space = 0.30 m

According to these inputs, L is obtained as 0.0012 H/km and C is get as 9.63×10^{-9} F/km. Surge impedance of the phase conductor is calculated (Z_{surge}) as 352 ohm and wave velocity (ϑ) is calculated as 294000 km/s. These calculated values are used in the model in this thesis study.

For the shield wires, the calculations are also performed according to the CIGRE [15] equations. The result is obtained as 340 ohms for equivalent surge impedance of the shielding wire.

Line insulators are the fourth term of the OHL modeling. There are different options for the insulator modeling [4]. One is related with the critical flashover voltage that is the impulse voltage level at which the probability of flashover of the insulator is 50%. The other is the leader propagation model which is based on that the leader propagation stops if the gradient in the un-bridged part of the gap falls below E_{10} which is the critical leader inception gradient. The other one is the voltage-time curve flashover model. According to the voltage-time curve flashover model, flashover voltage is as following;

$$V_{fo} = K_1 \times \frac{K_2}{t^{0,75}} \quad (12)$$

where K_1 and K_2 are 400 and 710 times of the air gap length (L), respectively and τ is the elapsed time after lighting stroke. The used insulator model in this thesis is study based on this equation.

2.4. Lightning (Surge) Arrester Model

Since the goal of installing lightning arresters is to provide protection at high voltages, it should conduct no or little current at normal operation voltages and conduct current at overvoltages in order to prevent a fault due to high voltages, as defined in [11]. Hence, the lightning arrester model should have a nonlinear voltage versus current characteristics. This nonlinear characteristic is provided by silicon-carbide (SiC) material with series connected spark gaps previously. Spark gaps cause high impedance and no current conduction. After the spark over of the spark gaps, silicon carbide material provides current flow. However, nowadays metal oxide (MO) material that inherently provides nonlinear characteristic is used at lightning arresters. In this type, number of metal oxide discs determines the voltage rating and the diameter and parallel columns of the discs define the energy ratings of the MO lightning arresters.

The types of models for surge arresters can be classified in three groups; non-linear resistance model, frequency dependent model, simplified frequency dependent model. Non-linear resistance model is frequency-independent and this model is appropriate for low frequency transients and slow front transients according to [11]. As it is described in [18], for fast front transient studies, although temperature dependent V-I characteristic is negligible; frequency dependent V-I characteristic, MOV block inductance and ground lead inductance is important. These requirements refer to the frequency dependent models. Although different types of frequency dependent models are proposed, IEEE working group [4] compose a complete model. The frequency-dependent arrester model proposed by IEEE WG takes into account its dynamic behavior. This model is shown in Figure 8.

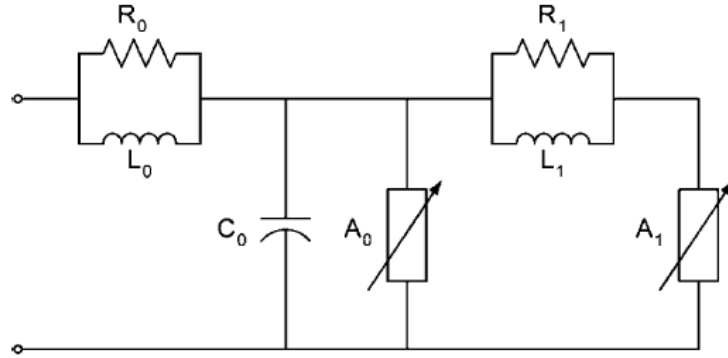


Figure 8 IEEE Working Group MO surge arrester model for fast front surges

Non-linear resistor provides the requirements of the voltage versus current characteristic; inductor gives the frequency dependent behavior, as seen from Figure 8. Resistor R_1 and inductor L_1 form a lowpass filter.

The values of these parameters are calculated according to the formulas as given below;

$$L_0 = 0.2 \times \frac{d}{n} \quad R_0 = 100 \times \frac{d}{n} \quad (13)$$

$$L_1 = 15 \times \frac{d}{n} \quad R_1 = 65 \times \frac{d}{n}$$

$$C = 100 \times \frac{n}{d} \text{ (pF)}$$

where d is the height of the arrester in meter, n is the number of parallel columns of MO disks, V_{20} is the discharge voltage for a 10 kA, 8/20 μ s current in kilovolts, V_{ss} is the switching surge discharge voltage for an associated switching surge current in kilovolts.

These formulas give the linear parameter values. IEEE Working Group proposes a procedure for other parameters. This procedure is as following;

- 1) Determine linear parameters from the previously given formulas, and derive the nonlinear characteristics of A_0 and A_1 .

- 2) Adjust and match the switching surge discharge voltage for current with a time-to-crest of about 45 s.
- 3) Adjust the value of L_1 to match the V_{10} voltages.

Also a simplified frequency model is valid for fast front over voltage studies. This type model is seen from Figure 9. In this type, series linear resistors are eliminated. Since the importance of the capacitance C in IEEE model is negligible according to [11]; it is also reduced in this model.

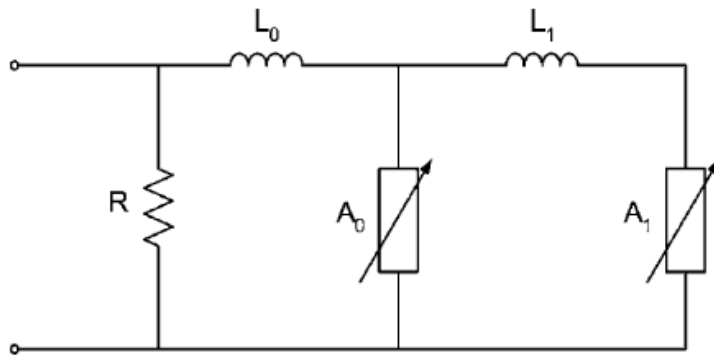


Figure 9 Simplified Lightning Arrester Model

2.5. Substation Equipment Models

Substation equipment is modeled according to the [4]. As known, substations consist of several equipment; such as transformer, the most expensive equipment which should be well protected, circuit breaker, disconnector switch, current transformer, voltage transformer, surge arrester, bus support insulator, conductor and etc. Disconnector, circuit breaker, instrument transformers, and bus support insulator can be modeled with their stray capacitances to ground according to [4] and [16]. The reference values in [4] are demonstrated in Figure 10. These values are minimum capacitance values used in lightning studies that provide pessimistic assumption. These values are also accepted by IEC [3].

It is proposed that power transformer can be represented by its stray capacitances to earth [3]. The value simulated for power transformer is 3000 pF which is in accordance with the values in [3] and [4].

Equipment	Capactiance-to-Ground		
	115 kV	400 kV	765 kV
Disconnecter Switch	100 pF	200 pF	160 pF
Circuit Breaker (Dead Tank)	100 pF	150 pF	600 pF
Bus Support Insulator	80 pF	120 pF	150 pF
Capacitive Potential Transformer	8000 pF	5000 pF	4000 pF
Magnetic Potential Transformer	500 pF	550 pF	600 pF
Current Transformer	250 pF	680 pF	800 pF
Autotransformer*	3500 pF	2700 pF	5000 pF

* Capacitance also depends on MVA.

Figure 10 Typical capacitance to ground values for substation equipment [4]

In addition, it is possible to model some of equipment which are close to each other (3 and 5 m) with group capacitances [4]. For the conductor used in the substation, the same values calculated at overhead line model are considered.

2.6. Substation Model

Busbar type of the substation is designed according to the importance of the substation. This means that effects of energy interruption versus capital expenditure of the substation. A substation where energy interruption is less important and capital expenditure cost should be low is designed as simple type. However, in some substations, energy availability is so critical that more expensive but more reliable busbar type is designed. The main busbar types of substations are;

- Single Main Busbar,
- Single Main Busbar with Transfer Busbar,
- Double Main Busbar,
- Double Main Busbar with Transfer Busbar,
- Ring Busbar.

Since this study is focused on THVES and double main busbar with transfer busbar is the most common type, the busbar type of the substation used in this thesis study is accepted as double main busbar with transfer busbar. The important advantage of the double main busbar with transfer busbar is the isolation of feeders for the repair and maintenance. Since this system makes flexibility possible, energy availability rate is increased. The double main busbar with transfer busbar provides more reliable system so it is preferred more than the others.

The single line diagram of the feeders modeled in this study is shown in Figure 11. This figure demonstrates the typical 420 kV single line diagram consisting of line feeder, transformer feeder and coupling-transfer feeder. It is obvious that although substations are designed according to double main busbar with transfer busbar type, the arrangement can be changed upon the substation area and direction of the lines and transformers in order to fit the site and connect to OHL with lower investment. Substations can have more than one feeder for lines and transformers, but only one transformer, one line feeder and one coupling-transformer feeder is modeled. Although it has more feeders, it is assumed that the other feeders are out of service in order to analyze the worst possible condition. Therefore, the lightning waveform is not divided and proceeds from the line feeder to the transformer feeder.

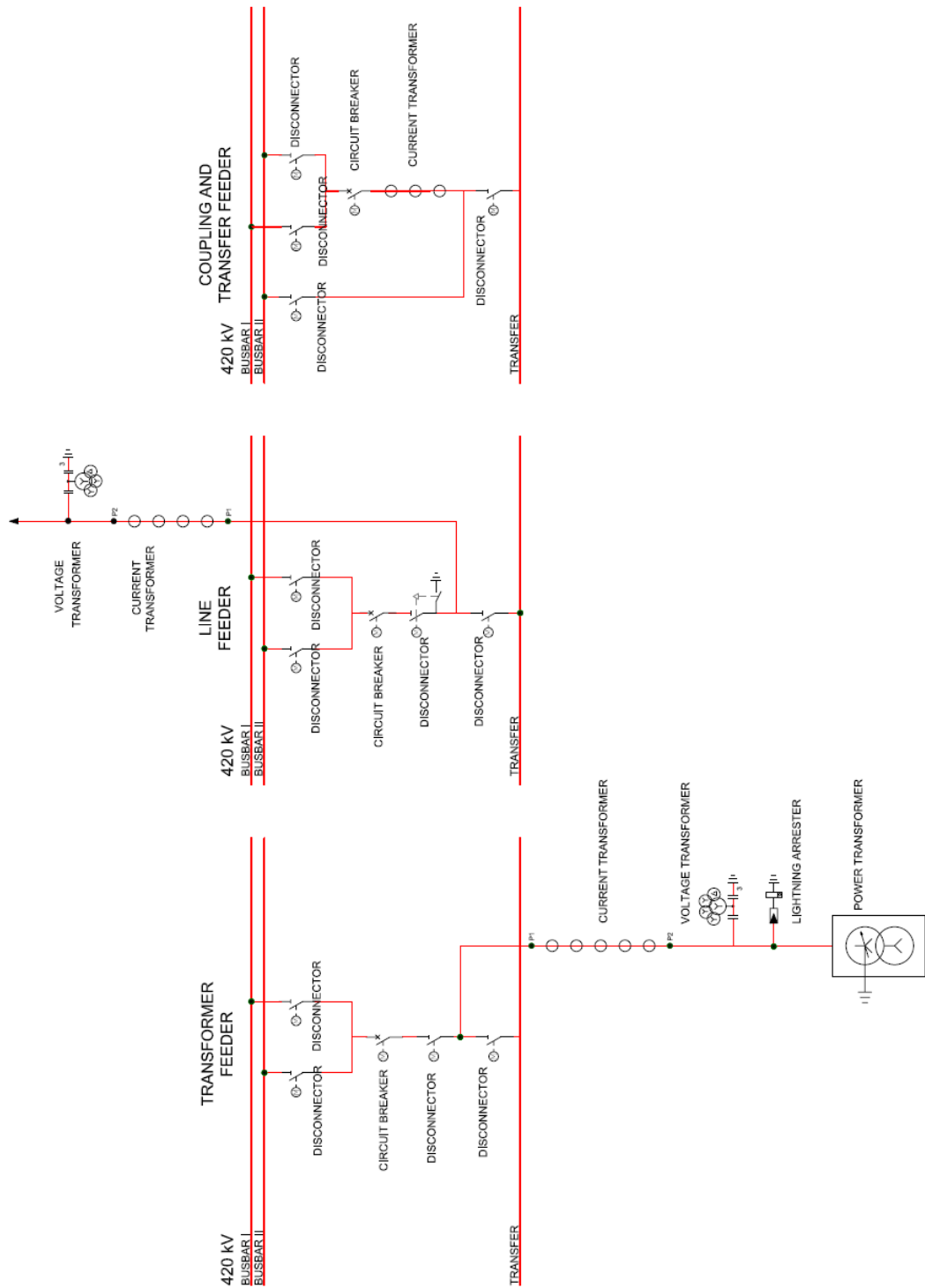


Figure 11 Typical single line diagrams of 420 kV substation double busbar with transfer busbar for transformer feeder, line feeder and coupling and transfer feeder

Figure 12 shows the typical general layout drawing of the line feeder of 420 kV substations with double busbar system with transfer busbar. This is the top view of the substation and equipment. Pantograph type disconnectors are used in this substation configuration. As seen from the figure, the line entrance is from right hand side. At the end of the bay, there are voltage transformer and lightning arrester. After this equipment, line is connected directly to the upper line, and then there is a connection between the upper line and current transformer. After that, the line is connected to the busbars via pantograph type disconnectors.

The typical general layout of the bus coupler-transfer feeder and transformer feeder of 420 kV substations are shown in Figure 13 and Figure 14, respectively. As seen from the figures, since the transformer is located at the left end side of the transformer bay, there is no need for the upper line. Transformer is connected directly to the transformer bay through the lightning arrester and voltage transformer at the transfer busbar side.

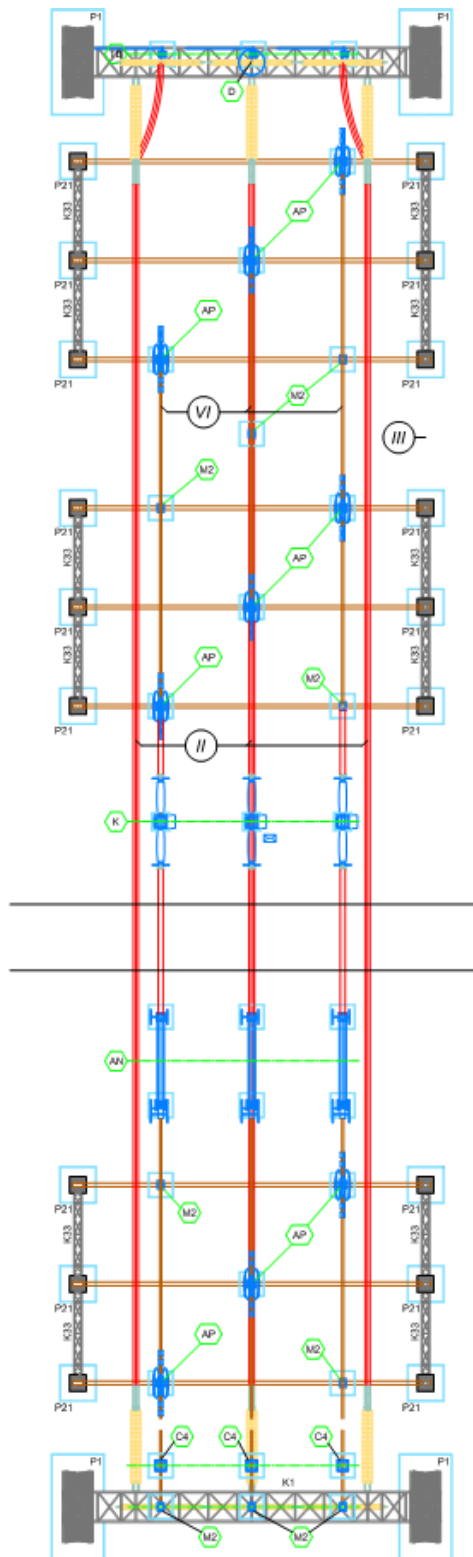


Figure 12 Typical general layout of line feeder

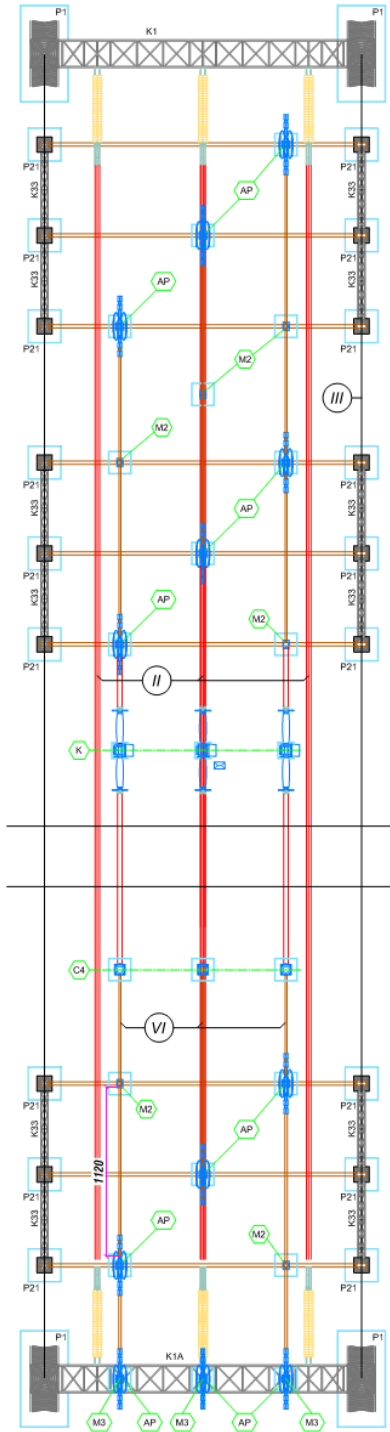


Figure 13 Typical general layout of the bus coupler and transfer feeder

2.7. Complete Simulation Models

At the previous parts of this chapter, the sections introduce the lightning strike model, overhead line model, lightning arrester model, substation equipment model and substation model. These models are connected to compose the complete simulation models. The complete models where simulations performed on are presented in this section.

As explained in previous parts, two different models are developed in the scope of this thesis study; the shielding failure model and the back flashover failure model. The model used on the shielding failure analyses is given in Figure 15. The parameters of shielding failure which are calculated at the previous parts are used at this model. The signed lightning arrester model is not fixed for the defined different cases. The model implemented for the back flashover failure analyses is in Figure 16. The parameters of back flashover failure used at this model are calculated at the previous sections. The signed lightning arrester model with red circular is not fixed for all cases. These models, presented in Figure 15 and Figure 16, are base models whose parameters and configurations will be changed for different simulation cases.

In both shielding failure and back flashover failure models, the corona effect, which is an important factor reducing the steepness of the incoming surge as described in [4], is neglected in this thesis study in order to analyze the worst case scenarios. In addition, since the lightning strike locations are close to the substation and the path, that surge propagates through, is short in simulations of this thesis, the effect of corona is very limited [13].

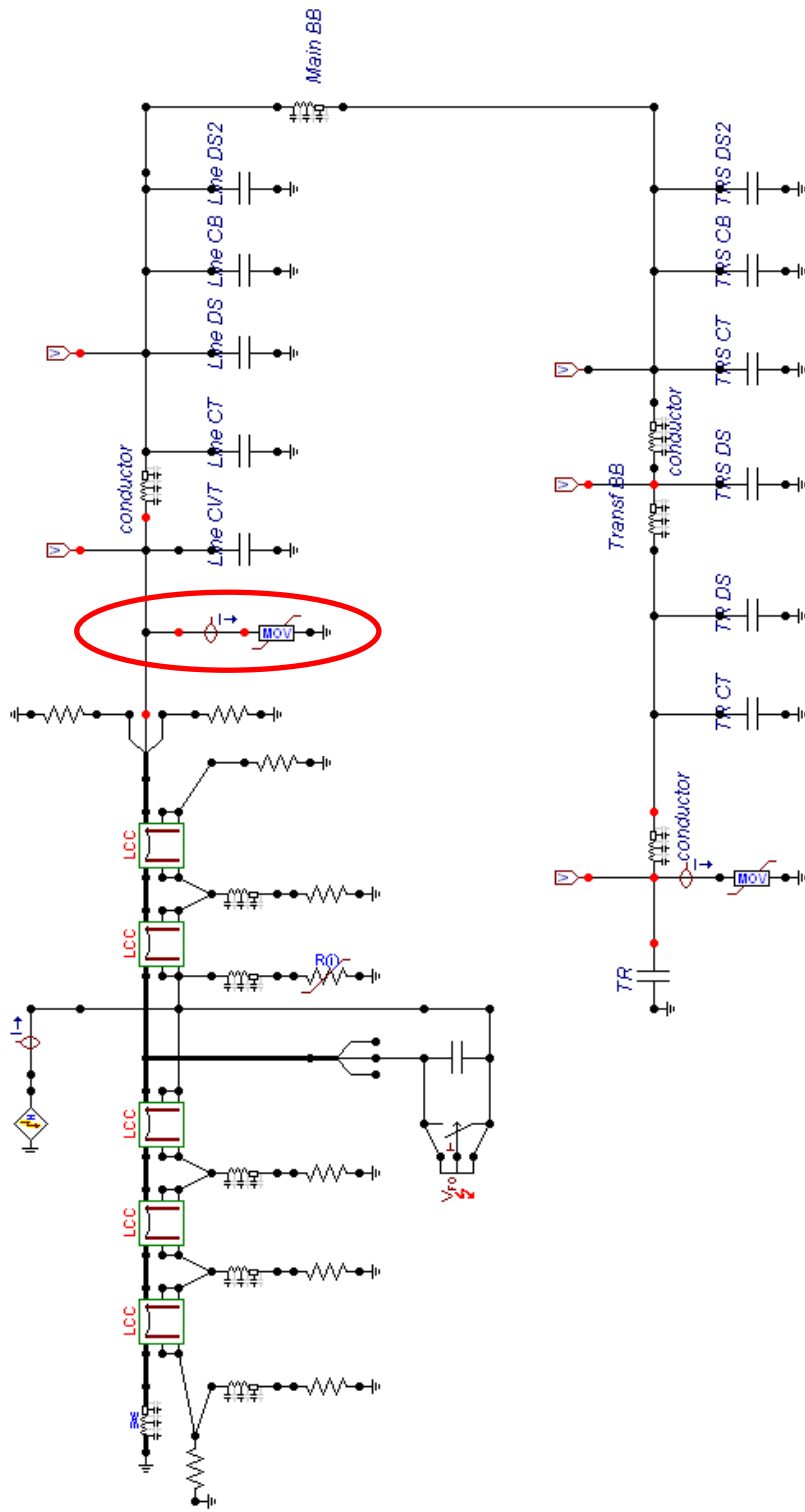


Figure 16 Back flashover failure model on ATP

CHAPTER 3

SIMULATIONS AND RESULTS

3.1. Introduction

After digital electromagnetic transients programs became available in the late 1960's and early 1970's for mainframe computers, and later for personal computers, it is possible to make transient analysis on computers [20]. The analyses in this thesis study are performed on the ATP for both shielding failure and back flashover failure. The cases are determined in order to analyze the possible situations and observe the worst case scenarios. In this scope, 32 different cases are determined. In order to obtain the effect of changes obviously, the cases are classified in groups with four situations. In each case, a variable parameter has been changed and the results are observed. For these 32 cases, defined variable parameters are as follows;

- Failure Type
- Connection Type
- Lightning Arrester Location
- Current Amplitude
- Connection Length
- Lightning Stroke Location

In the analyses, as explained in the modeling chapter, two types of failure are evaluated. These are back flashover failure and shielding failure. For lightning arrester location, in only four cases, lightning arresters are located only at front of

the power transformer; in other cases they exist both at front of the power transformer and at the line entrance. Connection type refers that the line feeder is connected to the transformer feeder directly or through transfer feeder. The lightning stroke current amplitude is defined as variable parameter and it is increased to the higher values from the calculated ones. Therefore, both worst case scenarios are performed and possible modeling errors are eliminated. Connection length refers to the busbar length between the line feeder and transformer feeder. This length is increased and also decreased in order to see the effects. The last variable parameter is lightning stroke location. In the standard cases, location of lightning stroke is used as defined in [2], second closest tower to the substation for back flashover failure and closest tower to the substation for shielding failure. These cases and the obtained results are explained below. In the analyses, lightning impulse withstand voltage levels of the equipment and power transformer have been reviewed separately.

3.2. Effect of the Location of Lightning Arresters for Main Busbar Connection Type

The details of Cases 1, 2, 3 and 4 are given at Table 2. In the analyses classified in Group 1, the main objective is to investigate the effect of the lightning arrester at the line entrance when line feeder is connected to transformer feeder through the main busbar. For that purpose, four different cases are analyzed.

Table 2 Group 1 Cases

CASES	Failure Type	LA Location	Connection Type	Current Amplitude	Connection Length	Lightning Location
1	BFO	<i>TR</i>	Main Busbar	185 kA	Medium	2. Tower
2	BFO	<i>TR + LE</i>	Main Busbar	185 kA	Medium	2. Tower
3	SF	<i>TR</i>	Main Busbar	19 kA	Medium	1. Tower
4	SF	<i>TR + LE</i>	Main Busbar	19 kA	Medium	1. Tower

The back flashover failure type is performed with existing lightning arrester only at the front of the power transformer in Case 1 and existing lightning arrester both at the front of the power transformer and at the line entrance in Case 2. In Cases 3 and 4, shielding failures are analyzed. There are lightning arresters only at the front of the power transformer in Case 3, but both at the front of the power transformer and at the line entrance in Case 4. In these four cases, it is assumed that the energized one line feeder and one transformer feeder are connected through main busbar. In other words, the line feeder is connected to one of the main busbars and the transformer feeder is also connected to the same busbar. For the lightning current amplitudes, the calculated values in the previous chapter are used for both back flashover and shielding failure, which are 185 kA and 19 kA, respectively. As seen, connection length is defined as “medium” which refers to the assumption of 3 bays between the line bay and transformer bay. In the analyses, lightning location is the second tower for back flashover failure and the first tower for shielding failure as defined at the modeling phase. The model and the remaining determined parameters are kept the same.

The resultant waveforms obtained for Case 1 are shown in Figure 17. As it follows from the figure, in Case 1, the highest voltage at the equipment is 1085 kV. The transformer is exposed to a peak voltage of 893 kV. Case 2 result graph is demonstrated in Figure 18. As it can be seen from the figure, in Case 2, the highest voltage at the equipment is 1000 kV. The transformer is exposed to a peak voltage of 863 kV.

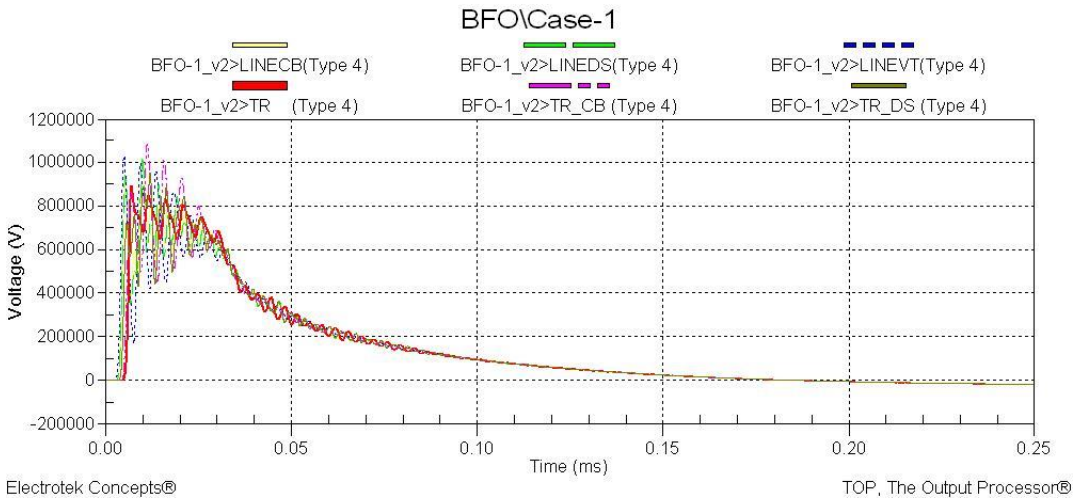


Figure 17 Resultant voltage waveforms for Case 1

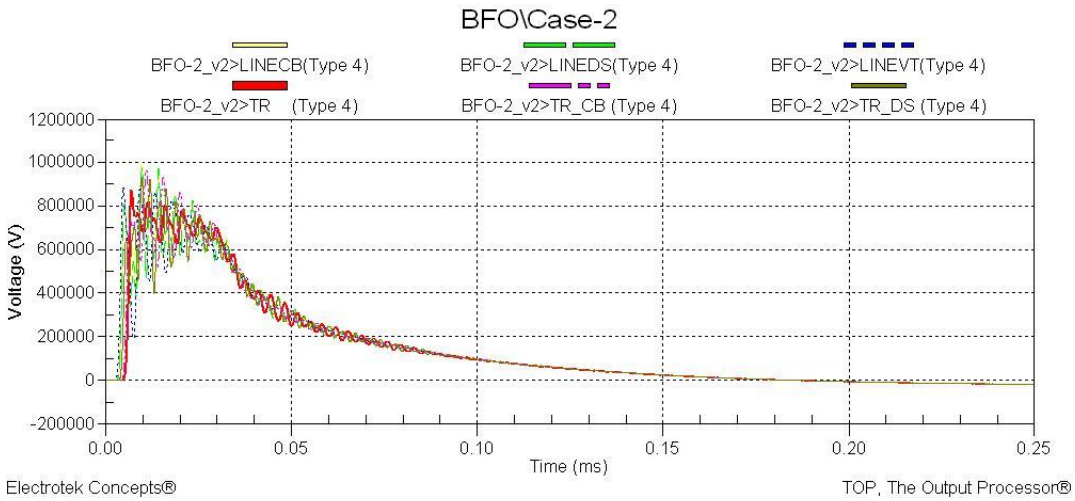


Figure 18 Resultant voltage waveforms for Case 2

The result obtained for Case 3 is shown in Figure 19. As followed from the figure, in Case 3, the highest voltage at the equipment is 1153 kV. The transformer is exposed to a peak voltage of 898 kV. The result of Case 4 is demonstrated in Figure 20. As it can be seen from the figure, in Case 4, the highest voltage is 1055 kV at the equipment and 876 kV at the transformer.

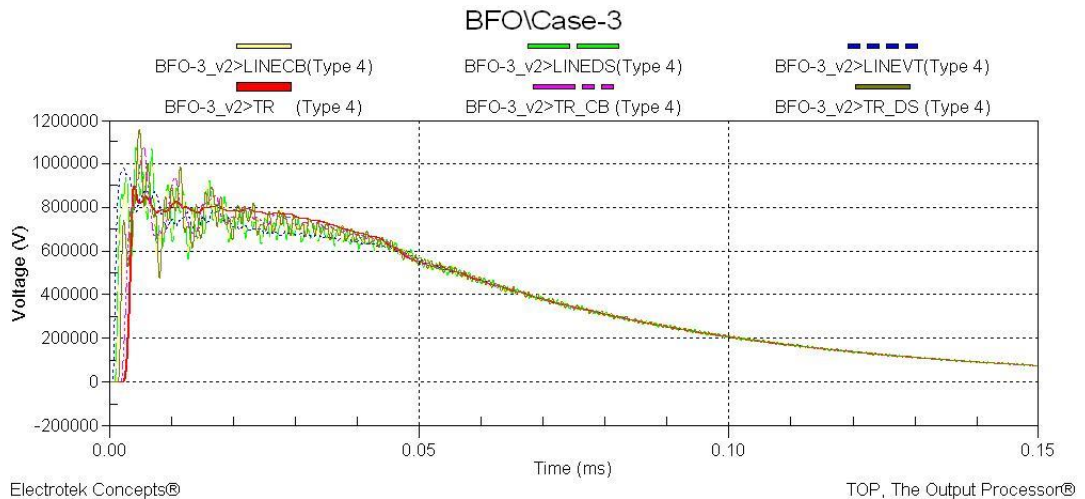


Figure 19 Resultant voltage waveforms for Case 3

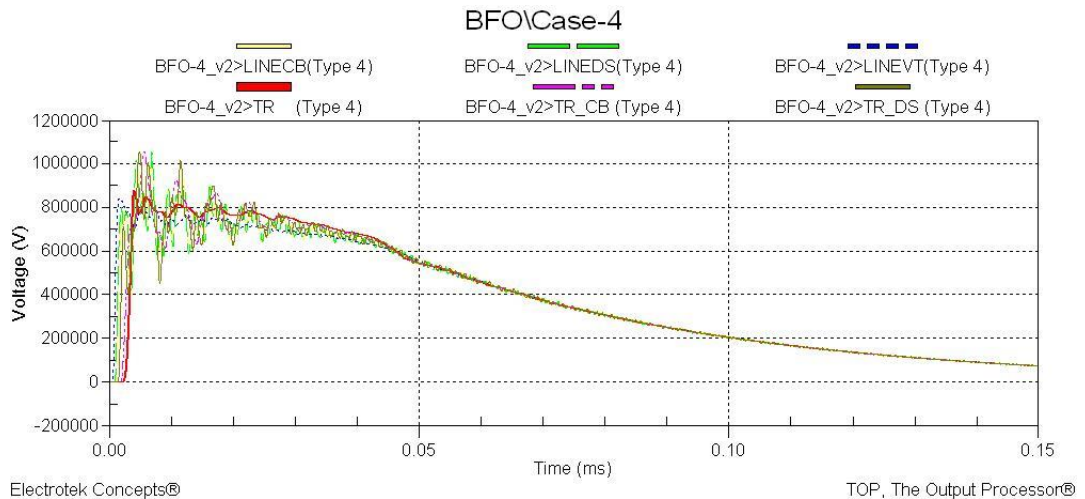


Figure 20 Resultant voltage waveforms for Case 4

3.3. Effect of the Location of Lightning Arresters for Transfer Busbar Connection Type

The details of the analyses for Cases 5, 6, 7 and 8 are shown at Table 3. In these analyses which are classified in Group 2, the main objective is similar with the Group 1. It is to investigate the effect of the lightning arrester at the line entrance when line feeder is connected to transformer feeder through the transfer busbar. In addition, the difference between results of Group 1 and Group 2 due to the connection types, main busbar and transfer busbar, is also evaluated. In order to achieve these aims, four different cases are analyzed.

Table 3 Group 2 Cases

CASES	Failure Type	LA Location	Connection Type	Current Amplitude	Connection Length	Lightning Location
5	BFO	<i>TR</i>	Transfer Busbar	185 kA	Medium	2. Tower
6	BFO	<i>TR + LE</i>	Transfer Busbar	185 kA	Medium	2. Tower
7	SF	<i>TR</i>	Transfer Busbar	19 kA	Medium	1. Tower
8	SF	<i>TR + LE</i>	Transfer Busbar	19 kA	Medium	1. Tower

Group 2 cases are very similar to the ones in Group 1. The only difference is at the connection type. In all four Group 2 cases, the line feeder is connected to the transformer feeder through the transfer feeder. It is assumed that the transformer feeder is transferred to the transfer feeder. In detailed explanation, line feeder is connected to the one of the main busbars, and then main busbar is connected to the transfer busbar via transfer feeder since transformer feeder is transferred. Finally, transfer busbar is connected to the transformer feeder through the transfer disconnector of the transformer feeder. The other situations are the same for Case 5 with Case 1, Case 6 with Case 2, Case 7 with Case 3 and Case 8 with Case 4.

The result observed for Case 5 is shown in Figure 21. As it can be seen from the figure, in Case 5, the highest voltage at the equipment is 1150 kV. The transformer is exposed to a peak voltage of 853 kV. Resultant graph Case 6 is demonstrated in Figure 22. As it follows, in Case 6, the highest voltage is 1075 kV at the equipment and is 850 kV at the transformer.

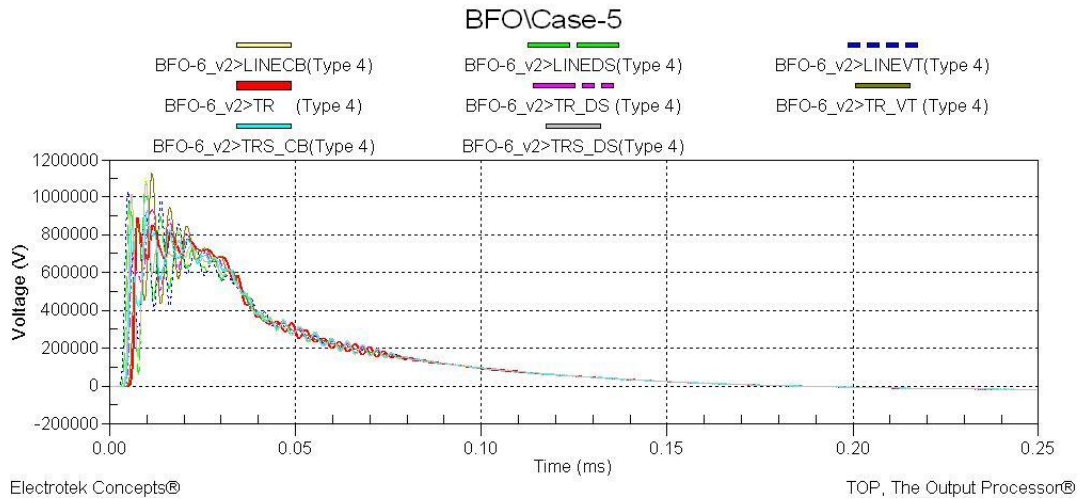


Figure 21 Resultant voltage waveforms for Case 5

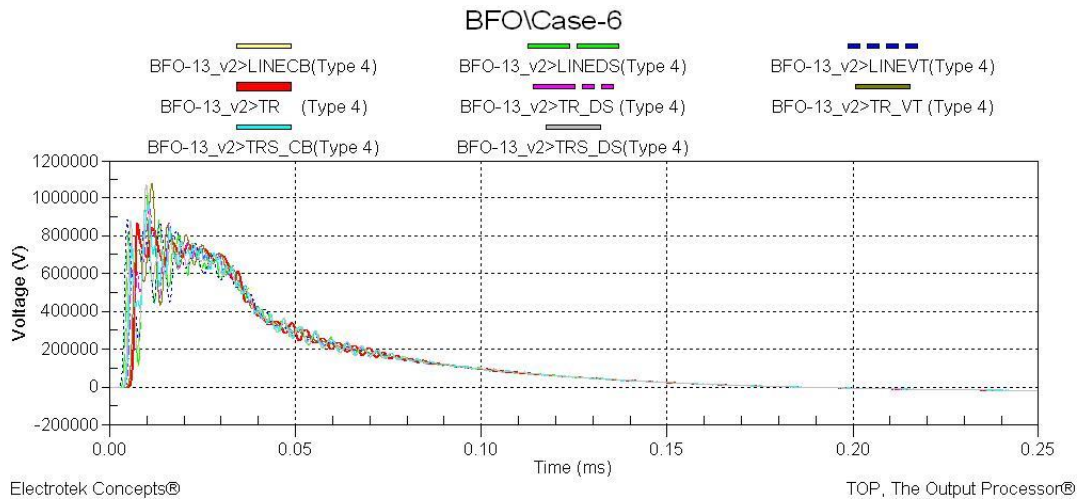


Figure 22 Resultant voltage waveforms for Case 6

The result obtained for Case 7 is shown in Figure 23. As it can be seen from the figure, in Case 7, the highest voltage at the equipment is 1227 kV. The transformer is exposed to a peak voltage of 958 kV. The obtained result for Case 8 is shown in Figure 24. As seen from the figure, in Case 8, the highest voltage at the equipment is 1163 kV. The transformer is exposed to a peak voltage of 871 kV.

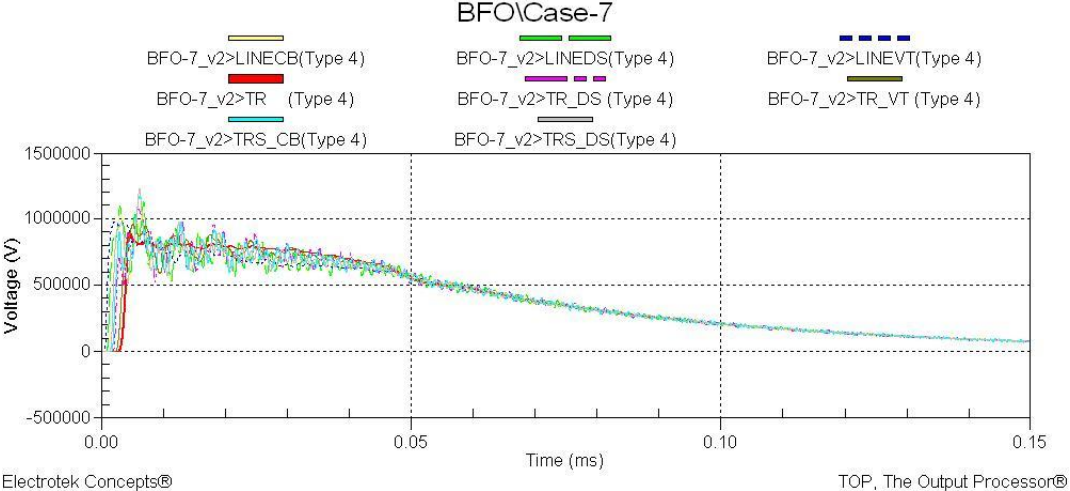


Figure 23 Resultant voltage waveforms for Case 7

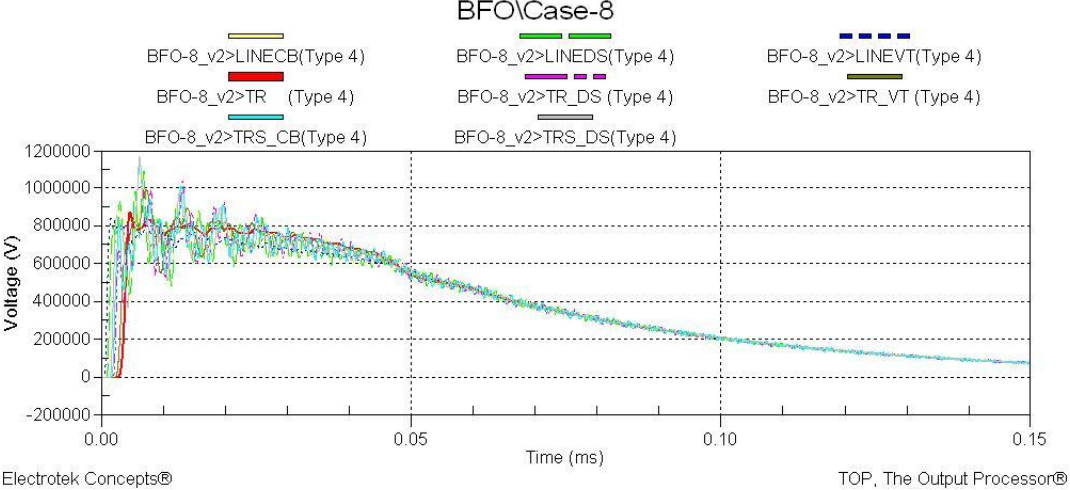


Figure 24 Resultant voltage waveforms for Case 8

3.4. Effect of the Current Amplitude of Lightning Strike for Main Busbar Connection Type

The details of the configurations for Cases 9, 10, 11 and 12 are demonstrated at Table 4. In these analyses, classified in Group 3, the main objective is to investigate the effect of the current amplitude of lightning stroke when line feeder is connected to the transformer feeder directly. By this way, it is possible to prevent the calculation and modeling errors. Four different cases are analyzed to get these goals.

Table 4 Group 3 Cases

CASES	Failure Type	LA Location	Connection Type	Current Amplitude	Connection Length	Lightning Location
9	BFO	TR + LE	Main Busbar	<i>190 kA</i>	Medium	2. Tower
10	BFO	TR + LE	Main Busbar	<i>200 kA</i>	Medium	2. Tower
11	SF	TR + LE	Main Busbar	<i>19.5 kA</i>	Medium	1. Tower
12	SF	TR + LE	Main Busbar	<i>20 kA</i>	Medium	1. Tower

In Group 3 cases and the next cases, lightning arrester location is standardized as both at the front of the power transformer and at the line entrance. The second difference from the previous Group cases, lightning current amplitude is increased to 190 kA for Case 9 and 200 kA for Case 10 from 185 kA at the back flashover failure type. In shielding failure type lightning stroke current amplitude is redefined 19.5 kA for Case 11 and 20 kA for Case 12.

The resultant waveforms of Case 9 are shown in Figure 25. As followed, in Case 9, the highest voltage at the equipment is 1020 kV. The transformer is exposed to a peak voltage of 872 kV. The obtained result for Case 10 is shown in Figure 26. In Case 10, the highest voltage at the equipment is 1046 kV. The transformer is exposed to a peak voltage of 876 kV.

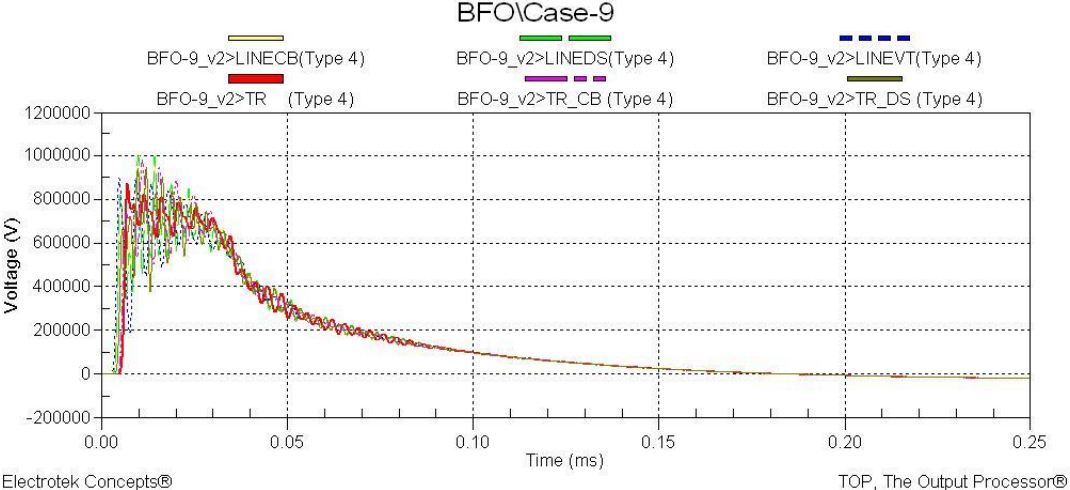


Figure 25 Resultant voltage waveforms for Case 9

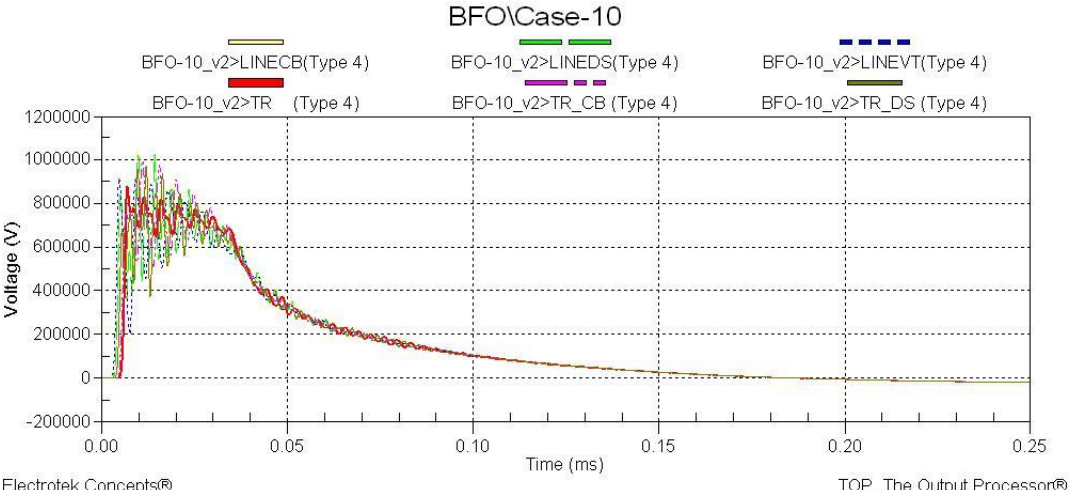


Figure 26 Resultant voltage waveforms for Case 10

The result obtained for Case 11 is shown in Figure 27. In Case 11, the highest voltage at the equipment is 1065 kV. The transformer is exposed to a peak voltage of 878 kV. The obtained result for Case 12 is shown in Figure 28. As it can be seen from the figure, in Case 12, the highest voltage at the equipment is 1077 kV. The transformer is exposed to a peak voltage of 880 kV.

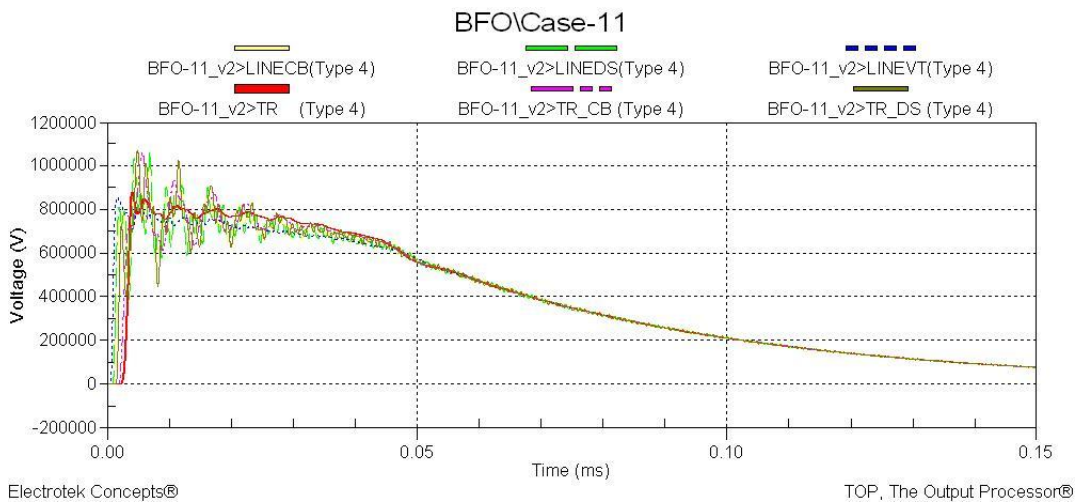


Figure 27 Resultant voltage waveforms for Case 11

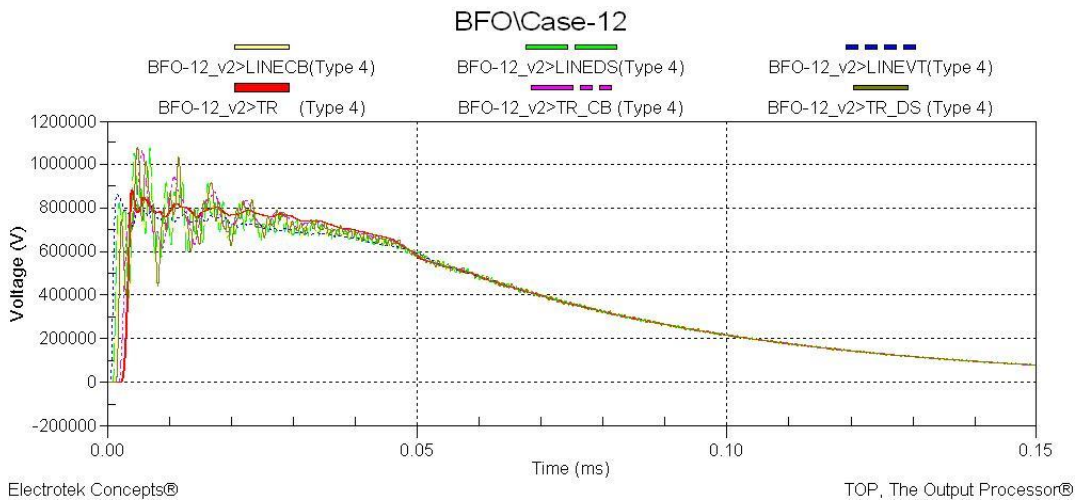


Figure 28 Resultant voltage waveforms for Case 12

3.5. Effect of the Current Amplitude of Lightning Strike for Transfer Busbar Connection Type

The details of Cases 13, 14, 15 and 16 are illustrated at Table 5. In these analyses classified in Group 4, the main objective is to investigate the effect of the current amplitude of lightning stroke when line feeder is connected to the transformer feeder through the transfer busbar. In addition, with comparison between Group 1, Group 2 and Group 3, Group 4 cases, it is possible to evaluate the outcomes of the connection type. In this scope, four different cases are analyzed.

Table 5 Group 4 Cases

CASES	Failure Type	LA Location	Connection Type	Current Amplitude	Connection Length	Lightning Location
13	BFO	TR + LE	Transfer Busbar	<i>190 kA</i>	Medium	2. Tower
14	BFO	TR + LE	Transfer Busbar	<i>200 kA</i>	Medium	2. Tower
15	SF	TR + LE	Transfer Busbar	<i>19.5 kA</i>	Medium	1. Tower
16	SF	TR + LE	Transfer Busbar	<i>20 kA</i>	Medium	1. Tower

The only difference between the Group 3 and Group 4 cases is the connection type. In Group 4 cases, it is assumed that the transformer feeder is connected to the line feeder through the transfer feeder and transfer busbar. Therefore, the lightning impulse voltage wave propagates a longer path including transfer feeder and transfer busbar.

The resultant waveforms obtained for Case 13 is shown in Figure 29. As it can be seen from the figure, in Case 13, the highest voltage at the equipment is 1081 kV. The transformer is exposed to 868 kV. The result observed for Case 14 is shown in Figure 30. As shown, in Case 14, the highest voltage, is 1092 kV at the equipment and 872 kV at the transformer

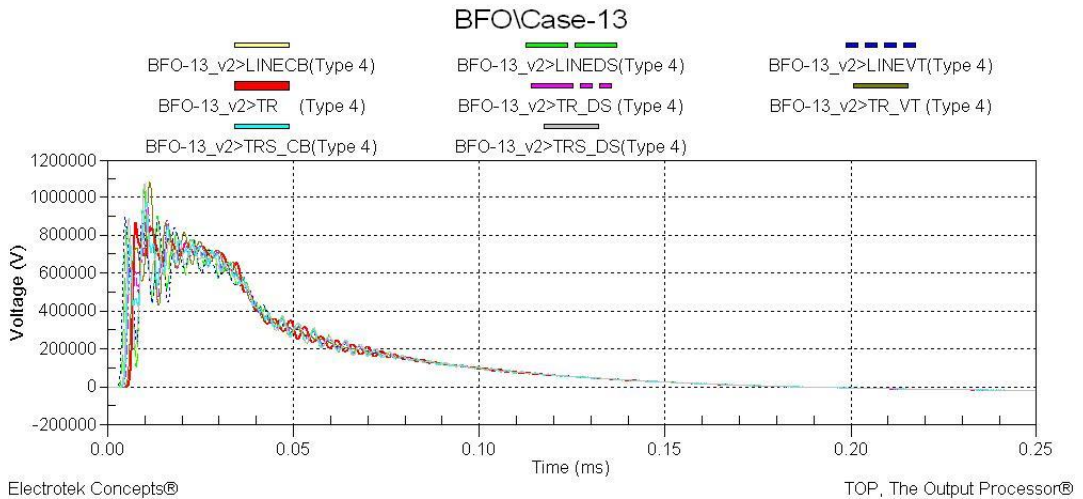


Figure 29 Resultant voltage waveforms for Case 13

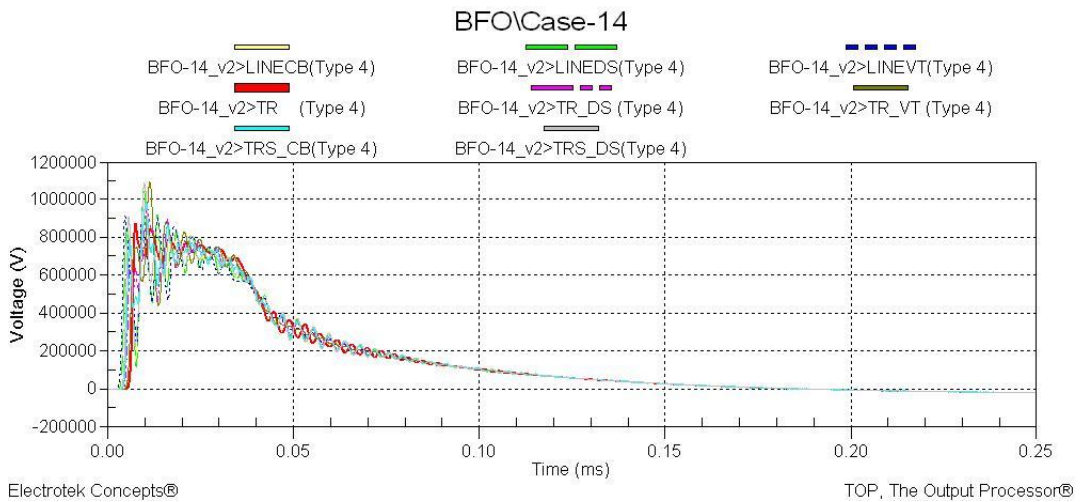


Figure 30 Resultant voltage waveforms for Case 14

The result observed for Case 15 is shown in Figure 31. As it can be seen from the figure, in Case 15, the highest voltage at the equipment is 1178 kV. The transformer is exposed to a peak voltage of 873 kV. The obtained result for Case 16 is shown in Figure 32. As it can be seen from the figure, in Case 16, the highest voltage at the equipment is 1193 kV. The transformer is exposed to a peak voltage of 875 kV.

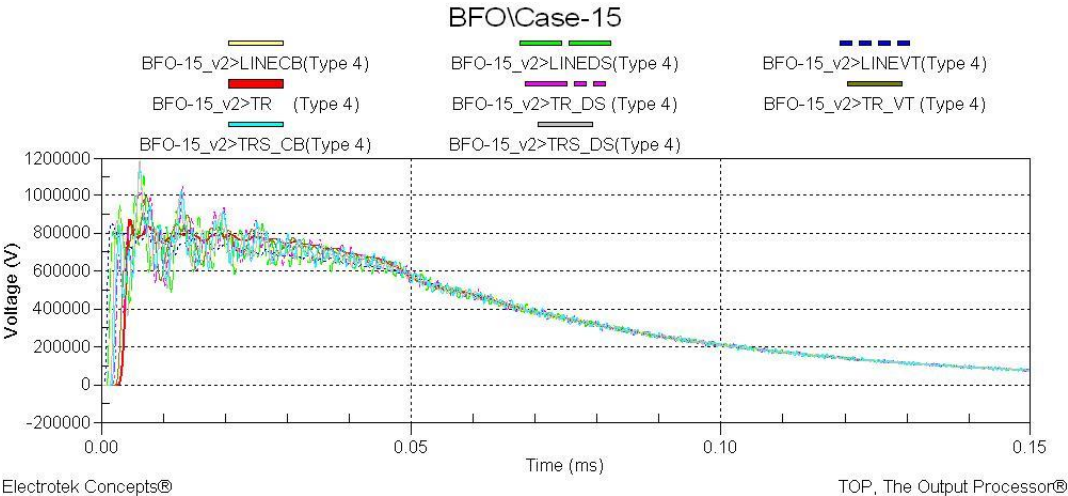


Figure 31 Resultant voltage waveforms for Case 15

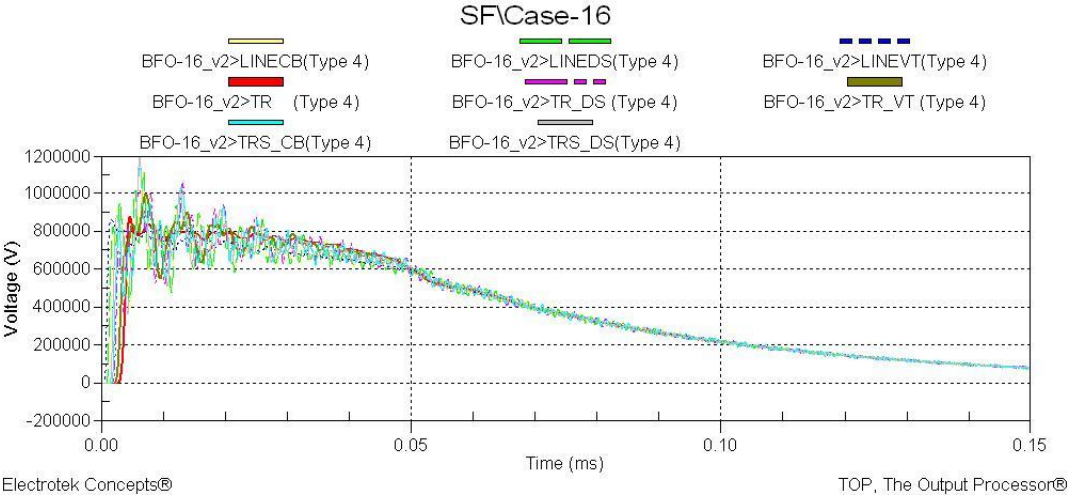


Figure 32 Resultant voltage waveforms for Case 16

3.6. Effect of the Connection Length for Main Busbar Connection Type

Table 6 shows the details of the analyses for Cases 17, 18, 19 and 20. In these analyses classified in Group 5, the main objective is to investigate the effect of the length of the path that lightning impulse waveform propagates along when the line feeder is connected to the transformer feeder directly. This length of the path is defined as connection length. Four different cases are analyzed for that purpose.

Table 6 Group 5 Cases

CASES	Failure Type	LA Location	Connection Type	Current Amplitude	Connection Length	Lightning Location
17	BFO	TR + LE	Main Busbar	185 kA	<i>Closer</i>	2. Tower
18	BFO	TR + LE	Main Busbar	185 kA	<i>Longer</i>	2. Tower
19	SF	TR + LE	Main Busbar	19 kA	<i>Closer</i>	1. Tower
20	SF	TR + LE	Main Busbar	19 kA	<i>Longer</i>	1. Tower

In Group 5 cases, variable parameter is selected as the connection length. As it is explained previously, in the other Group cases connection length is defined as “medium” which refers that there are three bays span between the line feeder and transformer feeder. In Group 5 cases, it is assumed that there is no bay between the line bay and transformer bay. This situation means that they are side by side referring to “shorter” for Case 17 and Case 19. On the other hand, it is assumed that there are five spans between the line bay and the transformer bay for Case 18 and Case 20 which refers to “longer”.

The result observed for Case 17 is demonstrated in Figure 33. As it can be seen from the figure, in Case 17, the highest voltage at the equipment is 1021 kV. The transformer is exposed to a peak voltage of 872 kV voltage level. The obtained result for Case 18 is shown in Figure 34. As it can be seen from the figure, in Case 18, the highest voltage at the equipment is 966 kV. The transformer is exposed to a peak voltage of 870 kV.

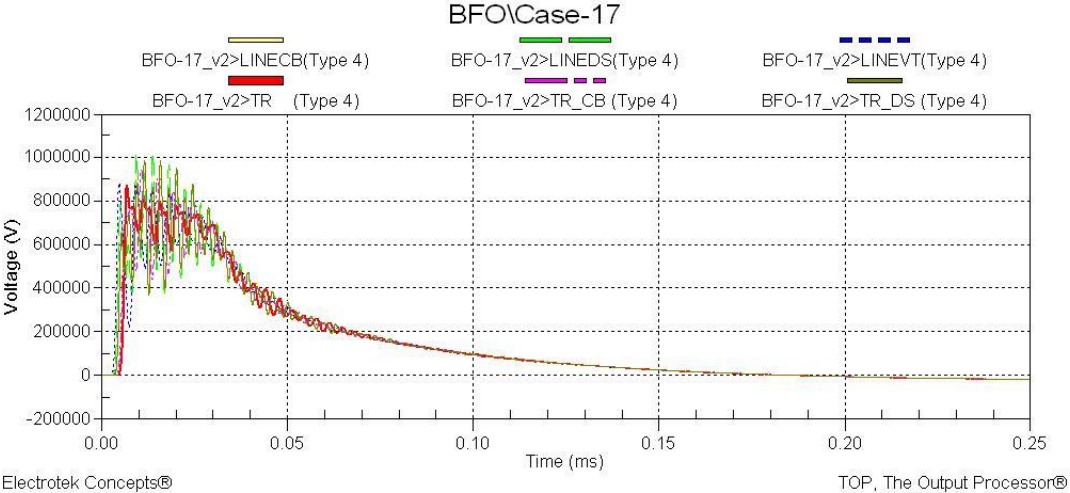


Figure 33 Resultant voltage waveforms for Case 17

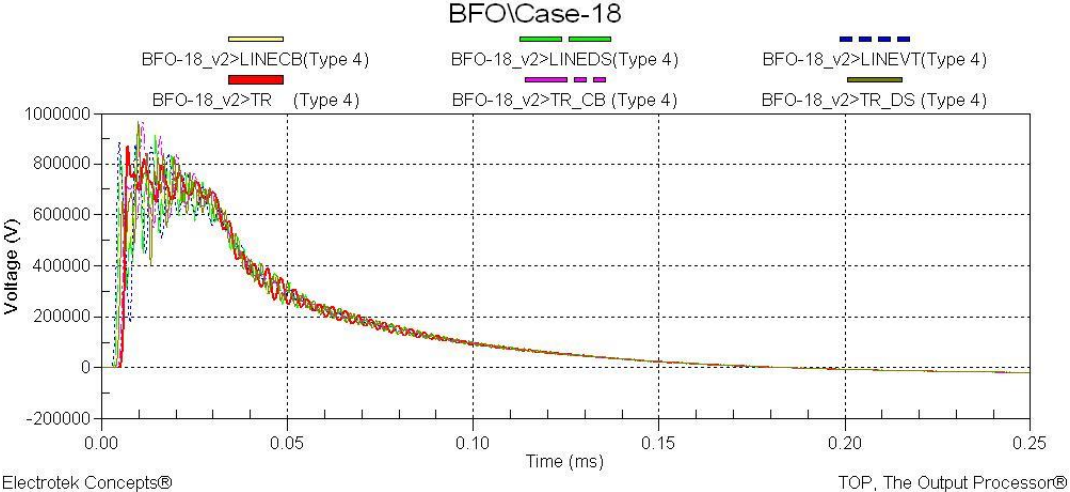


Figure 34 Resultant voltage waveforms for Case 18

The resultant waveforms obtained for Case 19 are shown in Figure 35. As it can be seen from the figure, in Case 19, the highest voltage at the equipment is 1069 kV. The transformer is exposed to a peak voltage of 879 kV. The obtained result for Case 20 is shown in Figure 36. As it can be seen from the figure, in Case 20, the highest voltage at the equipment is 1070 kV. The transformer is exposed to a peak voltage of 875 kV.

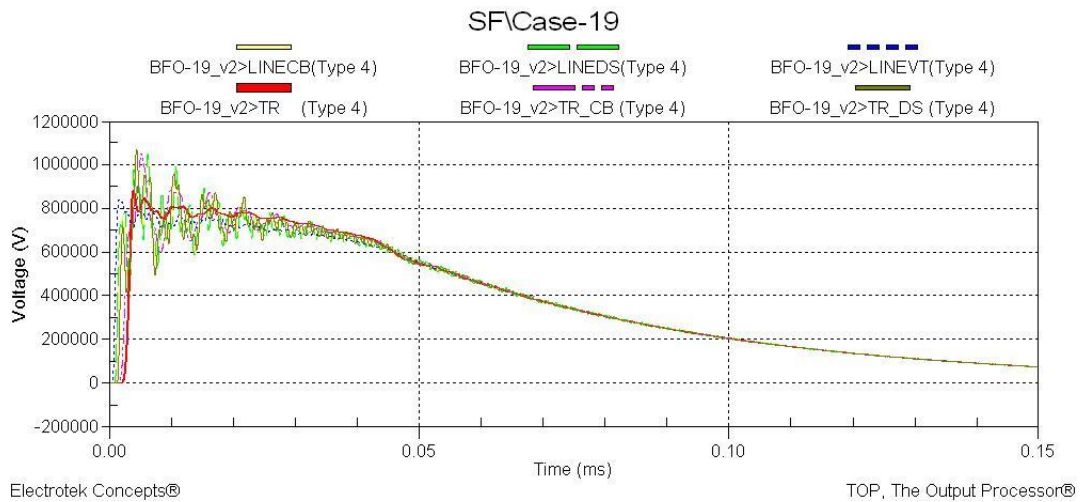


Figure 35 Resultant voltage waveforms for Case 19

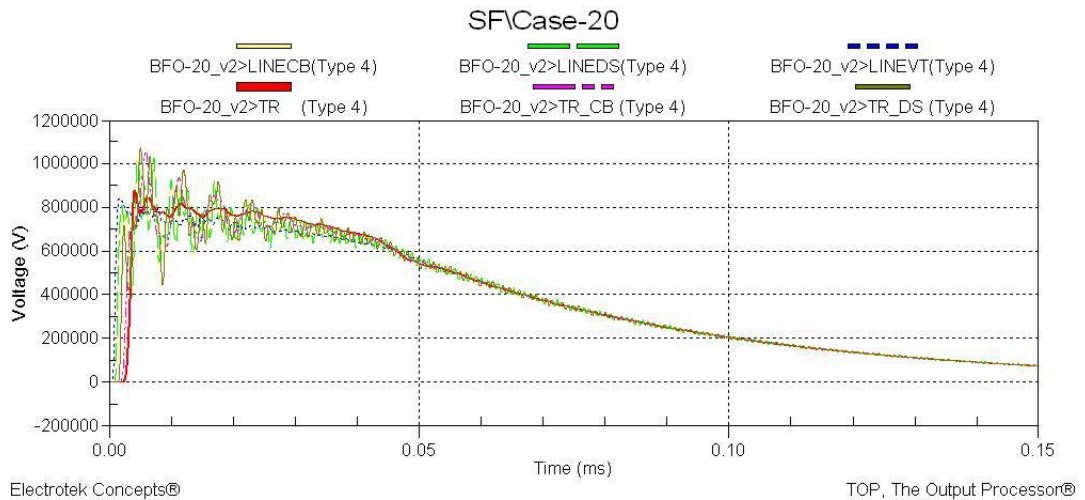


Figure 36 Resultant voltage waveforms for Case 20

3.7. Effect of the Connection Length for Transfer Busbar Connection Type

The details of the analyses for Cases 21, 22, 23 and 24 are shown at Table 7. In these analyses classified in Group 6, the main objective is to investigate the effect of the length of the path that lightning impulse waveform propagates along when the line feeder is connected to the transformer feeder through transfer feeder. This length of the path is defined as connection length. In order to achieve aims, four different cases are analyzed.

Table 7 Group 6 Cases

CASES	Failure Type	LA Location	Connection Type	Current Amplitude	Connection Length	Lightning Location
21	BFO	TR + LE	Transfer Busbar	185 kA	<i>Closer</i>	2. Tower
22	BFO	TR + LE	Transfer Busbar	185 kA	<i>Longer</i>	2. Tower
23	SF	TR + LE	Transfer Busbar	19 kA	<i>Closer</i>	1. Tower
24	SF	TR + LE	Transfer Busbar	19 kA	<i>Longer</i>	1. Tower

In Group 6 cases, the only difference from the Group 5 cases is the connection type. In Group 4 cases, it is assumed that the transformer feeder is connected to the line feeder through the transfer feeder and transfer busbar. Therefore, the lightning impulse voltage wave propagates a longer path including transfer feeder and transfer busbar.

The obtained result for Case 21 is shown in Figure 37. As seen, in Case 21, the highest voltage at the equipment is 869 kV. The transformer is exposed to a peak voltage of 941 kV. The obtained result for Case 22 is shown in Figure 38. As it can be observed from the figure, in Case 22, the highest voltage at the equipment is 1200 kV. The transformer is exposed to a peak voltage of 865 kV.

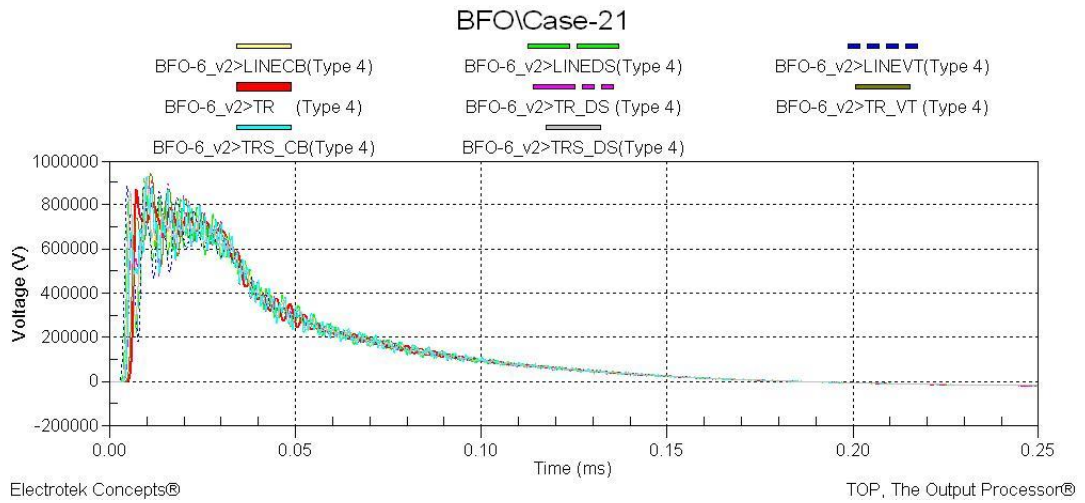


Figure 37 Resultant voltage waveforms for Case 21

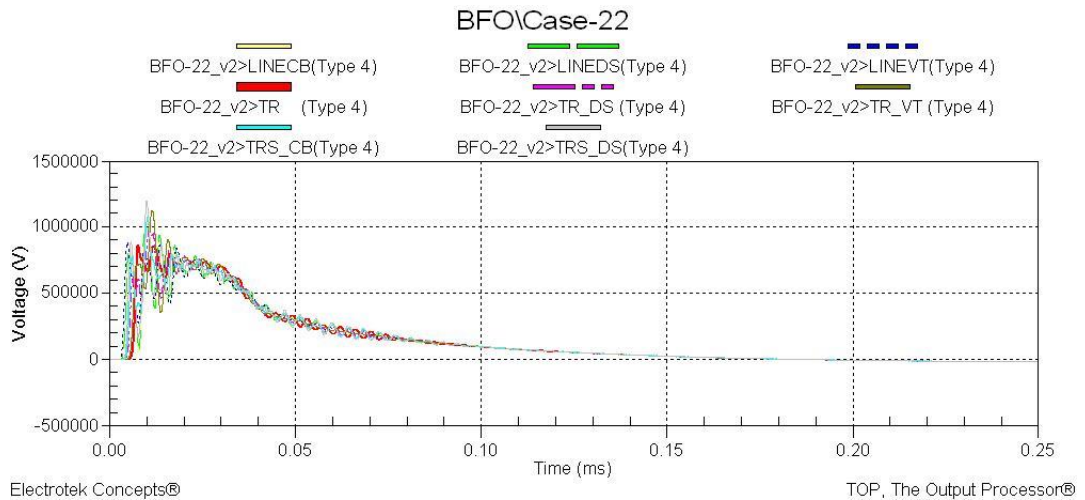


Figure 38 Resultant voltage waveforms for Case 22

The result observed for Case 23 is illustrated in Figure 39. As it can be seen from the figure, in Case 23, the highest voltage at the equipment is a 1108 kV. The transformer is exposed to 876 kV. The obtained result for Case 24 is shown in Figure 40. As it can be seen from the figure, in Case 24, the highest voltage at the equipment is 1166 kV. The transformer is exposed to 870 kV.

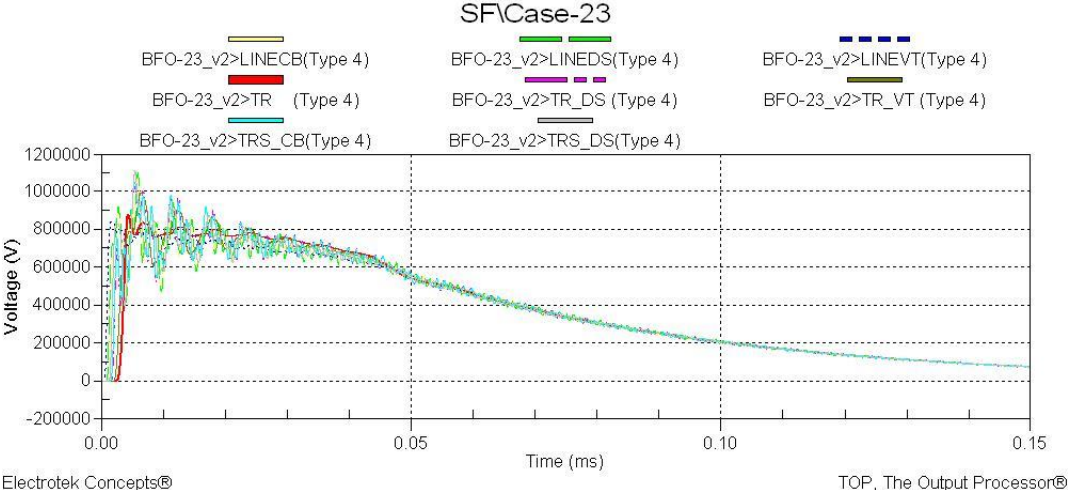


Figure 39 Resultant voltage waveforms for Case 23

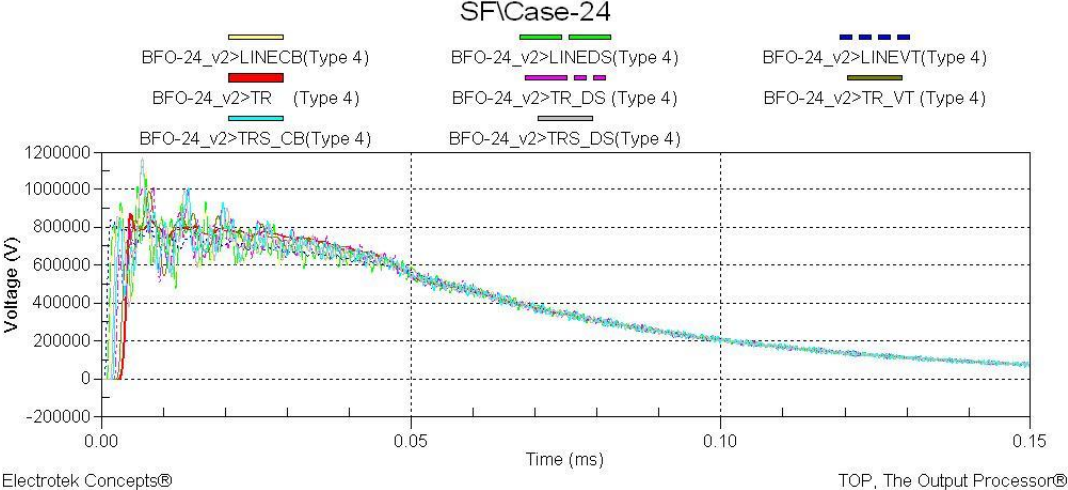


Figure 40 Resultant voltage waveforms for Case 24

3.8. Effect of the Lightning Strike Location for Main Busbar Connection Type

The details of Cases 25, 26, 27 and 28 are illustrated at Table 8. In these analyses classified in Group 7, the main objective is to investigate the effect of the lightning stroke location. For this purpose, four different cases are analyzed.

Table 8 Group 7 Cases

CASES	Failure Type	LA Location	Connection Type	Current Amplitude	Connection Length	Lightning Location
25	BFO	TR + LE	Main Busbar	185 kA	Medium	<i>3. Tower</i>
26	BFO	TR + LE	Main Busbar	185 kA	Medium	<i>4. Tower</i>
27	SF	TR + LE	Main Busbar	19 kA	Medium	<i>2. Tower</i>
28	SF	TR + LE	Main Busbar	19 kA	Medium	<i>3. Tower</i>

In all cases except Group 7 and Group 8 cases, the minimum strike distance defined in [2], the second tower for back flashover failure and the first tower for shielding failure, is used in the analyses. In Group 7 cases, the lightning stroke location is changed to the third tower from the second tower for back flashover failure type and from the first tower for shielding failure type.

The result obtained for Case 25 is shown in Figure 41. As it can be seen from the figure, in Case 25, the highest voltage at the equipment is 882 kV. The transformer is exposed to 860 kV. The obtained result for Case 26 is shown in Figure 42. As it can be seen from the figure, in Case 26, the highest voltage at the equipment is 840 kV and at the transformer is 857 kV.

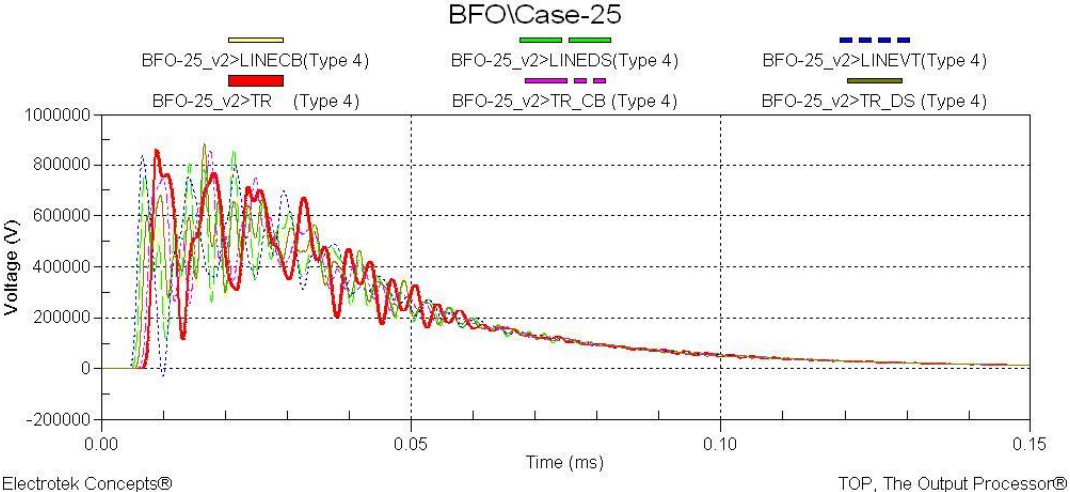


Figure 41 Resultant voltage waveforms for Case 25

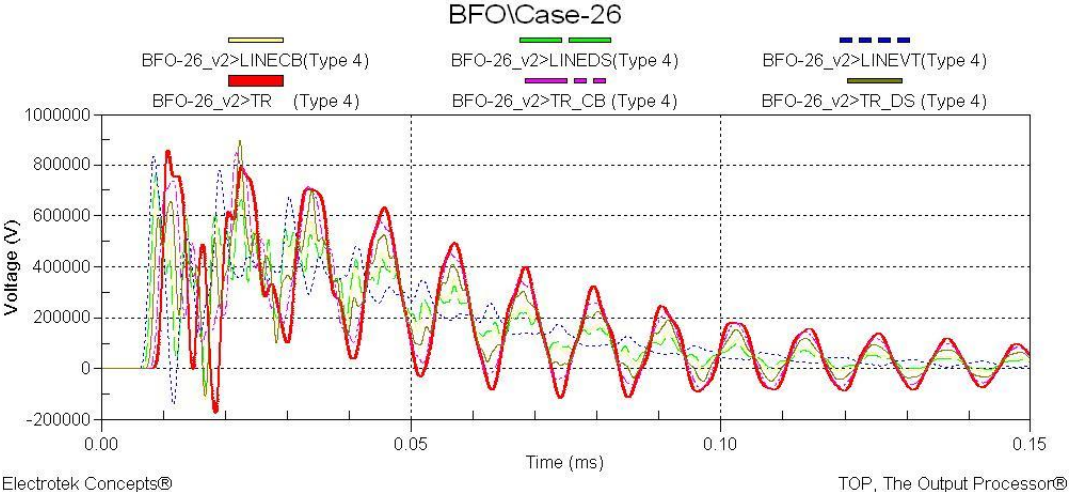


Figure 42 Resultant voltage waveforms for Case 26

The result observed for Case 27 is shown in Figure 43. As it can be seen from the figure, in Case 27, the highest voltage at the equipment is 1050 kV and at the transformer is 872 kV. The obtained result for Case 28 is shown in Figure 44. As it can be seen from the figure, in Case 28, the highest voltage at the equipment is 1139 kV. The transformer is exposed to a peak voltage of 868 kV.

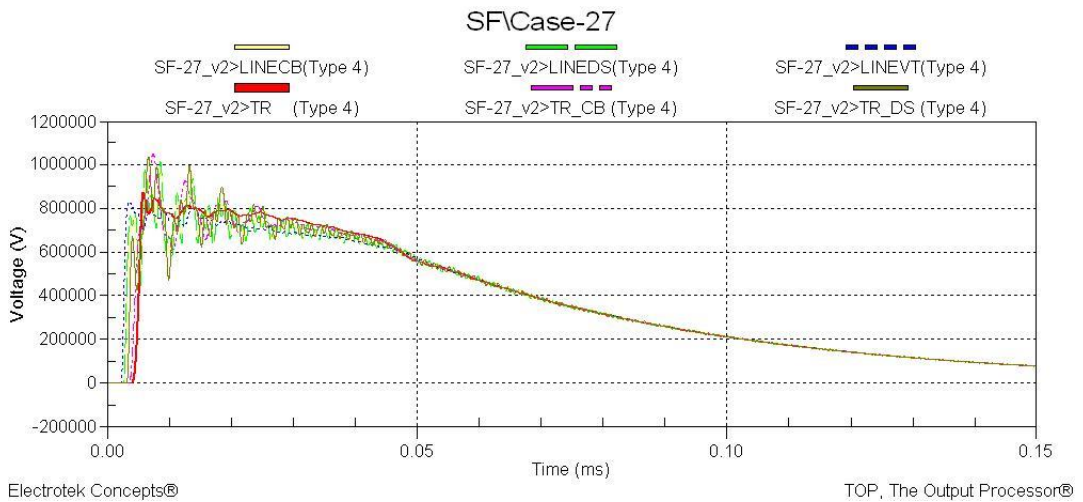


Figure 43 Resultant voltage waveforms for Case 27

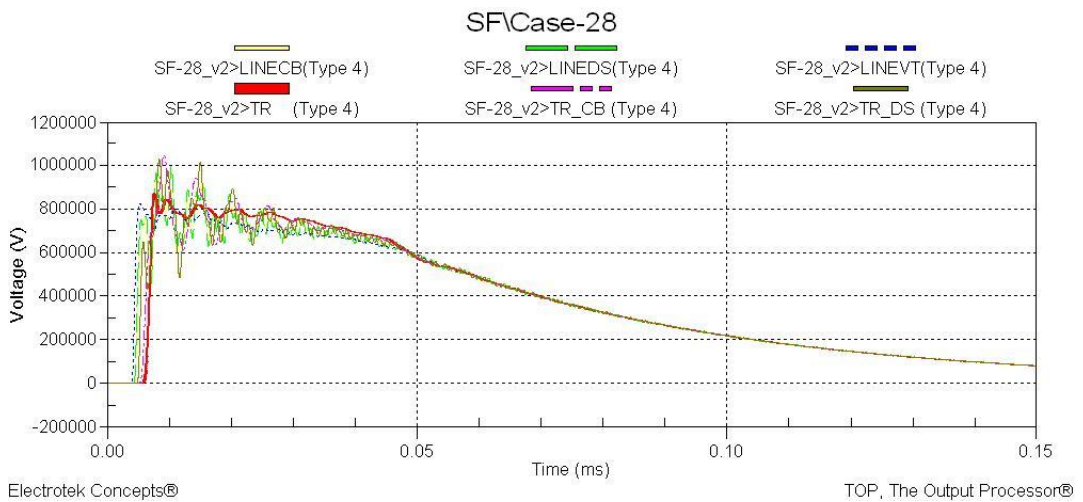


Figure 44 Resultant voltage waveforms for Case 28

3.9. Effect of the Lightning Strike Location for Transfer Busbar Connection Type

The details of the analyses for Cases 29, 30, 31 and 32 are shown at Table 9. In these analyses classified in Group 8, the main objective is to investigate the effect of the lightning stroke location. In this scope, four different cases are analyzed.

Table 9 Group 8 Cases

CASES	Failure Type	LA Location	Connection Type	Current Amplitude	Connection Length	Lightning Location
29	BFO	TR + LE	Transfer Busbar	185 kA	Medium	3. Tower
30	BFO	TR + LE	Transfer Busbar	185 kA	Medium	4. Tower
31	SF	TR + LE	Transfer Busbar	19 kA	Medium	2. Tower
32	SF	TR + LE	Transfer Busbar	19 kA	Medium	3. Tower

In all cases, except Group 7 and Group 8 cases, the minimum strike distance defined in [2], second tower for back flashover failure and first tower for shielding failure, is used in the analyses. In Group 8 cases, similar to Group 7 cases, the lightning stroke location is changed to third tower from second tower for back flashover failure type and from first tower for shielding failure type.

The resultant voltage waveforms for Case 29 are shown in Figure 45. As it can be seen from the figure, in Case 29, the highest voltage at the equipment is 882 kV. The transformer is exposed to 860 kV. The obtained result for Case 30 is shown in Figure 46. As it can be seen from the figure, in Case 30, the highest voltage at the equipment is 840 kV. The transformer is exposed to a peak voltage of 857 kV.

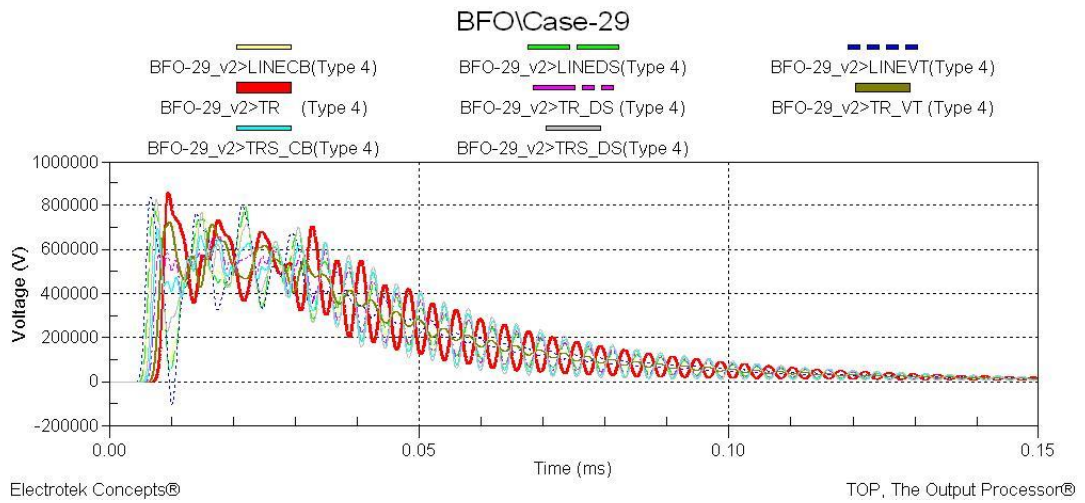


Figure 45 Resultant voltage waveforms for Case 29

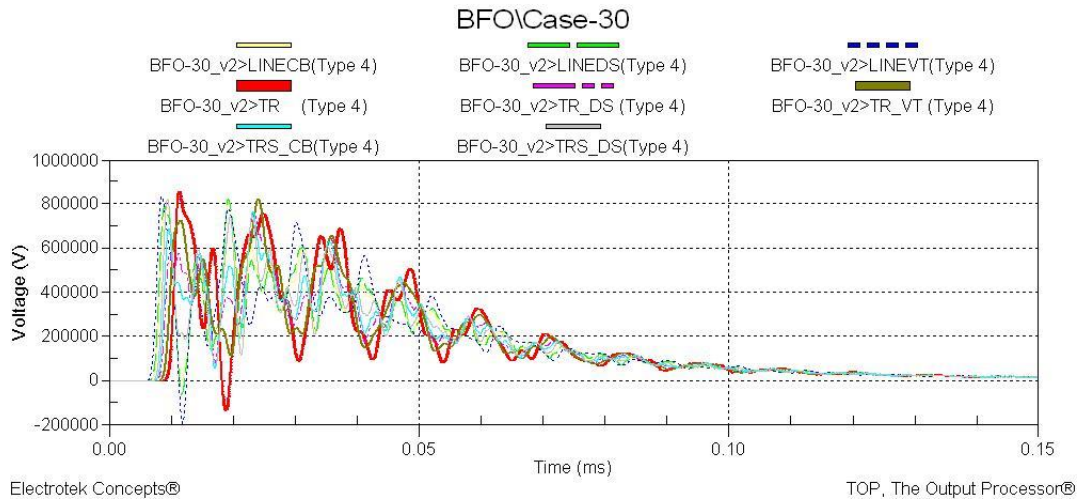


Figure 46 Resultant voltage waveforms for Case 30

The obtained result for Case 31 is shown in Figure 47. As it can be seen from the figure, in Case 31, the highest voltage at the equipment is 882 kV. The transformer is exposed to 860 kV. The obtained result for Case 32 is shown in Figure 48. As it can be seen from the figure, in Case 32, the highest voltage at the equipment is 840 kV and at the transformer is 857 kV.

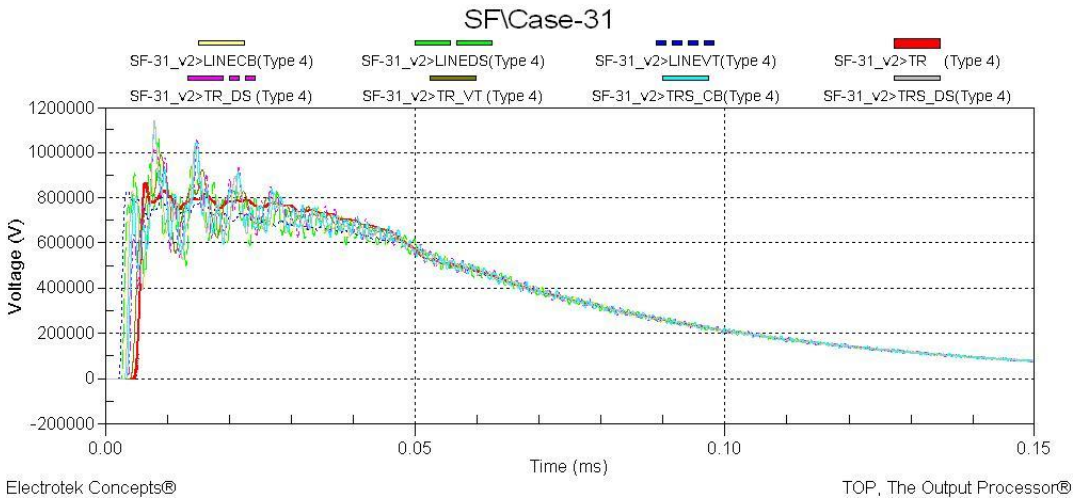


Figure 47 Resultant voltage waveforms for Case 31

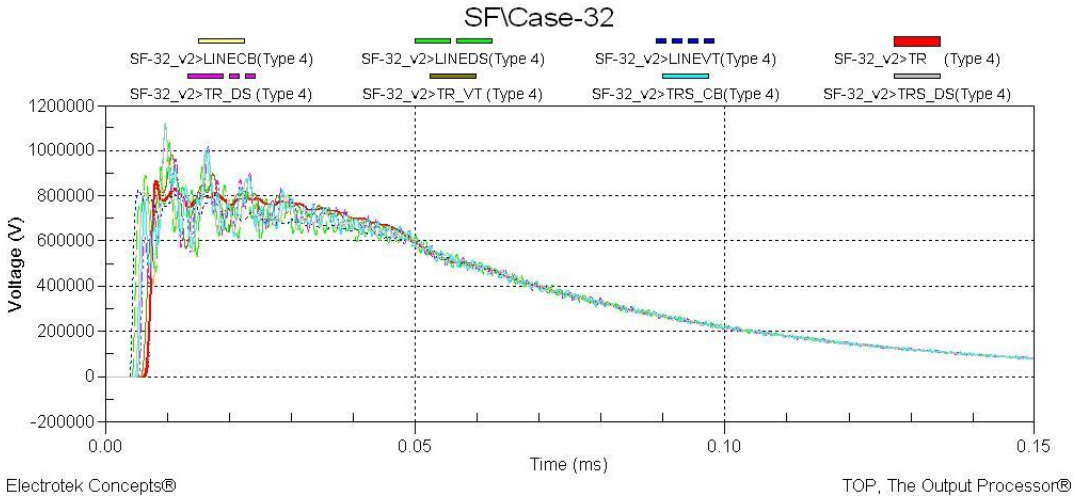


Figure 48 Resultant voltage waveforms for Case 32

CHAPTER 4

DISCUSSION OF RESULTS

4.1. Introduction

In this chapter, the results of the simulation cases defined in previous chapter are presented and discussed. The graphs are prepared from the results obtained by the simulations according to the objectives of the cases. According to the variables defined in previous chapter, two types of graphs are presented in order to see the effects of the variables. For each variable, the results are discussed for both main busbar connection type and transfer busbar connection type.

In the following sections, the effects of failure types, the effects of connection types, the effects of location of lightning arresters, the effects of current amplitude of lightning strike, the effects of connection length and the effects of location of lightning strike are evaluated separately. In the last section of this chapter, maximum voltages observed at the simulations for power transformer and other equipment are discussed by considering standard lightning impulse withstand voltage levels defined in IEC [1], safety factor for simulations and cost of equipment and lightning arrester.

4.2. Analyses of Effect of Location of Lightning Arresters

As described in Chapter 3, the objective of the first 8 cases is to observe the effect of location of lightning arresters. In order to obtain this aim, simulations are performed for two situations in terms of location of lightning arresters; at only the front of the power transformer and both at line entrance and at front of the power transformer. In Figure 49 and Figure 50, the effect of location of lightning arresters can be seen for the main busbar connection and the transfer busbar connection.

As shown in Figure 49 and Figure 50, maximum voltages, seen at the equipment and power transformer with lightning arresters both at the front of the power transformer and at the line entrance, are lower than the configuration when the lightning arresters are only at the front of the power transformer. Hence, with the implementation of additional lightning arresters to the entrance of the line feeders, equipment and power transformer are exposed to lesser voltage. This decrease in the peak voltage is approximately 100 kV for equipment and 20 kV for power transformer. This result shows that in order to adequately protect the transformer and other substation equipment, it is necessary to provide lightning arresters at the following locations in the substation; at front of every power transformer and at the entrance of outgoing and incoming feeders on the substation, as described in [24]. Moreover, it is obviously obtained that the equipment is exposed to higher overvoltages than the power transformer. That is an expected result because of the fact that the lightning arresters are located close to the power transformer. Another outcome of Figure 49 and Figure 50 is that shielding failure causes higher voltages both at equipment and power transformer. Although the current amplitude of lightning strike at the back flashover failure is higher than the shielding failure, the maximum voltages seen at the shielding failure are higher since the lightning strike is directly to one of phase conductors and lightning strike has different characteristics at the shielding failure. However, the situation depends on the location of the substation and on the characteristics of the lightning strike.

The outcomes of the first 8 cases, which have the main objective of investigating effect of location of lightning arresters, are not limited with the above explanations. Besides the above mentioned, it is possible to analyze the effect of connection type which is seen in Figure 51 and Figure 52. The difference between the main busbar connection and transfer busbar connection is that at the main busbar connection, the line feeder is connected to the transformer feeder directly; however, at the transfer busbar connection, the transformer feeder is fed from the line feeder through the transfer busbar. This situation causes difference at the connection length. Lightning strike at the transfer busbar connection propagates through a longer path between the point of lightning strike at the transmission line and the power transformer. This increase in the path causes two different results. Since lightning impulse wave attenuates while it propagates, the maximum voltages seen at the power transformer are lower for transfer busbar connection. However, voltages, which equipment is exposed to, decrease because the distance between the lightning arresters and equipment increases. As seen from Figure 51 and Figure 52, these results are valid for both back flashover and shielding failures. Although the decrease at the maximum voltage of power transformer is approximately only 5 kV, this reduction gives the decay tendency.

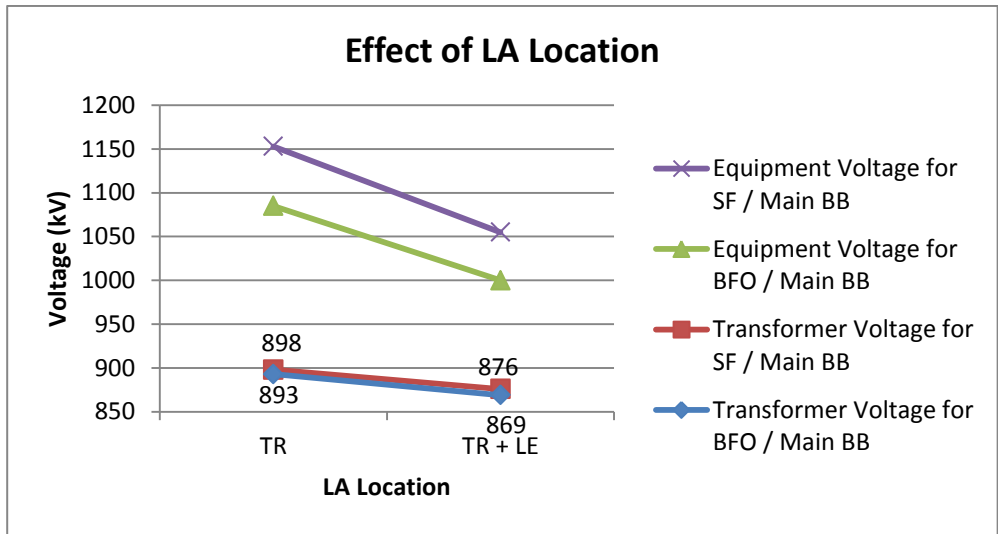


Figure 49 Effect of location of lightning arresters for main busbar connection type in Case 1, 2, 3 and 4

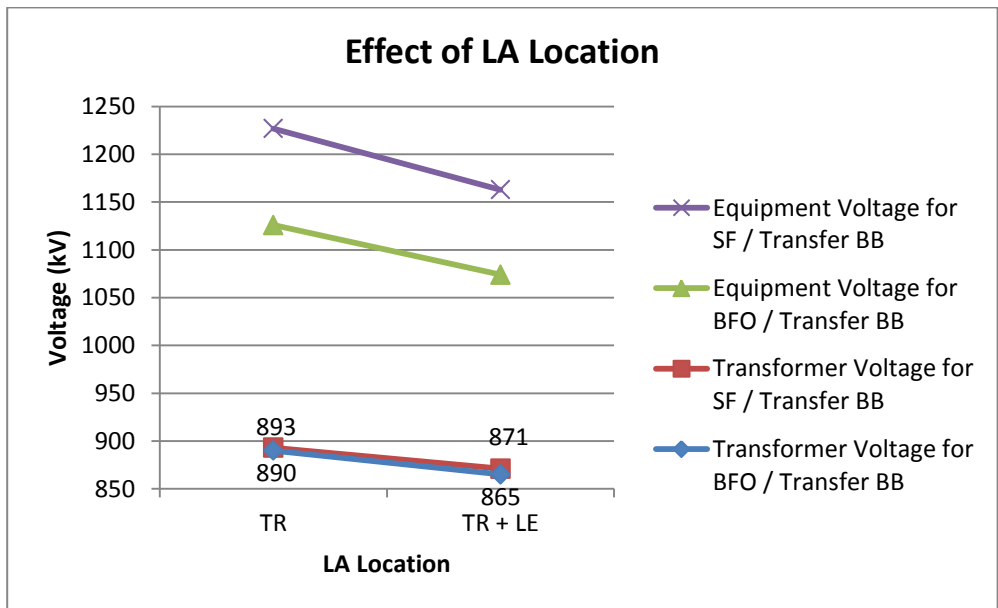


Figure 50 Effect of location of lightning arresters for transfer busbar connection type in Case 5, 6, 7 and 8

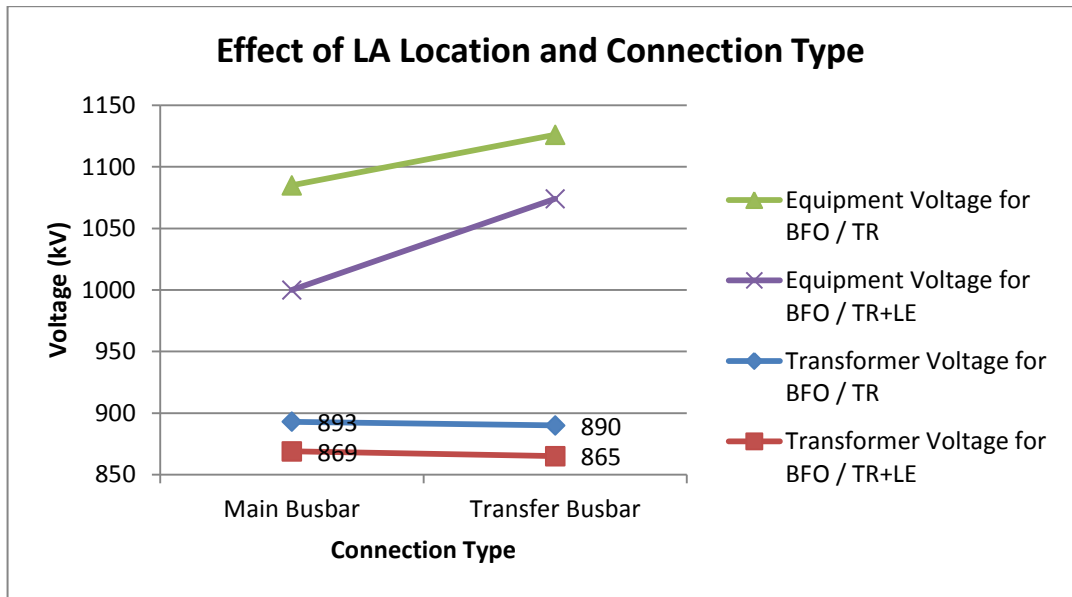


Figure 51 Effect of location of lightning arresters and connection type for back flashover failure in Case 1, 2, 5 and 6

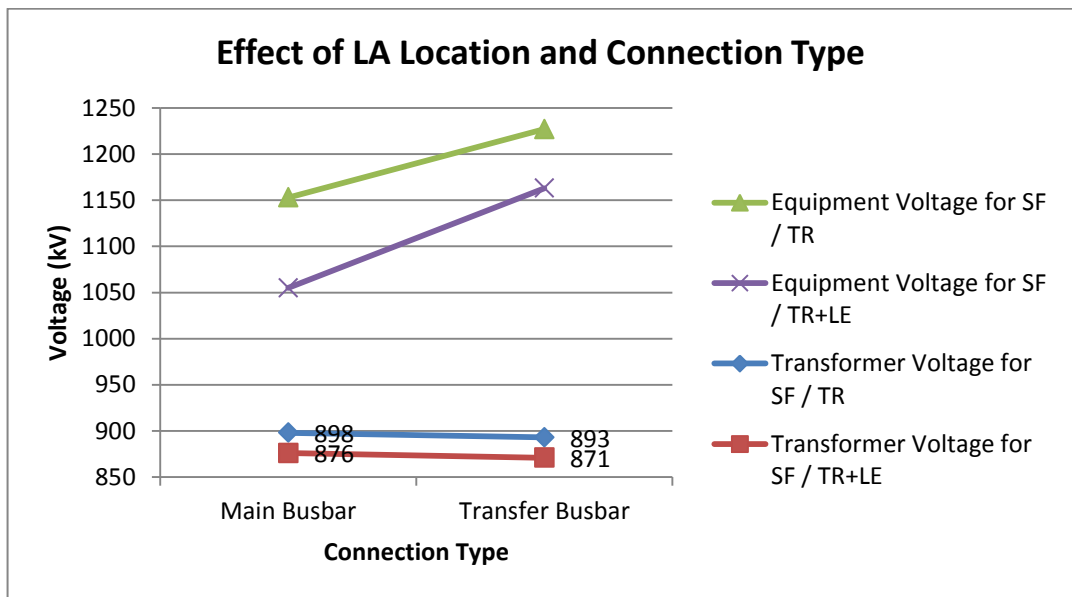


Figure 52 Effect of location of lightning arresters and connection type for shielding failure in Case 3, 4, 7 and 8

4.3. Analyses of Effect of Current Amplitude of Lightning Strike

The main aim of the second 8 cases, which are Case 9-10-11-12-13-14-15-16, is to see the effect of current amplitude of lightning strike to the transmission line. Hence, simulations are performed for three situations in terms of current amplitude of lightning strike; 185 kA, 190 kA and 200 kA for the back flashover and 19 kA, 19.5 kA and 20 kA for the shielding failure. In Figure 53 and Figure 54, the effect of current amplitude of lightning strike is shown for main busbar connection and transfer busbar connection.

Figure 53 and Figure 54 illustrate that maximum voltages, observed at the equipment and power transformer, increase by higher current amplitude of lightning strike for both shielding failure and back flashover failure. In other words, while the current amplitude of the applied lightning strike increases, equipment and power transformer are exposed to higher voltages. This is an expected result since there is a linear correlation between the current amplitude of the lightning strike and maximum voltages observed at the equipment and power transformer. The results are also in accordance with [22]. The increase obtained in simulations does not exceed 50 kV for equipment and 10 kV for power transformer. This explains that there is a direct but limited proportion between maximum voltages and current amplitude for 10 kA increase in back flashover failure and 0.5 kA increase in shielding failure. In addition, it is obviously obtained that the equipment is exposed higher overvoltages than the power transformer. That is expected result because of the lightning arresters located close to the power transformer. Another outcome of Figure 53 and Figure 54 is that shielding failures cause higher voltages both at equipment and power transformer. Although the current amplitude of lightning strike at the back flashover failure is higher than the shielding failure, the maximum voltages seen at the shielding failure are higher since the lightning strike is directly to one of phase conductors

and lightning strike has different characteristics at the shielding failure. However, since the situation depends on the location of substation and characteristics of lightning strike, this could not be generalized.

The outcomes from the second 8 cases, are not limited with the above explanations. In addition, it is possible to analyze also the effect of connection type that is seen in Figure 55 and Figure 56. The difference between the main busbar connection and transfer busbar connection is that at the main busbar connection, the line feeder is connected to the transformer feeder directly but at the transfer busbar connection, the transformer feeder is fed from the line feeder through the transfer busbar. This situation causes difference at the connection length. Lightning strike at the transfer busbar connection propagates through a longer path between the point of lightning strike at the transmission line and the power transformer. This increase in the path causes two different results. Since lightning impulse wave attenuates while it propagates, the maximum voltages seen at the power transformer are lower for transfer busbar connection. However, equipment exposed to the highest voltages decrease because the distance between the lightning arresters and equipment increases. As seen from Figure 55 and Figure 56, these results are valid for both back flashover and shielding failures. Although the decrease at the maximum voltage of power transformer is approximately only 4kV and 5 kV, this decrease gives the tendency.

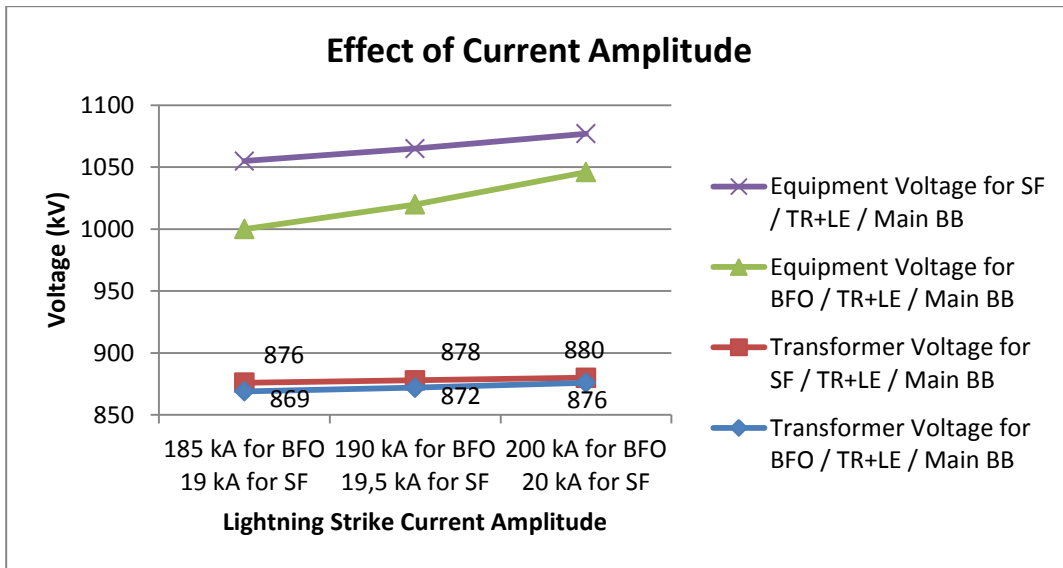


Figure 53 Effect of current amplitude of lightning strike for main busbar connection type in Case 9, 10, 11 and 12

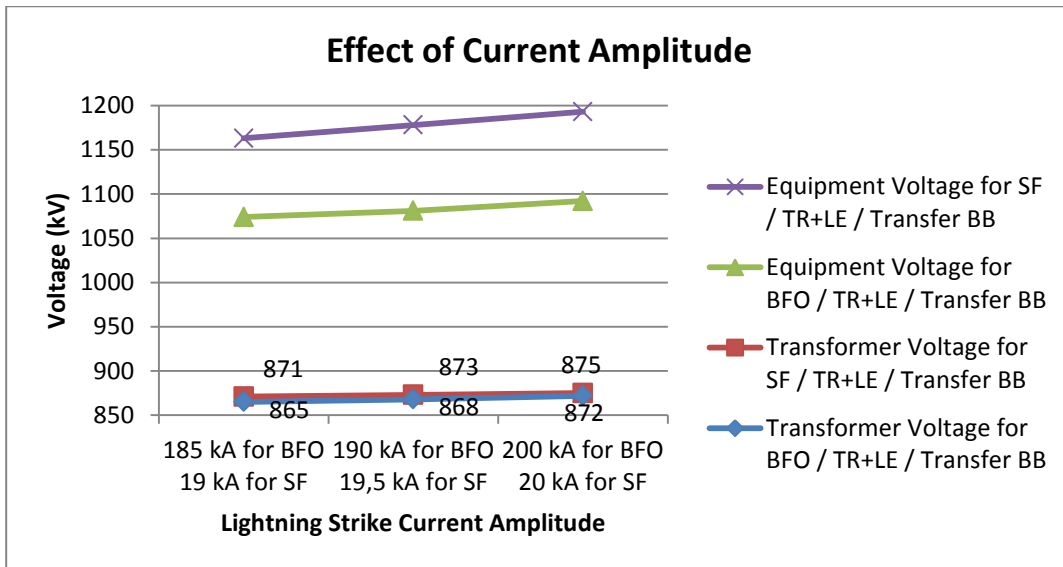


Figure 54 Effect of current amplitude of lightning strike for transfer busbar connection type in Case 13, 14, 15 and 16

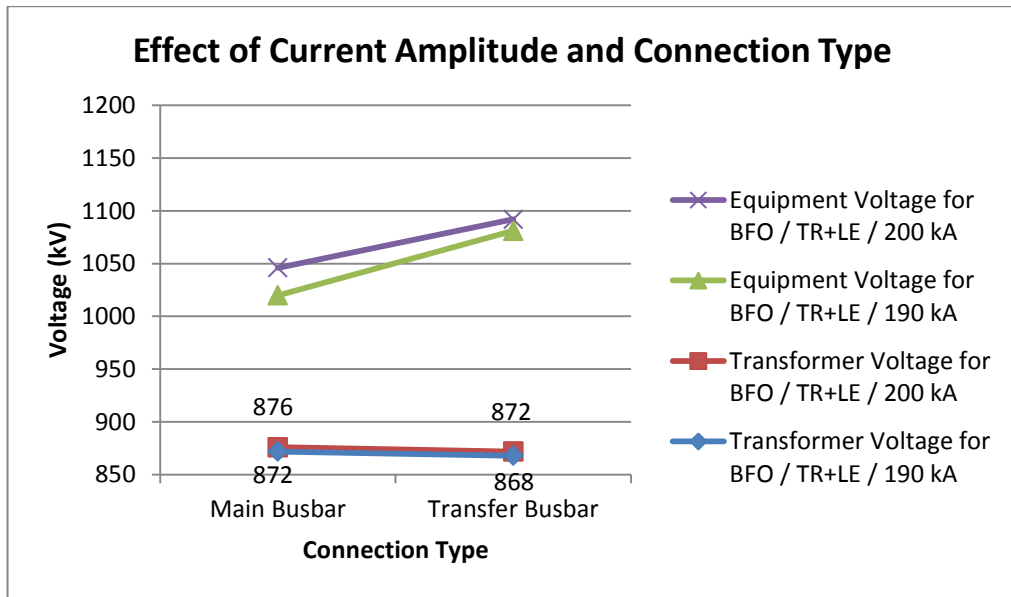


Figure 55 Effect of current amplitude and connection type for back flashover failure in Case 9, 10, 13 and 14

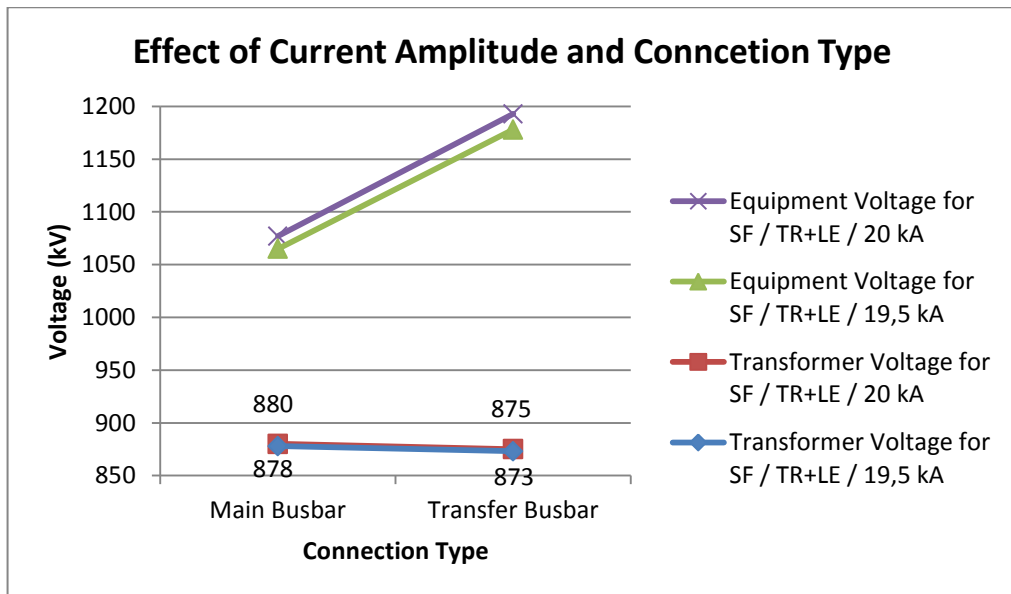


Figure 56 Effect of current amplitude and connection type for shielding failure in Case 11, 12, 15 and 16

4.4. Analyses of Effect of Connection Length

The third 8 cases, which are Case 17-18-19-20-21-22-23-24, have the objective of observing the effect of connection length which describes the length of the path that lightning strike propagates. In order to obtain this aim, simulations are performed for three situations in terms of connection length; shorter, medium and longer for both back flashover and shielding failure. The terms of shorter, medium and longer refers to the distance between line feeder and transformer feeder. In Figure 57 and Figure 58, the effect of connection length is demonstrated for main busbar connection and transfer busbar connection.

As illustrated in Figure 57, maximum voltages, seen at the equipment and power transformer, decrease with increase of connection length of the line feeder and transformer feeder for both back flashover and shielding failure when line feeder is connected to the transformer feeder directly. In Figure 58, it is shown that maximum voltage seen at the power transformer at the transfer busbar connection has the same tendency with the main busbar connection. However, equipment maximum voltage increases as the connection length increases for transfer busbar connection. In addition, it is obviously obtained that the equipment is exposed higher overvoltages than the power transformer. That is expected result because of the lightning arresters located close to the power transformer. Another outcome of Figure 53 and Figure 54 is that shielding failures cause higher voltages both at equipment and power transformer. Although the current amplitude of lightning strike at the back flashover failure is higher than the shielding failure, the maximum voltages seen at the shielding failure are higher since the lightning strike is directly to one of phase conductors and lightning strike has different characteristics at the shielding failure. However, this is not a general concept. In other words, the situation depends on the location of substation and characteristics of lightning strike.

In addition, it is possible to analyze also the effect of connection type that is seen in Figure 59 and Figure 60. The difference between the main busbar connection and transfer busbar connection is that at the main busbar connection, the line feeder is connected to the transformer feeder directly; but, at the transfer busbar connection, the transformer feeder is fed from the line feeder through the transfer busbar. This situation causes difference at the connection length. Lightning strike at the transfer busbar connection propagates through a longer path between the point of lightning strike at the transmission line and the power transformer. This increase in the path causes two different results. Since lightning impulse wave attenuates while it propagates, the maximum voltages seen at the power transformer are lower for transfer busbar connection. However, equipment exposed voltages decrease because the distance between the lightning arresters and equipment increases. As seen from Figure 59 and Figure 60, these results are valid for both back flashover and shielding failures.

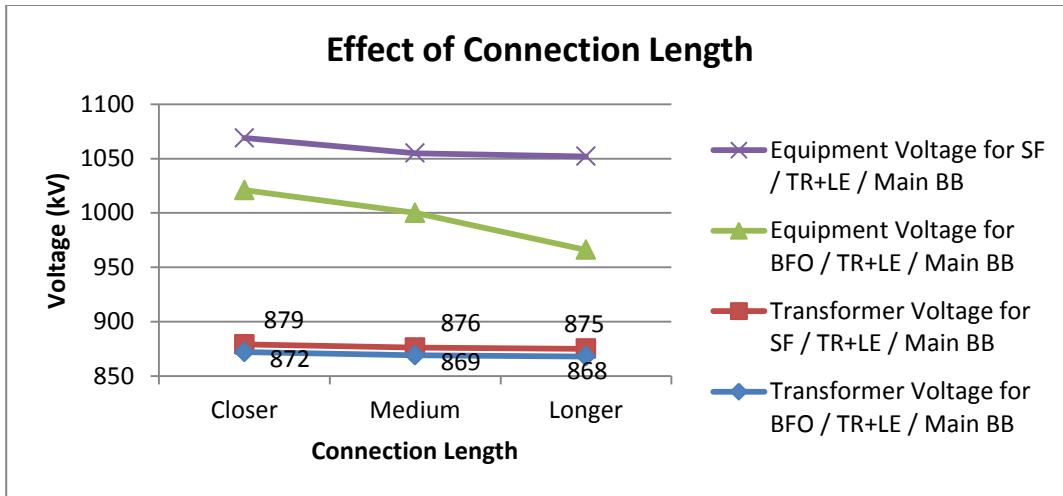


Figure 57 Effect of connection length for main busbar connection type in Case 17, 18, 19 and 20

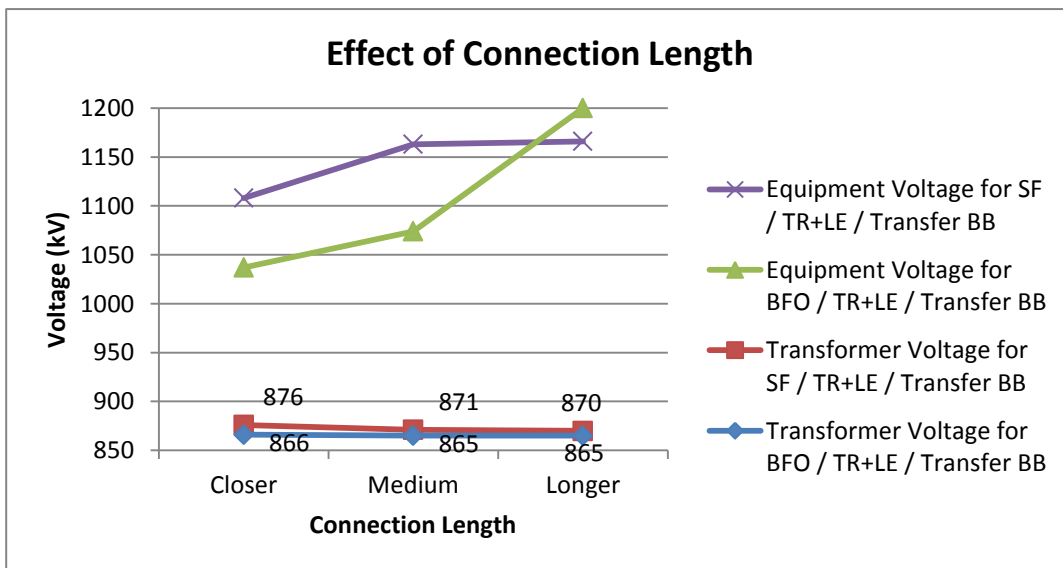


Figure 58 Effect of connection length for transfer busbar connection type in Case 21, 22, 23 and 24

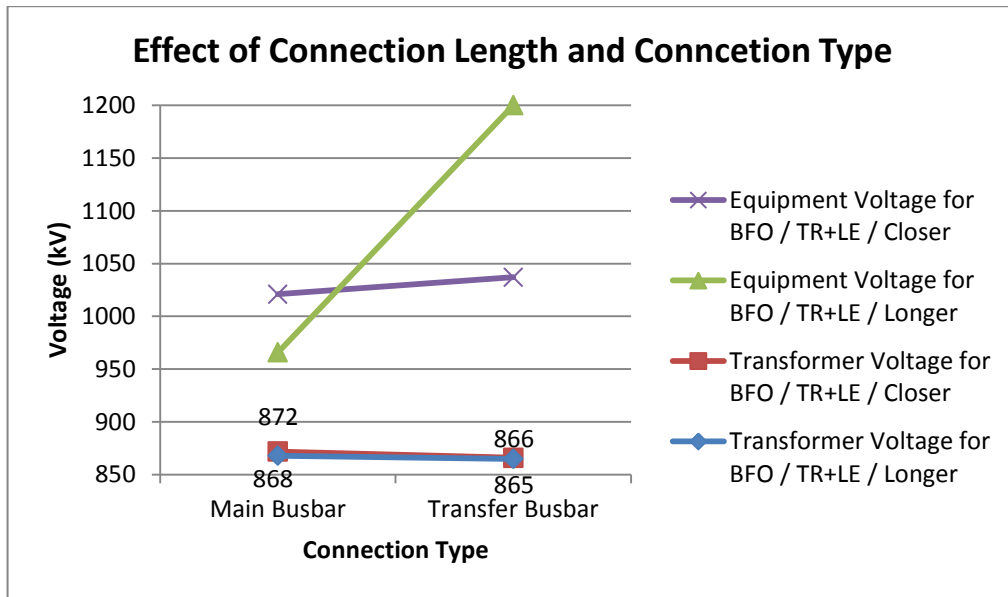


Figure 59 Effect of connection length and connection type for back flashover failure in Case 17, 18, 21 and 22

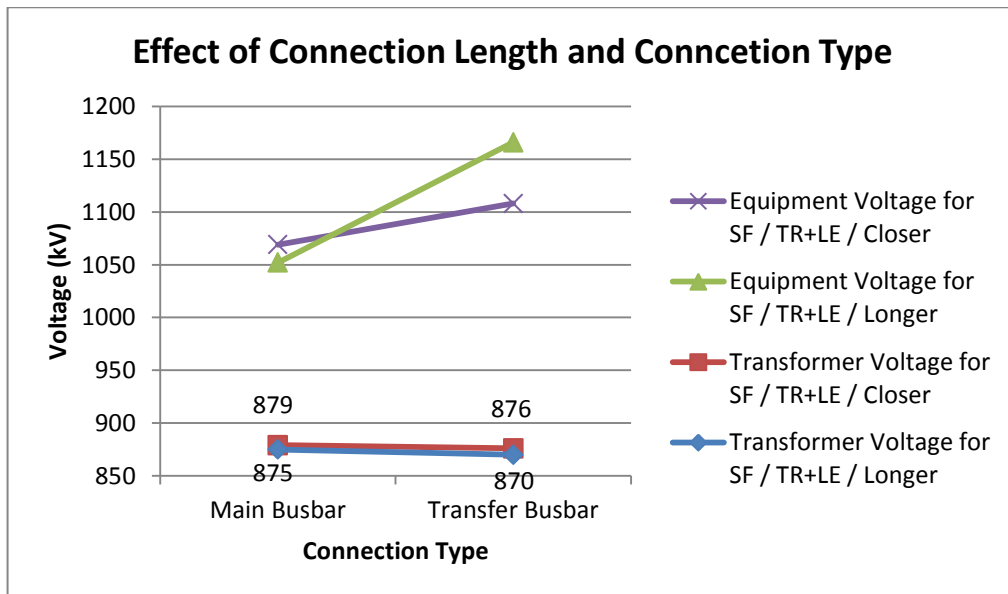


Figure 60 Effect of connection length and connection type for shielding failure in Case 19, 20, 23 and 24

4.5. Analyses of Effect of Location of Lightning Strike

The goal of the forth 8 cases, which are Case 25-26-27-28-29-30-31-32, is to see the effect of location of the lightning strike at the transmission line. In order to achieve this aim, simulations are performed for three situations in terms of lightning strike location; second, third and fourth tower for both back flashover and first, second and third tower for shielding failure. In Figure 61 and Figure 62, the effect of connection length can be seen for main busbar connection and transfer busbar connection.

As given in Figure 61 and Figure 62, maximum voltages, seen at the equipment and power transformer, decrease as the location of lightning strike becomes far from the substation. In other words, while the distance between the lightning strike point at the transmission line and entrance of the substation decreases, equipment and power transformer are exposed to lower voltages. Attenuation of the wave of lightning strike through the transmission line explains this situation and it is accordance with [13]. Hence, these simulations also prove that second tower for back flashover failure and first tower for shielding failure as lightning strike location are the worst case scenarios in terms of maximum voltages seen at the equipment and power transformer. In addition, it is obviously obtained that the equipment is exposed higher overvoltages than the power transformer. That is expected result because of the lightning arresters located close to the power transformer. Another outcome of Figure 61 and Figure 62 is that shielding failures cause higher voltages both at equipment and power transformer. Although the current amplitude of lightning strike at the back flashover failure is higher than the shielding failure, the maximum voltages seen at the shielding failure are higher since the lightning strike is directly to one of phase conductors and lightning strike has different characteristics at the shielding failure. However, this is not a general concept. In other words, the situation depends on the location of substation and characteristics of lightning strike.

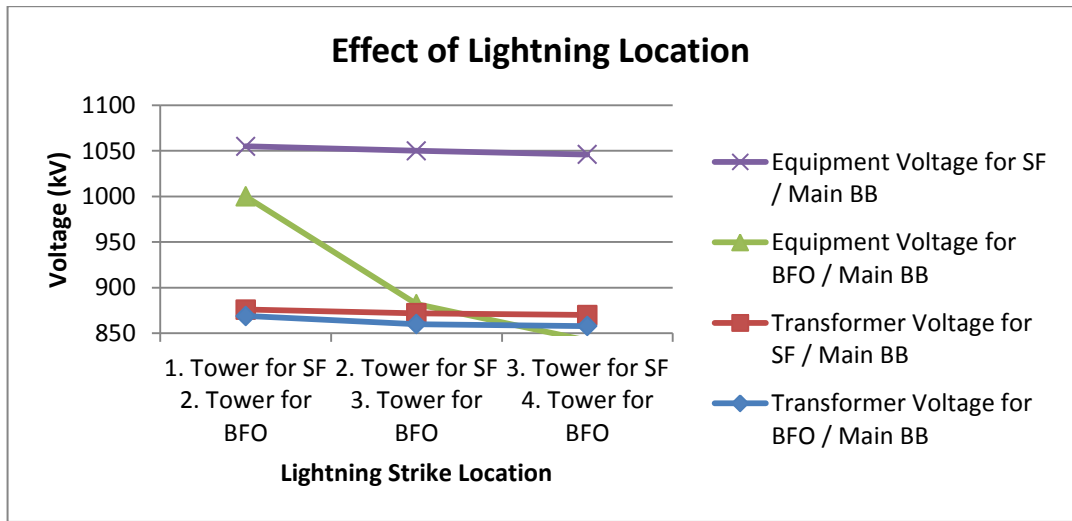


Figure 61 Effect of location of lightning strike for main busbar connection type in Case 25, 26, 27 and 28

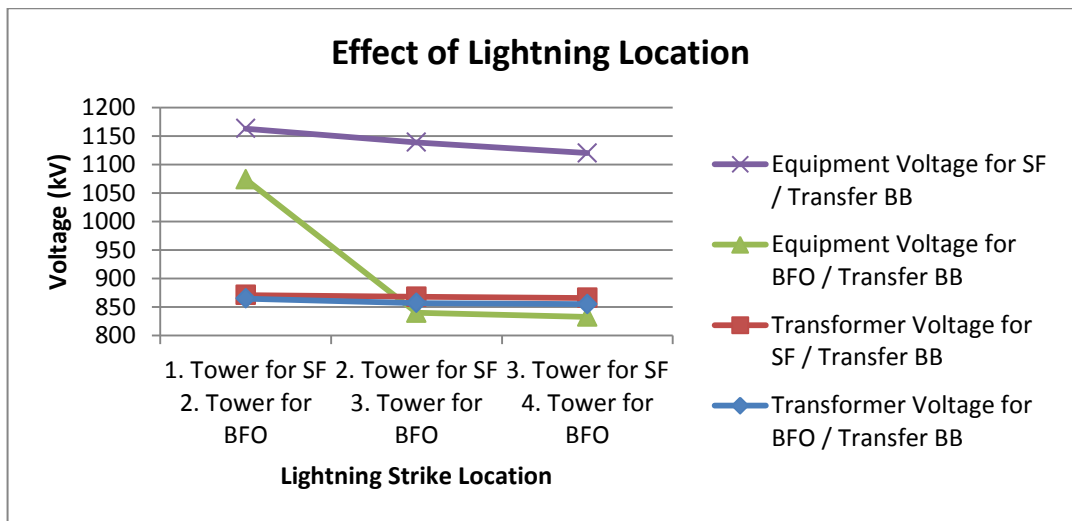


Figure 62 Effect of location of lightning strike for transfer busbar connection type in Case 29, 30, 31 and 32

4.6. Analyses of Results

In this part of the chapter, all results obtained from simulations are discussed in terms of safety factor and cost of equipment. In order to compare the final results observed in the simulations with the standard lightning impulse withstand voltage levels in [2], the safety factor shall be taken into account. The safety factor, called also as correction factor, is applied to compensate the difference in the equipment assembly, the dispersion in the product quality, the quality of installation, the ageing of the insulation during the expected lifetime and other unknown influences according to IEC [2].

Safety factors (K_s) recommended in IEC [2] are 1.15 for internal insulation and 1.05 for external insulation. [27] also proposes 1.15 as a safety factor in insulation coordination studies. In his thesis study, safety factor utilized for all simulations is 1.15. In order to evaluate the standard lightning impulse withstand voltage (LIWV) levels defined in IEC [1], the values should be divided to the safety factor accepted. Therefore, standard LIWV levels for highest group of 525 kV in IEC [1], 1425 kV for power transformer and 1550 kV for other equipment, should be taken into account as 1239.1 kV for power transformer and 1347.8 kV for other equipment. Similarly, standard levels for highest group of 420 kV in IEC [1] should be taken into account as 1130.4 kV for power transformer and 1239.1 kV for other equipment. These calculated values, 1239.1 kV for power transformer and 1347.8 kV for other equipment in 525 kV and 1130.4 kV for power transformer and 1239.1 kV for other equipment in 420 kV, can be considered as the limits for simulation results.

The maximum voltages obtained from simulations for Case 1, 3, 5 and 7, where lightning arrester configuration is the same with current application of Turkish High Voltage Electricity System, i.e. there are lightning arresters only at the front

of the transformer and no lightning arresters at the line entrance, are 898 kV for power transformer and 1227 kV for other equipment. Although these values, 898 kV and 1227 kV, are not close to the valid standard LIWV levels in THVES which are for 525 kV systems in IEC [1], since the effects of lightning arresters located at the line entrance at decrease of the maximum voltage can be obviously observed, additional lightning arresters located at the entrance of the line feeders are recommended. This recommendation is also in accordance with [24]. The remaining cases are simulated for only lightning arresters located both at the front of the power transformer and at the line entrance.

In remaining cases, the maximum voltages observed on the simulations are 880 kV for power transformer at Case 12 and 1200 kV for other equipment at Case 22. These values are under the standard LIWV levels defined in [1] for 420 kV power systems. Hence, in THVES, additional lightning arresters should be located at the line entrance of the line feeders in order to enable the decrease of LIWV levels of equipment to standard LIWV levels defined in [1]. However, as explained in Chapter 1, there are three groups of standard LIWV levels for 420 kV systems in IEC [1]. For THVES, decrease of LIWV levels to only highest group of standard LIWV levels is possible since the values observed exceed LIWV levels defined in lower groups.

When the decrease of LIWV levels in 420 kV substations in THVES is evaluated in economical manner, cost of additional lightning arresters and cost reduction of equipment shall be taken into account. Hence, with the additional lightning arrester application at the line entrance, there will be further cost of three lightning arresters located at the line entrance of each of three phases. The budgetary price of one lightning arrester in 2013 price list of several producers is approximately 3,000 €. This cost means that for each line feeder, the additional cost is roughly 9,000 €. On the other hand, decreasing the LIWV levels of equipment in 420 kV

substations in THVES is going to result in a reduction of cost of equipment. For primary equipment in 420 kV THVES, such as power transformers, circuit breakers, disconnector switches and instrument transformers, cost reduction due to adapting LIWV levels to 1300 kV for power transformer and 1425 kV for other equipment is approximately 10% according to existing market prices. When the cost of circuit breaker for 420 kV highest system voltage and 1550 kV LIWV level, approximately 100,000 €, is taken into account, it is concluded that additional cost of lightning arresters at the entrance of line feeders can be compensated by the cost of reduction of only a circuit breaker. Therefore, changing LIWV levels in 420 kV substations in THVES, from 1425 kV to 1300 kV for power transformer and from 1550 kV to 1425 kV, is technically applicable according to the simulation results and is also economically feasible according to the cost reduction comparison.

CHAPTER 5

CONCLUSION AND FUTURE WORK

Insulation coordination still is an important phenomenon in power systems in order to design the system properly in terms of equipment insulation levels. These insulation coordination studies provide both technically correct and economically feasible systems.

As explained, lightning impulse withstand voltage (LIWV) levels of 420 kV equipment in Turkish High Voltage Electricity System (THVES), defined as 1425 kV and 1550 kV for power transformer and for other equipment, are higher than standard LIWV levels for 420 kV determined in IEC [1]. One of the results of this situation is that the equipment in power system with higher LIWV level in THVES has non-standard values. Since most of European countries use LIWV values defined in IEC [1] for 420 kV, the manufactures have to make custom production for Turkish Market. The obvious outcome of this custom production for the related equipment is higher costs than standard production. The second result of having higher LIWV is that if the LIWV levels of equipment in 420 kV THVES is not correctly selected, higher LIWV values cause overinvestment on equipment.

In this thesis, insulation coordination study is performed for lightning overvoltage in 420 kV substations in THVES through computer simulations using Alternative Transient Program (ATP). The study simulates and reviews different cases in terms of failure types, connection types, location of lightning arresters, current amplitude of lightning strike, connection length and location of lightning strike. With this scope, the objective is to optimize number and location of lightning arresters in 420 kV substations in THVES.

One of the important conclusions of this thesis study is that current LIWV levels of the equipment in 420 kV substations in THVES, 1425 kV for power transformer and 1550 kV for equipment, are high enough for the protection of equipment against lightning overvoltages. With the standard lightning arrester application in 420 kV THVES, lightning arresters located only at front of power transformer, LIWV levels for equipment are satisfied with safety constant higher than 1.15 which is defined in [1] as safety constant for external insulation.

The other outcome is that when additional lightning arresters are located at the entrance of line feeders, maximum voltages observed at equipment and power transformer decrease in 420 kV THVES. By evaluating the peak values obtained from simulations under worst case scenarios, it is concluded that maximum voltages, 880 kV for power transformer and 1200 kV for other equipment, are lower than standard LIWV levels defined in [1]. The peak values observed at the and are and When the safety factor as 1.15 is taken into account, the maximum voltages obtained through simulations also do not exceed standard LIWV levels. Since the worst case approach is used throughout the thesis study in order to get conclusive results, LIWV levels of power transformer and other equipment in 420 kV substations in THVES can be reduced to standard values given in IEC [1] in order to eliminate the negative and undesirable consequences of the existing practice which are non-standard production of equipment in 420 kV power system in THVES and overinvestment.

Since only lightning impulse withstand voltage levels are analyzed in this thesis, switching impulse withstand voltage levels valid in THVES should also be examined through computer simulations as a future work. Therefore, since standard overvoltage levels in a power system is an important planning criterion, standard overvoltage levels defined in IEC [1] can be evaluated as a whole.

REFERENCES

- [1] IEC Publication 60071.1, “Insulation Coordination Part 1: Definitions, Principles and Rules”, 1993

- [2] IEC Publication 60071.2, “Insulation Coordination Part 2: Application Guide”, 1996

- [3] IEC Publication 60071.4, “Insulation Coordination Part 4: Computational Guide to Insulation Co-Ordination and Modelling of Electrical Networks”, 2004

- [4] “IEEE Modeling Guidelines for Fast Front Transients”, The Fast Front Transients Task Force of the IEEE Modeling and Analysis of System Transients Working Group, Dec. 1997.

- [5] A. R. Hileman, “Insulation Coordination for Power Systems”, CRC Press, 1999.

- [6] World Distribution of Thunderstorm Days, “World Meteorological Organization”, Geneva, Switzerland, WMO No. 21, 1056.

- [7] J. A. Martinez-Velasco, “Power System Transients Parameter Determination”, CRC Press, 2010

- [8] IEEE Std 1313.2-1999, “Guide for the Application of Insulation Coordination”, 1999

- [9] Ü. Hızıroğlu, “Overvoltage in Electric Substations and Protection with Metal Oxide Surge Arresters”, Master Thesis, METU, 1993

- [10] S. Şerifeken, "Insulation Coordination Study for Hilal/Izmir Gas Insulated Substation", Master Thesis, METU, 1990
- [11] "Parameter Determination for Modeling Systems Transients - Part V: Surge Arresters", IEEE Transactions on Power Delivery, Vol. 20, No. 3, 2005
- [12] A. J. Eriksson, "The Incidence of Lightning Strikes to Transmission Lines," IEEE Transactions on Power Delivery, July 1987
- [13] J. Takami, S. Okabe, E. Zaima, "Lightning Surge Overvoltages at Substations Due to Backflashover With Assumed Lightning Current Waveforms Based on Observations", IEEE Transactions on Power Delivery, Vol. 25, No. 4, October 2010
- [14] "Elektrik Tesisleri Genel Teknik Sartnamesi ve Uygulama Esasları", Chamber of Electrical Engineers (EMO), TY/2011/2, Ankara, 2012
- [15] "Guide to Procedures for Estimating the Lightning Performance of Transmission Lines," CIGRE Working Group 01 (Lightning) of Study Committee 33 (Overvoltages and Insulation Co-ordination), October 1991
- [16] H. Mokhlis, A. H. A. Bakar, H. A. Illias, M. F. Shafie, "Insulation Coordination Study of 275kV AIS Substation in Malaysia", IEEE 978-1-4577-0547-2/12, 2012
- [17] H. Mokhlis, A. H. A. Bakar, H. A. Illias, M. F. Shafie, "Lightning Overvoltage performance of 132kV GIS Substation in Malaysia", IEEE International Conference on Power System Technology, 2010

- [18] P. Pinceti, M. Giannettoni, “A simplified model for zinc oxide surge arresters”, IEEE Transactions on Power Delivery, Vol. 14, No. 2, April 1999
- [19] P. N. Mikropoulos, T. E. Tsovilis, Z. G. Datsios and N. C. Mavrikakis, “Effects of Simulation Models of Overhead Transmission Line Basic Components on Backflashover Surges Impinging on GIS Substations”, 45th International Universities' Power Engineering Conference (UPEC) in Cardiff, Wales, UK., 2010
- [20] H. W. Dommel, “An Overview of Computer Simulation Methods for Electromagnetic Transients in Power Systems”, Australasian Universities Power Engineering Conference (AUPEC), 2005
- [21] D. Xu, Z. Hao, “Research of The Lightning Protection Performance for 220 kV Double-circuit Transmission Line” 7th Asia-Pacific International Conference on Lightning, Chengdu, China, November 2011
- [22] A. Ametani, T. Kawamura, “A Method of a Lightning Surge Analysis Recommended in Japan Using EMTP”, IEEE Transactions on Power Delivery, Vol. 20, No. 2, April 2005
- [23] T. Ueda, T. Ito, H. Watanabe, T. Funabashi, “A Comparison between Two Tower Models for Lightning Surge Analysis of 77kV System”, IEEE 0-7803-6338-8, 2010
- [24] A. Annamalai, A. Gulati, R. Koul, “Sizing of Surge Arresters for 400kV Substation - A Case study”, IEEE International Conference on Emerging Trends in Electrical and Computer Technology (ICETECT), 2011

[25] R. L. Witzke, T. J. Bliss, "Co-ordination of Lightning Arrester Location with Transformer Insulation Level", AIEE Summer and Pacific General Meeting, Pasadena, 1950

[26] A. Bayadi, N. Harid, K. Zehar, "Dynamic Surge Arrester Protection Performance on High Voltage Systems Using EMTP", 2003

[27] K. H. Week, "Principles and Procedures of Insulation Co-Ordination", IEE Proceedings, Vol. 134, Pt. C, No. 2, March 1987

[28] M. J. Heathcote, "The J&P Transformer Book", Newnes, 2007

APPENDIX A

SIMULATION RESULTS FOR CASES IN TABULATED FORM

Table 10 Results for Case 1

	A	B	C	D	E
1	Name	Min	Max	Abs Max	Avg
2	LINECB	-22552	1.02173E+006	1.02173E+006	46053.7
3	LINEDS	-22495.7	1.02702E+006	1.02702E+006	46053.4
4	LINEVT	-22454.7	1.03189E+006	1.03189E+006	46052
5	TR	-22749.6	893585	893585	46055.4
6	TR_CB	-22634.7	1.08421E+006	1.08421E+006	46055.1
7	TR_DS	-22580.5	950500	950500	46054.6

Table 11 Results for Case 2

	A	B	C	D	E
1	Name	Min	Max	Abs Max	Avg
2	LINECB	-22572.2	1.00011E+006	1.00011E+006	45979.8
3	LINEDS	-22491.3	976321	976321	45979.4
4	LINEVT	-22404.7	884930	884930	45978.1
5	TR	-22876.9	869529	869529	45982.1
6	TR_CB	-22698.3	966917	966917	45981.3
7	TR_DS	-22650.8	931367	931367	45980.7

Table 12 Results for Case 3

	A	B	C	D	E
1	Name	Min	Max	Abs Max	Avg
2	LINECB	-285.108	1.05044E+006	1.05044E+006	62822.9
3	LINEDS	-381.909	1.07432E+006	1.07432E+006	62827.9
4	LINEVT	-205.653	977166	977166	62822.7
5	TR	-232.332	898363	898363	62820.4
6	TR_CB	-251.844	1.07911E+006	1.07911E+006	62821.3
7	TR_DS	-433.902	1.15295E+006	1.15295E+006	62829.8

Table 13 Results for Case 4

	A	B	C	D	E
1	Name	Min	Max	Abs Max	Avg
2	LINECB	-268.661	1.00518E+006	1.00518E+006	61826.6
3	LINEDS	-352.796	1.05142E+006	1.05142E+006	61830.6
4	LINEVT	-197.994	840652	840652	61826.3
5	TR	-232.971	876155	876155	61824.7
6	TR_CB	-244.24	1.05528E+006	1.05528E+006	61825.4
7	TR_DS	-401.395	1.05204E+006	1.05204E+006	61832.1

Table 14 Results for Case 5

	A	B	C	D	E
1	Name	Min	Max	Abs Max	Avg
2	LINECB	-22925.3	1.1037E+006	1.1037E+006	46049.8
3	LINEDS	-22513.3	1.0784E+006	1.0784E+006	46048.7
4	LINEVT	-22468.9	1.03192E+006	1.03192E+006	46047.4
5	TR	-22786.1	890249	890249	46052.4
6	TR_DS	-22955.8	932000	932000	46052.3
7	TR_VT	-22659.5	1.12622E+006	1.12622E+006	46052.3
8	TRS_CB	-23509	926266	926266	46053.8
9	TRS_DS	-23021.7	1.07709E+006	1.07709E+006	46051.1

Table 15 Results for Case 6

	A	B	C	D	E
1	Name	Min	Max	Abs Max	Avg
2	LINECB	-22780.2	1.0719E+006	1.0719E+006	45978.1
3	LINEDS	-22441.8	1.03147E+006	1.03147E+006	45977.5
4	LINEVT	-22404.1	884930	884930	45975.9
5	TR	-22693.5	865953	865953	45981.3
6	TR_DS	-22771.5	944798	944798	45980.6
7	TR_VT	-22591.9	1.07432E+006	1.07432E+006	45981.1
8	TRS_CB	-23216.4	967787	967787	45981
9	TRS_DS	-22843.4	1.06843E+006	1.06843E+006	45979.3

Table 16 Results for Case 7

	A	B	C	D	E
1	Name	Min	Max	Abs Max	Avg
2	LINECB	-784.444	1.12029E+006	1.12029E+006	62742.5
3	LINEDS	-385.033	1.12524E+006	1.12524E+006	62709.3
4	LINEVT	-227.108	977166	977166	62706.9
5	TR	-279.892	893665	893665	62704.3
6	TR_DS	-1063.92	1.06988E+006	1.06988E+006	62768.6
7	TR_VT	-316.969	958116	958116	62705.7
8	TRS_CB	-1653.2	1.17013E+006	1.17013E+006	62867.5
9	TRS_DS	-1002.78	1.22736E+006	1.22736E+006	62763.1

Table 17 Results for Case 8

	A	B	C	D	E
1	Name	Min	Max	Abs Max	Avg
2	LINECB	-750.296	1.08233E+006	1.08233E+006	61764.8
3	LINEDS	-360.465	1.08867E+006	1.08867E+006	61734.3
4	LINEVT	-217.144	840652	840652	61732.2
5	TR	-259.099	871436	871436	61730.3
6	TR_DS	-1008.87	1.03694E+006	1.03694E+006	61789.3
7	TR_VT	-297.609	992964	992964	61731.4
8	TRS_CB	-1528.9	1.12171E+006	1.12171E+006	61881.4
9	TRS_DS	-932.081	1.16355E+006	1.16355E+006	61783.8

Table 18 Results for Case 9

	A	B	C	D	E
1	Name	Min	Max	Abs Max	Avg
2	LINECB	-23092.4	1.01932E+006	1.01932E+006	47160.9
3	LINEDS	-22993.4	996766	996766	47160.5
4	LINEVT	-22956.6	894555	894555	47159.3
5	TR	-23328.2	871686	871686	47163.1
6	TR_CB	-23190.5	979658	979658	47162.5
7	TR_DS	-23113.3	944107	944107	47161.9

Table 19 Results for Case 10

	A	B	C	D	E
1	Name	Min	Max	Abs Max	Avg
2	LINECB	-24157	1.0463E+006	1.0463E+006	49518.7
3	LINEDS	-24132.6	1.02311E+006	1.02311E+006	49518.4
4	LINEVT	-24065.7	914247	914247	49517.2
5	TR	-24279.9	876014	876014	49521.2
6	TR_CB	-24204.4	996045	996045	49520.4
7	TR_DS	-24210.3	972588	972588	49519.7

Table 20 Results for Case 11

	A	B	C	D	E
1	Name	Min	Max	Abs Max	Avg
2	LINECB	-272.602	1.01236E+006	1.01236E+006	62995.3
3	LINEDS	-360.665	1.06295E+006	1.06295E+006	62999.4
4	LINEVT	-201.509	851630	851630	62995
5	TR	-229.954	878475	878475	62993.2
6	TR_CB	-245.208	1.05975E+006	1.05975E+006	62994
7	TR_DS	-408.291	1.06567E+006	1.06567E+006	63001

Table 21 Results for Case 12

	A	B	C	D	E
1	Name	Min	Max	Abs Max	Avg
2	LINECB	-274.741	1.01705E+006	1.01705E+006	64130.4
3	LINEDS	-369.236	1.0719E+006	1.0719E+006	64134.8
4	LINEVT	-204.928	862741	862741	64130.1
5	TR	-223.062	880607	880607	64128.1
6	TR_CB	-243.471	1.0636E+006	1.0636E+006	64129
7	TR_DS	-414.422	1.07744E+006	1.07744E+006	64136.4

Table 22 Results for Case 13

	A	B	C	D	E
1	Name	Min	Max	Abs Max	Avg
2	LINECB	-23394.5	1.07579E+006	1.07579E+006	47160
3	LINEDS	-23017.3	1.03606E+006	1.03606E+006	47159.2
4	LINEVT	-22967.9	894555	894555	47157.6
5	TR	-23202.1	868031	868031	47162.9
6	TR_DS	-23422.8	950572	950572	47162.7
7	TR_VT	-23103.4	1.08072E+006	1.08072E+006	47162.9
8	TRS_CB	-23866.9	977764	977764	47163.7
9	TRS_DS	-23478.7	1.07243E+006	1.07243E+006	47161.3

Table 23 Results for Case 14

	A	B	C	D	E
1	Name	Min	Max	Abs Max	Avg
2	LINECB	-24621.1	1.08424E+006	1.08424E+006	49519.2
3	LINEDS	-24186	1.04487E+006	1.04487E+006	49518
4	LINEVT	-24086.4	914247	914247	49516.4
5	TR	-24290.7	872209	872209	49521.8
6	TR_DS	-24824.8	956013	956013	49522.2
7	TR_VT	-24247.3	1.09199E+006	1.09199E+006	49521.8
8	TRS_CB	-25305	986171	986171	49524.4
9	TRS_DS	-24785.5	1.08464E+006	1.08464E+006	49520.7

Table 24 Results for Case 15

	A	B	C	D	E
1	Name	Min	Max	Abs Max	Avg
2	LINECB	-719.787	1.09604E+006	1.09604E+006	62926.1
3	LINEDS	-364.789	1.10315E+006	1.10315E+006	62898.4
4	LINEVT	-219.732	851630	851630	62896.2
5	TR	-244.217	873495	873495	62894.1
6	TR_DS	-993.673	1.04672E+006	1.04672E+006	62949.6
7	TR_VT	-290.256	996062	996062	62895.3
8	TRS_CB	-1466.11	1.12906E+006	1.12906E+006	63036.1
9	TRS_DS	-912.542	1.17927E+006	1.17927E+006	62944.2

Table 25 Results for Case 16

	A	B	C	D	E
1	Name	Min	Max	Abs Max	Avg
2	LINECB	-726.194	1.1091E+006	1.1091E+006	64063
3	LINEDS	-371.776	1.11641E+006	1.11641E+006	64035.5
4	LINEVT	-223.315	862741	862741	64033.4
5	TR	-252.962	875413	875413	64031
6	TR_DS	-1002.6	1.05548E+006	1.05548E+006	64086.7
7	TR_VT	-297.531	998448	998448	64032.3
8	TRS_CB	-1488.56	1.13499E+006	1.13499E+006	64173
9	TRS_DS	-921.058	1.19384E+006	1.19384E+006	64081.3

Table 26 Results for Case 17

	A	B	C	D	E
1	Name	Min	Max	Abs Max	Avg
2	LINECB	-22518.2	995785	995785	45978.2
3	LINEDS	-22424.9	1.0209E+006	1.0209E+006	45977.9
4	LINEVT	-22398.6	883913	883913	45976.7
5	TR	-22893.7	871338	871338	45980.1
6	TR_CB	-22679.7	942883	942883	45979.5
7	TR_DS	-22462.4	985640	985640	45978.7

Table 27 Results for Case 18

	A	B	C	D	E
1	Name	Min	Max	Abs Max	Avg
2	LINECB	-22505	952614	952614	45981
3	LINEDS	-22532	926286	926286	45980.9
4	LINEVT	-22403.5	885161	885161	45978.9
5	TR	-22652.5	868997	868997	45983
6	TR_CB	-22546.6	963752	963752	45982.4
7	TR_DS	-22598.4	966218	966218	45982.4

Table 28 Results for Case 19

	A	B	C	D	E
1	Name	Min	Max	Abs Max	Avg
2	LINECB	-198.078	1.0081E+006	1.0081E+006	61849.5
3	LINEDS	-199.25	1.04924E+006	1.04924E+006	61849.7
4	LINEVT	-188.149	840652	840652	61850.1
5	TR	-219.236	879287	879287	61848.5
6	TR_CB	-206.72	1.04882E+006	1.04882E+006	61849
7	TR_DS	-197.471	1.06909E+006	1.06909E+006	61849.3

Table 29 Results for Case 20

	A	B	C	D	E
1	Name	Min	Max	Abs Max	Avg
2	LINECB	-217.355	1.01641E+006	1.01641E+006	61813.9
3	LINEDS	-300.807	1.02457E+006	1.02457E+006	61816.7
4	LINEVT	-193.907	840652	840652	61814.4
5	TR	-221.393	875622	875622	61812.8
6	TR_CB	-218.122	1.05612E+006	1.05612E+006	61813.3
7	TR_DS	-253.023	1.0707E+006	1.0707E+006	61814.3

Table 30 Results for Case 21

	A	B	C	D	E
1	Name	Min	Max	Abs Max	Avg
2	LINECB	-22847.5	1.0375E+006	1.0375E+006	45978.6
3	LINEDS	-22502.6	1.02838E+006	1.02838E+006	45978.1
4	LINEVT	-22411.2	884629	884629	45976.3
5	TR	-22695	866704	866704	45981.3
6	TR_DS	-22693.2	963106	963106	45980.8
7	TR_VT	-22588.7	1.03039E+006	1.03039E+006	45981.1
8	TRS_CB	-22852.2	966306	966306	45981.1
9	TRS_DS	-22713.5	996733	996733	45979.6

Table 31 Results for Case 22

	A	B	C	D	E
1	Name	Min	Max	Abs Max	Avg
2	LINECB	-22655	1.05457E+006	1.05457E+006	45977.4
3	LINEDS	-22635.4	1.00275E+006	1.00275E+006	45977.1
4	LINEVT	-22414.9	885161	885161	45975.2
5	TR	-22685.5	865430	865430	45981
6	TR_DS	-22891.5	966130	966130	45981.1
7	TR_VT	-22594	1.12351E+006	1.12351E+006	45980.9
8	TRS_CB	-23116.3	1.07435E+006	1.07435E+006	45980.8
9	TRS_DS	-22765.7	1.1956E+006	1.1956E+006	45978.9

Table 32 Results for Case 23

	A	B	C	D	E
1	Name	Min	Max	Abs Max	Avg
2	LINECB	-299.321	1.08449E+006	1.08449E+006	61782.4
3	LINEDS	-258.235	1.10071E+006	1.10071E+006	61781.7
4	LINEVT	-192.457	840652	840652	61781.2
5	TR	-208.332	876523	876523	61779.1
6	TR_DS	-298.647	1.02779E+006	1.02779E+006	61782
7	TR_VT	-209.259	991130	991130	61779.7
8	TRS_CB	-276.245	1.05236E+006	1.05236E+006	61781.7
9	TRS_DS	-263.896	1.10825E+006	1.10825E+006	61781.5

Table 33 Results for Case 24

	A	B	C	D	E
1	Name	Min	Max	Abs Max	Avg
2	LINECB	-1361.64	1.09496E+006	1.09496E+006	61812.2
3	LINEDS	-1049.27	1.05309E+006	1.05309E+006	61753.2
4	LINEVT	-269.606	840652	840652	61704.9
5	TR	-260.757	870336	870336	61702.3
6	TR_DS	-2248.32	1.01537E+006	1.01537E+006	61979.6
7	TR_VT	-327.841	988228	988228	61703.9
8	TRS_CB	-3715.69	1.11845E+006	1.11845E+006	62216.6
9	TRS_DS	-2192.54	1.16672E+006	1.16672E+006	61943.7

Table 34 Results for Case 25

	A	B	C	D	E
1	Name	Min	Max	Abs Max	Avg
2	LINECB	0	847758	847758	28764.1
3	LINEDS	0	865144	865144	28764.1
4	LINEVT	-28353.2	837554	837554	28786
5	TR	-28.3213	859571	859571	28764.2
6	TR_CB	0	855946	855946	28764
7	TR_DS	0	881951	881951	28764.1

Table 35 Results for Case 26

	A	B	C	D	E
1	Name	Min	Max	Abs Max	Avg
2	LINECB	-121898	739376	739376	29060.5
3	LINEDS	-74933.6	759419	759419	28691.5
4	LINEVT	-138200	833354	833354	28786.5
5	TR	-172510	858343	858343	34798.6
6	TR_CB	-75691.8	847914	847914	32758.9
7	TR_DS	-108186	895511	895511	30747.9

Table 36 Results for Case 27

	A	B	C	D	E
1	Name	Min	Max	Abs Max	Avg
2	LINECB	-104.853	979514	979514	61749
3	LINEDS	-147.565	1.01361E+006	1.01361E+006	61751.8
4	LINEVT	-71.0387	826704	826704	61749.1
5	TR	-89.8437	872648	872648	61747.4
6	TR_CB	-94.7666	1.0504E+006	1.0504E+006	61748
7	TR_DS	-171.129	1.03514E+006	1.03514E+006	61752.9

Table 37 Results for Case 28

	A	B	C	D	E
1	Name	Min	Max	Abs Max	Avg
2	LINECB	0	969863	969863	61619.6
3	LINEDS	0	994379	994379	61619.8
4	LINEVT	0	822457	822457	61620.2
5	TR	-1.34998	870925	870925	61618.4
6	TR_CB	0	1.04677E+006	1.04677E+006	61619
7	TR_DS	-3.18273	1.02618E+006	1.02618E+006	61619.4

Table 38 Results for Case 29

	A	B	C	D	E
1	Name	Min	Max	Abs Max	Avg
2	LINECB	0	790402	790402	28768.3
3	LINEDS	0	791352	791352	28768.3
4	LINEVT	-102370	837560	837560	28893.3
5	TR	0	856550	856550	28768.1
6	TR_DS	0	656308	656308	28768.2
7	TR_VT	0	724256	724256	28768.2
8	TRS_CB	-23.8018	693729	693729	28768.5
9	TRS_DS	0	826651	826651	28768.3

Table 39 Results for Case 30

	A	B	C	D	E
1	Name	Min	Max	Abs Max	Avg
2	LINECB	-574.369	812681	812681	28588.9
3	LINEDS	-63213.9	819916	819916	28657.6
4	LINEVT	-193636	833372	833372	28895.8
5	TR	-135277	855465	855465	28816.6
6	TR_DS	0	752157	752157	28588.7
7	TR_VT	0	821279	821279	28588.7
8	TRS_CB	0	762270	762270	28588.8
9	TRS_DS	0	820709	820709	28588.8

Table 40 Results for Case 31

	A	B	C	D	E
1	Name	Min	Max	Abs Max	Avg
2	LINECB	-427.718	1.06471E+006	1.06471E+006	61689.7
3	LINEDS	-173.972	1.0651E+006	1.0651E+006	61660.5
4	LINEVT	-84.7513	826704	826704	61658.3
5	TR	-117.06	868365	868365	61656.4
6	TR_DS	-607.317	1.06012E+006	1.06012E+006	61707.6
7	TR_VT	-135.84	987528	987528	61657.5
8	TRS_CB	-983.856	1.11412E+006	1.11412E+006	61775.5
9	TRS_DS	-567.979	1.13937E+006	1.13937E+006	61703.8

Table 41 Results for Case 32

	A	B	C	D	E
1	Name	Min	Max	Abs Max	Avg
2	LINECB	-151.494	1.05375E+006	1.05375E+006	61533.7
3	LINEDS	-6.03458	1.05041E+006	1.05041E+006	61523.5
4	LINEVT	0	822457	822457	61523.9
5	TR	-0.203971	866830	866830	61521.6
6	TR_DS	-273.512	1.01762E+006	1.01762E+006	61543.5
7	TR_VT	-0.225718	981673	981673	61522.2
8	TRS_CB	-550.187	1.10425E+006	1.10425E+006	61587
9	TRS_DS	-247.142	1.12023E+006	1.12023E+006	61541.7

APPENDIX B

THE DETAILS OF 3A1 TYPE TOWER

